UNESCO-IHE

INSTITUTE FOR WATER EDUCATION

COUPLED STRESS - SEEPAGE NUMERICAL DESIGN OF PRESSURE TUNNELS

Afis Olumide Busari

M.Sc Thesis WSE-HERBD - 11.03

April 2011

UNESCO-IHE
Institute for Water Education

Coupled stress-seepage numerical design of pressure tunnels

Master of Science Thesis

by

Olumide Afis Busari

Supervisors

Prof. A. E. Mynett (UNESCO-IHE)

Assoc. Prof. M. Marence (UNESCO-IHE)

Examination committee

Prof. A. E. Mynett (UNESCO-IHE), Chairman

Assoc. Prof. M. Marence Ph.D, M.Sc (UNESCO-IHE)

Dr. Ioana Popescu, Ph.D, M.Sc (UNESCO-IHE)

This research is done for the partial fulfilment of requirements for the Master of Science degree at the UNESCO-IRE Institute for Water Education, Delft, the Netherlands

Delft

April 2011

The findings, interpretations and conclusions expressed in this study do neither necessarily reflect the views of the UNESCO-mE Institute for Water Education, nor of the individual members of the MSc committee, nor of their respective employers.

Dedication

To the Almighty God - The giver of Knowledge

To my mentor - Sheik Ahmada Tijani ibn Muhammed Lawal

To the government of the Netherlands and its citizenry

To all lecturers - UNESCO-IHE Institute for Water Education, Delft, the Netherlands

Abstract

The design and construction of pressure tunnels are among the most complicated of tunnels. Therefore, special attention is required in the design and construction of these tunnels to prevent failure. This research introduce PLAXIS 2D fmite element program as a tool for numerical modeling of plain concrete pressure tunnels. The numerical model cannot portray the nature, but should simulate the materials and the loading cases. The rock behaviour was approximated using elasto-plastic Mohr - Coulombs model. The shotcrete and fmal lining defmed as permeable and elastic. Analyses were based on plain strain condition. Different phenomena in terms of loading cases during construction stage and operational loading of internal water pressure were simulated. The entire loading steps in the design of pressure tunnels modeled are: initial state of stresses, 2D simulation of 3D excavation, shotcrete installation, final lining construction, simulation of temperature/shrinkageeffect of concrete lining, shotcrete decay, grouting process with prestressing effect and finally, the modeling of operational loading of internal water pressure and external water pressure in empty tunnel. Special concern is taken on the modeling of the contact between the shotcrete and the fmal lining where during shrinkage and temperature change by first filling with cold water a gap can open. This gap is filled (closed) during prestressing.

Plain concrete lining of pressure tunnels is not absolutely tight lining and water seeps out of the tunnel. The seeped water is lost energy, but can also cause stability problems in the surrounding rock mass. Additionally, if the rock mass around the tunnel is tight (originally or tighten by grouting) the seeped water stays in the vicinity of the tunnel and increases the external water pressure. Such increased external water pressure decreases the gradients between internal and external pressure and reduce the seepage and losses. Modeling of this phenomenon is performed by coupled stress-seepage calculation performed by the same model. The coupling of stress - seepage was carried out by superimposing results of consolidation and water flow analyses.

Practical example was taken from the pressure tunnel of the HPP Ermenek Turkey. The calculation results are compared with results of existing tunnel and with analytical solutions. The entire simulation results for both: construction stages and operational loading by internal and external water pressure showed that PLAXIS 2D fmite element program can be used to observe and lor predict phenomena in pressure tunnels.

Keywords: *Pressure tunnel, plain concrete lining, permeable tunnel lining, stress-seepage analysis, PLAXIS 2D,jinite element simulation.*

Acknowledgement

The research was conducted in the course of my study as a Master of Science student at the UNESCO-IDE Institute for Water Education, Delft, the Netherlands and was funded by the Netherlands Fellowship Programme (NFP).

My profound gratitude to my thesis supervisor, Dr. Marence Miroslav, Associate Professor in Storage and Hydropower, Department of Water Science Engineering, UNESCO-IDE, for his personal support and technical advice during this research work. He took his time to couple principle of teaching and practice in the design and construction of pressure tunnel so that I can capture essence of the research work. I am glad to have worked with him as a master student. He made what I thought impossible to be possible regarding the complexity of the research topic. His encouragement gave me hope even when the going was tough, most especially the rigor of simulations. With him I have seen hydropower at the end of pressure tunnels.

Heartfelt thanks to Prof. Dr. A. E Mynett, Professor of Hydraulic Engineering and River Basin Development (UNESCO-IHE) for his constructive criticism and suggestions during progress report presentation and preparation of this manuscript. The relentless effort through time devotion for meetings and his readiness to attend to me in time of needs is highly appreciated.

Special thanks to the staff members of Hydraulic Engineering and River basin Development specialization and entire staff members of UNESCO-IDE for their invaluable contribution to human capacity building. lowe you all God - bless and wishing you the good knowledge and wisdom your esteemed offices demand.

I wish to appreciate Prof. S. Sadiku, Professor of Civil engineering and Head of Department of Civil Engineering, Federal University of Minna Nigeria for the great role he has played in making my dream a reality. Thanks to all staff members, academics and non-academics of Federal University of Technology, Minna, Nigeria.

I am indebted Mr. Yos Simanjuntak, Ph.D participant, Hydraulic Engineering and River Basin UNESCO-IDE for his support during my research. I am wishing you the best in all endeavours.

The role of my academic writing teachers, Mrs. Wendy Sturrock and Mrs. Davis Patricia cannot be overemphasized. They made research proposal a song worthy of singing.

Thanks to all friends who in one way or the other contributed to the success of this report. I remain eternally grateful to the 17 - member, River Basin family *(2009/2011)* academic session.

Afis Olumide Busari
Delft, April 2011.

Table of Contents

List of figures

List of tables

List of Symbols

Symbol	Unit	Meaning
Y,Yr	*kN/m3*	Unit weight of rock
Yw	*kN/m3*	Unit weight of water
p	*kg/m3*	Bulk density of rock
n		Porosity
e		Void ratio
ω	*kN/m2*	Stress
xx		Subscription for location in *x* direction
yy		Subscription for location in *y* direction
zz		Subscription for location in *z* direction
rr		Subscription for radial stresses
ee		Subscription for tangential stresses
re		Subscription for shear stress
v		Poisson's ratio
Ee		Uni-axial strain
c	*kN/m2*	Cohesion
¢	(0)	Friction angle
I	m4	Second moment of area
E		Strain
T	*kN/m2*	Shear strength
R	*m*	External radius
«:	*m*	Average radius
r	*m*	Internal radius
t/J	(0)	Segment angle
e	(0)	Polar angle
Ko		Coefficient of earth pressure at rest

feu	*N/mm2*	Characteristic strength of concrete
d_{eq}	*m*	equivalent thickness of liner
f.s		Factor of safety
y,h	*m*	Overburden depth
Pi	*kN/m2*	Inner liner pressure
P2	*kN/m2*	Outer liner pressure
Pi	*kN/m2*	Internal water pressure
Pr	*kN/m2*	External pressure
Po	*kN/m2*	Hydraulic pressure
q	*mls*	Seepage loss
."	*m2/s*	Kinematic viscosity
v	*m2/s*	Kinematic viscosity
η	*kN/s/m2*	Dynamic viscosity
Ke	*mlday*	Coefficient of permeability of concrete
Kr	*m/day*	Coefficient of permeability of rock
Ke2	*mlday*	permeability of liner after cracking
w	*mm*	Radial deflection in lining
wmax	*mm*	Maximum crack width
a	*per'iC*	thermal coefficient of concrete
KN	*kN/m2/m*	Normal stiffness of rock mass
KT	*kN/m2/m*	Tangential stiffness of rock mass
N		Number of cracks
2u or 2a	mm	Average crack
{3		Load reduction factor
BM	*kNm*	Bending moment
u	mm	Displacement
T	*kN*	Hoop force

1 Introduction

1.1 Preamble

The design and construction of pressure tunnels are among the most complicated of tunnels, because they include all steps of infrastructural tunnel construction and also special loading cases in construction and operation of the pressure tunnel. Therefore, special attention is required in the design and construction of these tunnels to prevent failure. The main function of the pressure tunnel is to convey water safe and with minimized losses from reservoir to the turbine. The pressure tunnels are mostly lined by plain or reinforced concrete lining, but sometimes the tunnels can be left unlined or just lined by shotcrete. In extreme cases, where all other methods in term of lining strength or permeability cannot give satisfactory results, a tightening element is needed. The tightening element, thin or thick steel lining and in some cases plastic foil or plastic pipe is commonly used. Implementation of the tightening element increases the construction costs and minimizing of the tunnel length with tightening element is an important target by pressure tunnel design.

Generally, unlined, shotcrete or simple concrete lined tunnels are not tight and water can leak in and out in the tunnel. Water leaked out is lost for the energy production and can also cause problems in tunnel surrounding (landslide or hydro-jacking of the surrounding rock mass). Especially the problem becomes serious if the method is used in the rock formations that are not resistant on loading by pressurized water.

In case of the rock mass that is not resistant on loading by pressurized water because of washing out of joint filling, slaking effect or erosion, the contact of rock mass with pressurized water and rock mass has to be omitted. The concrete lining represents a suitable solution. The plain concrete lining has limited tensile strength and therefore the bearing of the internal water pressure is limited. The bearing capacity of the plain concrete lining can be increased if the lining is before filling with water artificially pre-stressed. Pre-stressing of the concrete lining can be done by different methods; by cables - very expensive for long structures like tunnels and is used mostly in case of repair of short sections, or by high pressure grouting between the lining and the surrounding rock mass. Such grouting method is then limited by the compressive bearing capacity of the lining and is usually used up to the internal water pressures of 10-15 bars.

Other alternative is the use of reinforced concrete lining. By the reinforced concrete lining, the tensile stresses in the lining caused by internal water pressure are taken by steel reinforcement. The disadvantage of the reinforced concrete is again the limited tensile strength of the concrete. The concrete must crack that the reinforcement can become a bearing member. The reinforcement acts as a crack distributor allocating few wider open cracks in the number of thinner cracks. In case of pressure tunnels with pressures of 10 and more bars such reinforced concrete cannot be characterized as tight although the crack width is maybe under the limit defming tight concrete in the most of the international concrete codes.

If a tightening of tunnel is needed the tightening element in form of foil, thin plastic or steel lining and thick steel penstock has to be foreseen. The tightening element has function to protect leaking of the water out and also in the tunnel. Sometimes the tightening element can be seen also as a bearing member taking full or part of the water loading and design has to include this additional function.

A number of fundamental criteria and other important considerations have to be defined during the pressure tunnel design. Marence (2009) showed a possible flow chart (figure 1.1) defining design criteria that has to be taken into consideration during the power waterway design. The flow chart can be applied to each section along the power waterway and has to be included in the design of the vertical and horizontal tunnel alignment.

Figure 1.1: Flow chart for power waterway (Marence, 2009).

1.2 Research objectives

1.2.1 Overall objective

The overall objective of the research is to review common practice design methods with special attention on the plain concrete lined power waterways using PLAXIS 2D program.

1.2.2 Specific objectives

1. To define numerical model that include all important parameters and loading cases occurring during excavation of the tunnel, lining construction, grouting and operational loading by internal and external water pressure
11. To give unique and effective method for design of the permeable pressure tunnel linings.

Today, plain concrete lined pressure tunnels are mostly pre-stressed by grouting. Different grouting methods are used: gap grouting methods by circumferentially installed grouting pipes or

radially set grout holes are the most common used. Grouting through radially set grout holes additionally increase the rock mass strength and stiffness, but also reduce the rock mass permeability. Reduced permeability of the rock mass gives possibility for additional effect that was up to now not used in the design of the lining. Relatively tight rock mass around the concrete lined tunnel reduces water losses and produces external water pressure that, as a contra-pressure, reduces the tensile stresses in the concrete lining. Including of the increased external water pressure (contra-pressure) caused by water seepage through the concrete lining in the design gives possibility to extend the applicability of the plain concrete lining and will allow estimation of the water losses through the concrete lining.

1.3 Research questions

- ~ Can PLAXIS 2D program be used as a tool for the design of plain concrete pressure tunnel?
- ~ What are the restrictions of the program in modeling of construction stages and operational loading of internal water pressure?
- ~ Can the program account water leaking out of tunnel lining to the surrounding rock mass?
- ~ Is there any correlation between the model output results and results from existing theories in terms of seepage flow through liner?
- ~ Can the functionality of plain concrete liner be improved?

1.4 Purpose of proposed work

1.4.1 Plain concrete lining design

The research will focus on plain concrete lined pressure tunnels where the internal water pressure is restricted by low tensile strength of concrete. The internal water pressure generates tensile stresses in the concrete lining and if the lining stress exceeds tensile strength cracks in the concrete occurs, resulting in reduced lining functionality.

Bearing of internal water pressure by plain concrete lined pressure tunnels is limited by the low tensile strength of concrete. Shrinkage of concrete and cooling of the lining by first filling causes a gap between the concrete linings and surrounding rock mass and therefore the surrounding rock mass cannot be included in the bearing of the internal pressure as shown in figure 2(a). The low pressure grouting reconstitutes the contact with the surrounding rock mass and increases the bearing capacity, but still the bearing capacity of plain concrete lining is limited see figure 2(b). The bearing capacity of the plain concrete lining can be considerably increased if the surrounding rock mass is radially grouted with high pressure grouting causing so called "pre-stressing" of the [mal concrete lining figure 2(c). Such lining system dependent on the tunnel geometry and rock mass characteristics can be loaded by the internal pressures of up to 20 bars. This design method (developed by Seeber, 1985) is mostly used for the plain concrete lined tunnels in Austria and by the pressure tunnels around the world designed by Austrian designers.

1.4.2 Cracked plain concrete lining with high pressure grouting

The maximal grouting pressure is limited by lining strength and the stress level in the surrounding rock mass. The limitation of the grouting pressure restricts the bearing capacity of the plain concrete lining under assumption that the lining must stay in compressive state - no tensile cracks in the lining. Of course the bearing capacity of the concrete lining can be extended in the tensile zone up to the tensile concrete strength. If the internal pressure results in stresses higher than tensile strength the cracks in the concrete cannot be excluded. Cracked concrete is not tight

anymore and water will leak out the tunnel. In case of tight rock mass the high pressure grouting will additionally decrease the rock mass permeability and seeped water will stay in the vicinity of the tunnel, increasing the ground water level around the tunnel. Such increased ground water acts as counter pressure on the lining and will reduce the crack width and water leak out.

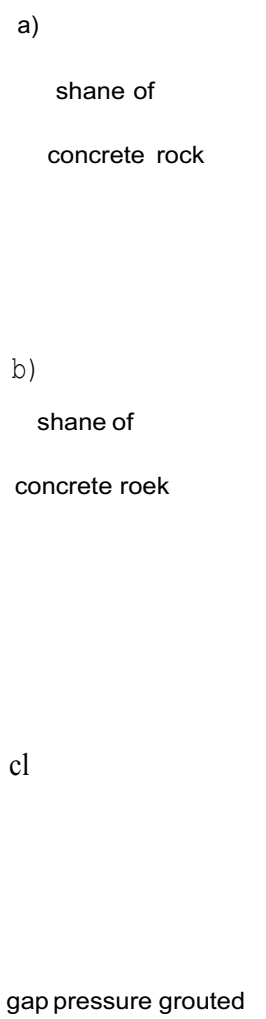

Figure 1.2: Effect of shrinkage, creep and temperature and internal pressure on a concrete lining
(a) Untreated (b) with simple grouting and (c) with pre-stressed grouting (Seeber, 1985)

1.5 Significance of the proposed work

Developed method can be used for design of plain concrete lining in case where standard plain concrete with high pressure grouting theory reaches its limits. In case of the good rock mass conditions and relatively tight rock mass the suggested method would extend the applicability of the plain concrete lining with pre-stressing and could reduce the length of much more expensive steel lined sections. Additionally, the method gives possibility to estimate the amount of lost - leaked out - water.

1.6 Research methodology

PLAXIS 2D Finite Element computer program for two dimensional coupled stress-seepage analyses is used for the research simulation. In the first project stage the simulation of different phenomena and loading (opening of the gap between lining, grouting, temperature changing, and seepage through the cracked concrete) is studied on small models. Finally, the partial results are summarized in the numerical simulation of excavation, construction and operation of the power tunnel. Calculation results is compared with the values collected from practical tunnel projects during calibration and validated using analytical design methods in case of seepage through cracked concrete lining.

1.7 Report layout

The thesis is structures as follows:

Chapter 2, *Background of study,* includes the basic concept of pressure tunnels. Different classifications of pressure tunnels are mentioned. It contains explanation on modes of failure in pressure tunnel, design approach for support systems, stresses around tunnel opening, seepage in tunnels, internal and external pressures, grouting techniques and different types of numerical methods used in tunnel design.

Chapter 3, *Design methods -Concrete lining,* shows specifically the existing analytical methods of designing pressure tunnel, their assumptions and design parameters. At the same time pointed out certain limitations peculiar to each method.

Chapter 4, *Model selection,* provides answers to the following questions: Why numerical modelling for tunnel design? Why PLAXIS 2D? Why Mohr-Coulomb's model for material modelling? Why plane strain condition? It also explains the salient features of PLAXIS 2D program.

Chapter 5, *Material and loading modelling,* includes the behaviour of rock and plain concrete as tunnelling materials. The relevance of the material behaviour to proper modelling of the materials as well as their interaction during construction and loading operation is presented. Nonetheless, a detail of how operational loadings are modelled is given.

Chapter 6, *Modelling considerations,* contains a step-by-step numerical design analysis of pressure tunnel. It shows simulations of construction stages and loading operation. It gives detail procedure of the model set-up, model testing and calibration, and simulation of loading cases during excavation phase, shotcrete lining installation, [mal lining installation, temperature and shrinkage effect of lining, decay of shotcrete, contact and consolidation grouting and finally, loading operation of internal water pressure.

Chapter 7, *Results and model calibration,* present simulation results both for construction stage and loading operation. The results of stresses and deformation in elements (using plastic and consolidation analyses), and results of seepage losses through cracked lining to the grouted zone (using groundwater flow analysis) are presented.

Chapter 8, *Discussion of results,* explain the result of model set up prior to calibration and relate the results to previous research work. Furthermore, the model calibration result using parametric analysis to simulate the 3D arching effect from 2D point of view. Explanation on how appropriate load reduction factor, {3 is selected for further simulation of construction stages and operation

loading. Step-by-step discussion of results for each construction stage as well as operational loading- internal water pressure is presented. The performance and accuracy of the model results are tested by comparing the model results with results of existing tunnel and with analytical solutions.

Chapter 9, *Conclusions and Recommendations,* gives the overall assessment ofPLAXIS 2D [mite element program as tool for design of pressure tunnels and recommendations for further research.

2 Background of study

2.1 Pressure tunnel

The term "pressure tunnel" in the general sense incorporates all hollow spaces, aligned along an axis and surrounded by rock, which conveyance water under pressure. It is an underground hydraulic structure built for water conveyance, either for hydropower, fresh water transport, or flood control. They take their name due to the fact that; the flow rate is always exceeding the capacity of the tunnels under free flow conditions and flow in tunnel is pressurized and mostly submitted to high water pressures pointing outwards the tunnel (USACE, 1997). The pressure tunnels can be classified in different categories.

2.1.1 Classification of pressure tunnels according to the head above its crown

According to Mosonyi, (1991) pressure tunnels are used at high-head installation oflow capacity. This implies that at a small discharge, water can be conveyed from the dam to the power house through a tunnel. Tunnels are thereby classified according to the height above the crown of the tunnel.

Low - pressure tunnel

Pressure tunnel falls under this category when the head above its crown is less than S meters ($y < Sm$).

Medium - pressure tunnel

Pressure tunnels with head between the ranges of Sm to 100m are categorized into this group.

High - pressure tunnel

Pressure tunnels with hydraulic head of greater than 100 m are referred to as high pressure tunnels.

Figure 2.1: Tunnel classification according to head above its crown.

2.1.2 Classification of pressure tunnels based on ground characteristics

Hendron, et al, (1987) and Fernandez, (1994) mentioned that the design decision if any section or the entire tunnel alignment should be left unlined or lined depends on the modes of failure and rock mass characteristics. The various modes of failure need to be evaluated. These potential modes of failure are mentioned in (section 2.1.4.1 and 2.1.4.2). In addition, (Hartmaier, 1998) mentioned clearly that confinement criteria must be checked and this is in line with the first step of the flow chart for the design of power waterway by (Marence, 2009) in figure 1.1.

According to (Benson, 1989) the confinement criteria calculations are governed by the following equation:

$$h_r = \frac{1 \cdot 3 h_w - h_s \gamma_s}{\gamma_r} \qquad (2.1a)$$

hs and *Ys* are overburden height of soil and unit weight of soil respectively. Where there is no soil cover, *hs Ys* = 0

Marence, (2009) defmed the factor of safety (FOS) for confmement criteria:

$$FOS = \frac{(Tmin,rock \sim yrhrko}{(Tmax(pi) \quad Ywhw} \qquad (2.1b)$$

where *(Jmax(pi)* is the maximum stress outside the tunnel caused by leakage water;

Yr and Yw are unit weights of rock and water respectively;

h; is the overburden height of rock (without soil overburden) and *hw* maximum static head;

ko is the ratio between minimum and maximum in-situ primary state of stress.

2.1.2.1 Unlined pressure tunnels

A pressure tunnel can be unlined if hydraulic confmement criteria is met - the minimum principal stress must be greater than the hydrostatic head (see figure 1.1). Additionally, the rock mass must be stiff strong, durable and impermeable enough and resistant to erosion and slaking (Benson, 1989, Hartmaier, et al., 1998, Pietro, 2008 and Marence, 2008). A tunnel can be unlined without significant risk if the probability of any of these modes of failure is low to nonexistent. It can be used in various geological environments if the following conditions are met:

- ~ The materials around the opening are of good quality, the rock is self supporting not liable to dissolution, erosion and substantial reduction in strength;
- ~ The permeability of surrounding rock mass around the opening is low. In case where the permeability of the rock mass is higher, the groundwater level above the tunnel should be equal to or exceeds the water head inside the tunnel;
- ~ The hydraulic pressures required to induce hydro-fracturing are larger than the internal pressures. A safety factor of 1.3 and 1.1 are recommended for static water pressure and dynamic surging conditions respectively;

Along the section of the tunnel alignment where these requirements are not met, a liner is required. The lining is usually cost competitive and time consuming. However, the lining provides a relatively watertight and hydraulically smooth inside surface (Benson, 1989 and USACE, 1997).

2.1.2.2 Lined pressure tunnels

Lined tunnels are the tunnels with concrete lining or tightened elements. If ground satisfies both confmement and Walch's border criterion - external ground water greater than the maximum internal water pressure, a concrete lining can be used. This can either be plain or unreinforced concrete lining with high pressure grouting or reinforced concrete lining. In most of such cases the lining cannot be classified as tight (due construction joints, cracks, imperfection, e.t.c.) and confmement criteria must be satisfied. Any portion of the tunnel where the confmement criteria is unsatisfied requires a tight tunnel lining. The element either is plastic foil, fibre glass or thin steel lining must be used to isolate the water in the pressure tunnel from the surrounding rock (Benson, 1989 and Marence, 2009).

2.1.3 Classification of pressure tunnels based on construction material and leakages

According to (Benson, 1989) linings can be classified into three groups namely pervious, semi-pervious and impervious. A full circular lining is expected to be capable of resisting external

loads, suitable to take internal pressure and protect the rock against the agressivity of conveyed water.

2.1.3.1 Pervious linings

These consist of shotcrete, also known as sprayed concrete and concrete lining without reinforcement (Benson, 1989). They are considered as pervious because they are characterised by local pervious zone due shrinkage cracks or placement imperfections that have occurred during curing. They can also easily cracked under internal pressure where the rock mass is less resistant and leakage occur through the cracks (Benson, 1989 and Alun, 2009).

2.1.3.2 Semi-pervious linings

By semi-pervious lining, also called technically tight lining, the lining is not absolutely tight but leakage out of tunnel is in order of allowable with respect to the rock mass and energy losses. They are reinforced concrete linings, more ductile than plain concrete. The ductility increases with the percentage of steel reinforcement. The reinforcement will distribute and control the cracks to a specific width. The cracks are much thinner and (better distributed) than in plain concrete lining. The leakage through numerous thin cracks in reinforced concrete lining with 0.1 - 0.3mm widths is one to two order magnitude less than through a single 5mm crack in plain concrete lining. This is because water loss is proportional to the third power of the crack width (Hendron, et al, 1987and Fernandez, 1994).

A plain concrete lining with high pressure grouting called prestressing can reduce the tensile stresses in the lining thereby reducing the permeability of the surrounding rock. Hence, prevent or reduced minimally the water loss from the tunnel to the surrounding rock. In case reinforcement bars are required, it has to be provided both radially and longitudinally to take care of shrinkage crack and tensile stress due internal water pressure respectively (Schleiss, 1997).

2.1.3.3 Impervious linings

Impervious linings are the lining systems that do not allow water to enter or pass through, for example, an impervious seal - steel or plastic. A composite liner of thin steel and an inside layer of concrete is also considered as impermeable provided that the grout-hole caps are sealed rightly (Benson, 1989). Steel liners are used at the powerhouse end of pressure tunnel where hydraulic pressures are high and the rock cover often low. Impervious linings provide buckling resistance against external pressure and are often used along the tunnel alignment in areas of permeable ground, water-sensitive rocks and low cover that are susceptible to unacceptable water losses (Benson, 1989).

2.1.4 Potential modes of failure of pressure tunnels

In the past there have been several cases where performance of pressure tunnels on hydroelectric projects has been unsatisfactory (Hendron, et al, 1987). It is useful to recognize and understand the difference between modes of failure that occur during construction and the failures that occurs during the operating life of pressure tunnels. A couple of failure mechanisms noted during construction stage if not controlled, might be present throughout the operating life. Nonetheless, understanding of the failure mechanisms is helpful in preparing for design work (USACE, 1997).

2.1.4.1 Modes of failure during construction

Failure modes are types of behavior that could be considered unacceptable in terms of hazard, risk to cost or schedule during construction, environmental effect, or long-term loss of production (USACE, 1997). The most common modes of failures observed in pressurized tunnels during

construction stage as described by (USACE, 1997) are failures controlled by discontinuities, rock failures affected by stresses and or mineralogy, and effect of groundwater.

2.1.4.2 Failure modes during operation

Most of the modes of failure during excavation, discussed in section 2.1.4.1, once properly handled, will pose no further treatment. However, if some of the conditions are not properly handled, they will affect the long term performance of the tunnels. The common modes of failures observed in pressure tunnels during operation according to (Hendron et al, 1987, Fernandez, 1994 and USACE, 1997) are excessive leakage, excessive pore-water pressure, failure of linings and collapse of openings.

2.2 Fundamental approach to ground support design

USACE, (1997) stated that underground design must achieve functionality, stability, and safety of the underground openings during and after construction and for as the entire design life of the underground structure.

There is no recognized standard, practice, or code for the design of underground structures. Designers often apply codes such as American Concrete Institute (ACI) Codes and Practices for concrete design (Sinha, 1989 and USACE, 1997). In Nigeria and some parts of Africa, British Standard (BS) 8110: Codes of practice for concrete design (part 1 and 2) combined with BS 8007: Code of practice for design of concrete structures for retaining aqueous liquids is mostly used. These codes were developed for structures above ground, not for underground structures. However, few parts of these codes apply to underground structures. Based on the above limitations, designers always approach tunnel design by searching for modes of failure that can be analyzed.

2.2.1 Layout design of pressure tunnels

As a result of intolerably high percentage of pressure tunnel failures and the cost of these failures, there is need to review the key decisions which are made in the design of a pressure tunnel as well as the technical basis for making these decisions (Hendron et al, 1987). In principle, realistic modes of behaviour or failure must be defmed (USACE, 1997). In addition, (Marence, 2008) mentioned the design of pressure tunnels as a complex decision-making procedure and suggested that technical basis has to be clearly specified and defmed. The key decisions which have to be made in the design of pressure tunnels are:

- horizontal and vertical alignment with respect to topography and existing groundwater levels,
- starting point and length of steel-lined section,
- length of the pressure tunnel which can be unlined or shotcrete lined,
- length of the tunnel which requires a plain concrete liner,
- length of the tunnel which requires a reinforced concrete liner,
- defmition of function and extent of contact and consolidation grouting,
- provision of specifications which allow flexibility in case of different conditions encountered during construction (Marence, 2008).

2.2.2 Basic design procedure in pressure tunnels

The fundamental steps in the design of pressure tunnel are outlined thus:

- The functional requirements such as hydraulics and geometric, ancillary and environmental, limitations, logistics, and maintenance requirements are defmed in broad sense (USACE, 1997).
- Collection of geologic, hydro-geologic and operational data including all information required to defme potential failure modes and analyze them. Field and laboratory data, and cultural data to defme environmental effect and constraints should be collected (Marence, 2008).
- Determination of convincing and possible failure modes including construction events, unsatisfactory long term performance, and failure to meet environmental requirements is required. Typical examples include instability problems or groundwater interruption during construction (USACE, 1997). Leakage criterion and settlements that may cause distress to adjacent existing structures should be considered. Also, the lining has to satisfy the structural, confmement and leakage criteria (Marence, 2008).
- Design of initial and fmal ground supports; Initial support encompasses all systems that are used to maintain a stable, safe opening during construction. Final supports are those systems needed to maintain a functional opening for the design life of the project (USACE, 1997). Initial support may be a part of the fmal supports or may be the final support, for example, precast segmental liner installed behind TBM.

2.3 Tunnel excavation methods

Today tunnels are mostly excavated continuously by the Tunnel Boring Machine (TBM) or in cycles by New Austrian Tunnelling Method (NATM) or so called Drill and Blast (DB) method.

2.3.1 Tunnel Boring Machine (TBM) excavation

Excavation with full face "Tunnel Boring Machine (TBM) " is mostly in use in recent transportation, irrigation and energy projects because it is fast, more economical and efficient compared to the analytical tunnel drill methods where classical drill-blast and small diameter mechanical excavators are used (Dimitrios, 2005). It has the advantage of higher advance rates, continuous operations, less rock damage, less support requirements and potential for remote, automated operations. However, higher capital cost, limited flexibility in response to extremes geological conditions are its main disadvantage (USACE, 1997 and Dimitrios, 2005). Tunnel excavated by TBM have circular cross section that is advantageous for pressure tunnels allowing construction with the same lining thickness and therefore stress level similar to the analytical solution. Excavation by TBM has been used in many projects with performance achievements in about 630 projects in early 1990's. One of recent construction that employed the use ofTBM is the ErmenekiTurkeypressure tunnel with length of 8028m and 6.60 m external diameter.

2.3.2 The New Austrian Tunneling Method (NATM)

The NA~ is a method for an underground structure which allows host ground surrounding excavation as an integral part of support structure. This implies that the host ground and the external support structure together take the full load. It saves costs of external support systems because the ground take part of the load and the support takes the remaining part of the ground load (Sinha, 1989 and Dimitrios, 2005).

2.4 Design of plain concrete pressure tunnel

Basically, the design can be divided into excavation, primary support, fmallinings and operational loading.

2.4.1 Design of excavation of underground tunnel

The underground excavation and use of support system is an interaction between ground properties and the selected excavation method in a stipulated period of time (Marence, 2003). The design is mostly started with defmition of the region of similar characteristics called homogenous regions. The geo-mechanical significant parameters and their characteristics have to be defmed for these regions (Marence, 2003). The groundwater information, primary state of stress and other specific parameters need to be included in the design. For each homogenous region strength and stiffness (elastic, plastic, rheological) parameters of the rock mass should be defmed (Marence, 2003,2005).

2.4.2 Design of primary support

One of the functions of primary support is to absorb the rock pressure before the fmal lining is installed (Seeber, 1984). Initial ground support is always installed shortly after excavation. The support system and measures (shotcrete, rock bolts, etc.) depend on the rock mass characteristics, expected failure mechanism but also on the excavation method (USACE, 1997).

The basic methodologies employed in the selection of primary ground support are highlighted in the manual USACE, 1997. The primary support system and excavation phases go hand in hand. The phase is an iterative design process where the selected excavation and support system is proved by applicable analytical and numerical methods (Marence, 2003).

2.4.3 Design of permanent, concrete linings

Most tunnels and shaft in rock are provided with a fmal lining. The required concrete lining for tunnels must be designed to meet functional criteria for water tightness, hydraulic smoothness, strength, durability, temperature change, appearance and, internal and external loads. Therefore, the liner must be designed for interaction with the rock mass and the hydrologic regime in the rock. The design should also consider constructability and economy (USACE, 1997 and Dimitrios, 2005).

The thickness of liner is determined from practical constructability point of view rather than structural requirements. The minimum practical lining thickness of 20 cm is recommended. However, thickness of 30 em or more is often used. "A 28-day compressive strength of 21 MPa and water cement ratio of 0.45 is satisfactory for most underground work" (USACE, 1997). Nevertheless, higher strengths up to 35 MPa may be adequate to achieve thinner lining, abrasion resistance or better durability or a higher modulus (Dimitrios, 2005). Lining reduces the flow surface roughness and protect the surrounding rock from scour by high velocity (Kang, 2009).

2.5 Materials for construction

2.5.1 Rock

The understanding of rock mass response to the construction of tunnel is important in assessing opening stability and the requirements for opening support. Even though several approaches of varying complexity being developed to assist designer to understand rock mass response, still the methods cannot take all aspects of rock response into consideration (USACE, 1997). Although, the methods are still helpful in quantifying rock response as well as providing guidance in support design.

The general concepts in rock analysis are the rational methods of design. The rational methods of design are based on theories of elasticity and plasticity and are applied through the concepts of stress and strain (Sinha, 1989, USACE, 1997, and Dimitrios 2005). These concepts have been discussed in detail in section 2.7 with special consideration to the non-linear elastoplastic Mohr-Coulomb model as a rock behaviour approximation (see chapter 4).

2.5.1.1 Rock strength

The strength of rock is characterised by friction and cohesion. The latter is connected with compression of the rock. Rock material is usually strong in compression where shear failure can occur and weak in tension (Dimitrios, 2005). Failure can occur when the induced stresses exceeded the maximum stress which the material can withstand or when the induced strains exceed the maximum strain which the material can withstand (Sinha, 1989). Rock exhibits brittle type behaviour when it is unconfined, but become more ductile (plastic) as the level of confinement increases (USACE, 1997 and Dimtrios, 2005).

The unconfined compressive strength is the geotechnical parameter often used to characterise the mechanical behaviour of rock (USACE, 1997). The tensile strength is less significant parameter for underground stability as compared to compressive strength. It is so low that when rock is in tension, it splits and the tensile stresses are of no concern (USACE, 1997, Hudson and Harrison, 2000 and Dirnitrios, 2005). As a rule of thumb, the compressive strength, σ_c of rock is about ten to twelve times the tensile strength, σ_t is only be true for a particular value of the friction angle (figure 2.2).

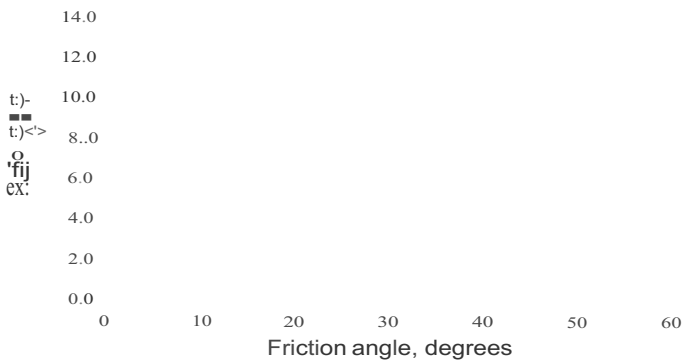

Figure 2.2: Relationship between Compressive strength and tensile strength of rock material *(Source: Hudson and Harrison, 2000).*

2.5.2 Shotcrete

Shotcrete is a concrete structure, functions as a primary support to stabilize the excavation. It is expected to carry the loads exerted by the surrounding rock mass (as a temporary lining). If found sufficient enough, a fmal lining can be neglected, then it is a very adaptable material when the tunnel is subjected to internal pressure (Dimitrios, 2005). Shotcrete improve the hydraulic efficiency (i.e. reduce roughness) and also prevent erosion of rock materials. It is mostly used in rock conditions and can also be used in conjunction with rock bolts. When it is used to improve the smoothness of tunnels; a Manning roughness value between 0.018 and 0.025 can be adopted depending on the thickness and contouring to be achieved (Brekke and Ripley, 1985, and Benson, 1989).

2.5.3 Rock bolts.

Rock just like concrete is strong in compression but weak in tension. Hence, rock reinforcement (for example rock bolt) enhances the performance of rock mass as a tunnel construction material by pinning individual loose blocks or as a support for unlined tunnels. It is proven that rock bolts ensures stability of excavation by the functions it rendered.

Sinha, (1989) and Dimitrios, (2005) mentioned the functions of rock bolts which include: controls of deformation around the rock mass towards excavation opening; counteracts the loosening of strata; stiffens the roof of excavation resulting in increase in bearing capacity of the roof; increase frictional forces on the discontinuities of rock mass as well as increases shear strength.

2.5.4 Concrete linings

Concrete lining needs formwork and is not practicable for primary support. Concrete lining is the most effective method to ensure stability while achieving a hydraulically efficiency tunnel. The main idea is that the applied load on shotcrete lining initially are reduced due to arching effect but then slowly increase (Dimitrios, 2005). More so, it is believed that shotcrete lining decays with time and hence, an inner lining of cast concrete is required (Dimitrios, 2005). The ideas are subject to confirmation, but there is no doubt that the inner lining will increase the safety of tunnels.

As for the construction, good design mix and construction techniques are essential while a construction method that provides homogenous concrete is needed. Nevertheless, the lining is still considered as pervious because of unavoidable imperfections and variable deformability of most rocks. Concrete liners must be considered by designers to be pervious or semi-pervious membranes because of cracks due to shrinkage and tensile stress from internal pressure (Benson, 1989, USACE, 1997 and Marence, 2009).

2.6 Properties of materials

In order to simulate the behaviour of ground and the associated structures, a suitable ground model and necessary material parameters must be assigned to the geometry. Different types of structures have different parameters and therefore different types of data are required. The properties of rocks and concrete materials used in the design of plain concrete pressure tunnels as discussed as follows:

2.6.1 Ground properties

The mechanical properties rock is worthwhile mentioning in order to understand how rock behaves. The properties of rock that defme the parameters of the ground in model are explained the sub-sections below.

2.6.1.1 Ground (bulk) unit weight *(y)*

This is the ratio of total weight to the total volume, i.e.:

$$\Upsilon = \frac{W}{\forall} = \frac{Mg}{\forall} = \rho g \qquad (2.2)$$

Where bulk density (ρ) is the ratio of total mass to the total volume of ground element.

The bulk unit weight depends on the type of rock, its porosity and the geological processes that take place in it. The igneous and metamorphic rocks have high unit weight as shown in table 2.1 while in sedimentary rocks the unit weights is lower but with larger range of variation see table 2.2

2.6.1.2 Porosity (n)

It is feature of rock and could be defmed as the ratio of volume of voids to the total volume of the rock sample and saturation, S is the ratio of free water volume to void volume (Vahid, 2010).

$$n = dV_v / dV \qquad S = dV_w / dV_v \qquad (2.3)$$

It may also be defmed in term of void ratio (Craig, 1992):

(2.4)

Where e and dV are void ratio and volume of solid sample respectively.

Tabl 2 1 B lk it . ht f i d t k

Granite and granite -gneiss	27	24-30
Granodiorite	27	24-28
Syenite	28	26-29
Diorite	28	27-29
Diabase, gabbro	29	27-33
Andesite	26	25-28
Basalt	30	26-33
Dunite,peridotite,pyroxenite	32	28-36
Serpentinite	26	24-30
Amphibolite	29	27-32
Gneiss	27	26-32
Ferruginous quartzite	25	32-43
Marble	27	23-30
Schist	26	25-28

(Source: Kazimierz, 1987).

	21	20-24	2-42
Loam	23	16-28	1-63
Gravel	15	14-17	33-55
Sandstone	23	21-28	0-55
Marl	22	20-26	2-31
Limestone, dolomite	25	21-29	1-37
Chalk	22	18-25	17-43
Anhydrite	28	24-30	0-5
Gypsum	23	21-25	0-5

(Source: Kazimierz, 1987).

2.6.1.3 Permeability *(k)*

The permeability of rock can be estimated from Darcy's law which defines the relationship between the flow rates of water through a porous media under hydraulic gradient.

$$q = AKi \qquad (2.5)$$

Where q = volume of water flowing per unit time; i = hydraulic gradient

A = cross - sectional area of the soil corresponding to the flow q;

K = coefficient of permeability measured in (m/s)

The coefficient K depends on the properties of the rock medium and on the physical properties such as unit weight, temperature and viscosity. In order to describe how water flow in a rock medium regardless of the physical properties of the fluid, the permeability coefficient k is used (Dimitrios, 2005). The unit for the coefficient k is darcy. The coefficients are connected by the general relationship:

$$K = k\frac{\gamma_s}{\eta} \qquad (2.6)$$

where γ_s is the unit weight of the seeping water and η is the dynamic viscosity of the water.

		0.1	0.7×10^{-4}
Sandstone:		0.2	0.6×10^{-3}
Carboniferous	$(0.29 - 6.0) \times 10^{-11}$	0.4	0.5×10^{-2}
Devonian	$(0.21 - 2.0) \times 10^{-11}$	0.7	2.5×10^{-2}
Granites	$(0.50 - 2.0) \times 10^{-10}$	1.0	0.7×10^{-1}
Schists	$(0.70 - 1.6) \times 10^{-10}$	2.0	0.6
Limestone	$(0.29 - 6.0) \times 10^{-9}$	4.0	0.5×10^{1}
Dolomites	$(0.50 - 1.2) \times 10^{-8}$	6.0	1.6×10^{1}

(Source: Kazimierz, 1987)

According to Kazimierz, (1987) the permeability of rock is lower than that of the rock mass because of low porosity and mostly not connected hollows, this is shown in Table 2.3 which provides a comparison of values of permeability coefficients in rock and rock mass.

	10 - 10-
Limestone	< 10-7
Hard coal	10-6 - 10-4
Magmatic and metamorphic rocks	10-12 - 10-11

(Source: Dimitrios, 2005)

2.6.1.4 Modulus of Elasticity (£)

Modulus of elasticity is defmed as the ratio of uniaxial stress to the corresponding unit longitudinal strain, elastic and reversible (during unloading). Table 2.4 gives approximate values of elastic moduli for typical rocks.

$$E = \frac{Uniaxial\ stress}{Uniaxial\ strain}$$

$$E = \frac{u_y}{\varepsilon_e} \qquad (2.7)$$

Table 2.4: Elastic moduli

Granite	2 - 6 x 104
Microgranite	3 - 8 x 104
Syenite	6 - 8 x 104
Diorite	7 -10 x 104
Dolerite	8 - 11 x 104
Gabbro	7 - 11 x 104
Basalt	6 - 10 x 104
Sandstone	0.5 - 8 x 104
Shale	1 - 3.5 x 104
Mudstone	2 - 5 x 104
Limestone	1 - 8 x 104
Dolomite	4 - 8.4 x 104
Coal	1 - 2 x 104

(Source: Kazimierz, 1987)

2.6.1.5 Poisson's ratio *(v)*

Poisson's ratio is the ratio of lateral strain to axial strain (figure 2.3).

$$v = \frac{lateral\ strain}{Axial\ strain} \qquad (2.8)$$

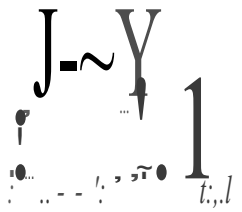

Figure 2.3: Strain on element of rock *(a)* axial strain, (b) lateral strain
(ModifiedHudson & Harrison, 1997)

2.6.1.6 Shear strength

According to (Dimitrios, 2005) the concept of shear strength is not precisely defmed but the shear deformation increases progressively in rock as the shear stresses increases. The shear strength of the rock mass resists deformation. **It** is a function of two parameters: Cohesion *(c)* and friction angle «({J) - described by (equation 2.9). The shear strength is a function of the normal stress on the plain of ground element as described by Mohr-Coulomb theory. Cohesion is the shear strength of the ground when normal stress is zero while ({J is equivalent to the angle of inclination of a surface sufficient to cause sliding of a layer block of similar material down the surface (Craig, 1992 and Dimitrios, 2005).

$$T = C + atarup \qquad (2.9)$$

The shear strength depends on the rock properties. These properties may be different for different ground layers making the ground parameters to vary from layer to layer. The range of variation of strength of some rocks is given in table 2.5

Granite	100-250	14-15	45-60
Diorite	180-300		
Dolerite	200-350	25-35	55-60
Gabbro	180-300		
Basalt	150-300	20-60	50-55
Sandstone	20-170	8-10	35-55
Shale	10-100	3-30	15-30
Limestone	30-250	10-50	35-50
Dolomite	80-250		
Coal	5-50		
Quartzite	150-300	10-60	50-60
Gneiss	50-200		
Marble	100-250	15-30	35-50
Slate	100-200		

(Source: Kazimierz, 1987)

2.6.2 Properties of a plain concrete.

The simple defmitions and/or explanations of concrete parameters are given below:

a) Modulus of elasticity, *Ee* - determined by subjecting concrete to a cube or cylindrical specimen to uniaxial compression and measuring deformation by means of dial gauge. The dial gauge reading divided by gauge length and applied load divided by cross sectional area of concrete give the respective strain and stress in the concrete. With series of reading being taken, stress - strain relationship is established. The graph is not always a straight line and the tangent of the curve is often used - tangent modulus (Shetty, 2005).
b) Poisson's ratio, *ve* - is the ratio between lateral strain to the longitudinal strain. It lies between 0.15 - 0.20 for normal concrete when actually determined from strain measurement.
c) Strength - the strength of a concrete is its resistance to rupture. It is often measured in a number of ways, such as strength in compression, in tension, in shear or flexure. All these are strength indicator with reference to a particular method of testing (Shetty, 2005).
d) Shrinkage - is the change in volume of concrete due to drying (a function of water - cement ratio), temperature change (known as thermal shrinkage) and lack of durability. It is often inducing cracks in concrete (Shetty, 2005).
e) Thermal coefficient, *a* - the effect of expansion and contraction of concrete when subjected to ambient increase or decrease in temperature and their effect on concrete cracking can be measured in terms of thermal shrinkage strainrs; = *a!J.T)* in concrete using thermal coefficient of concrete.

In computer programs, elastic parameters are often defmed together with lining geometrical characteristics. The parameters that define the plain concrete lining properties in model are:

(a) Normal stiffness *(EA)* - is required to estimate the deformation of concrete. It is given by modulus of elasticity and cross-sectional area of the member.

(b) Flexural rigidity *(El)* - is the product of modulus of elasticity and the second moment of area of the member.
(c) Others - other parameters are the thickness of the member, weight of member and Poisson's ratio.

2.7 Initial stress, stress and deformation fields around a deep tunnel

The behaviour of ground material instigates the behaviour of the overlying strata. Although ground modelling itself is an important issue, the modelling of structures as well as the interaction between the ground and structures are more common in researches and engineering projects. For instance, to understanding of behaviour of concrete as conduit in underground, one needs to understand the primary behaviour of concrete and that of the ground independently before interaction. These behaviours are function of the parameters that define the properties of the materials.

2.7.1 Stresses in ground materials

According to Hoek, et al, (1998) ground at depth is subjected to stresses resulting from weight of overlying strata (called the in-situ stresses). The magnitudes and directions of these in-situ stresses are very important in the underground excavation design. The stresses are analyzed in three dimensions.

2.7.2 Elastic strain

Elasticity is the simplest and most often applied theory relating stress and strain in a material. If the stress can be represented as function of deformation (see figure *2.7a),* then the material is elastic (Dimitrios, 2005). This implies that the history of deformation is irrelevant and accordingly remains unnoticed. In this theory, material is idealized as linear elastic, homogenous and isotropic -Hooke's law.

The lateral rock stress ratio is given by:

$$fCy) = k_o = VI\ 1 - V = (5YYI_{(5xx} \qquad (2.10)$$

The in-situ vertical stress is the stress due to the overlying rock and is given by:

(2.11)

where y represent the unit weight of the rock and y is the overburden depth. Generally, y lies between 20 and 30 kN/m3 (USACE, 1997) and (Dimitrios, 2005). According to USACE, (1997) for most rocks: $0.15 \sim v \sim 0.35$ and the value of ko lies between 0.2 and 0.55. As shown in figure *2.5a* from the conducted research and published results, the data shows that the vertical stresses measured in the field reasonably agree with equation 2.10.

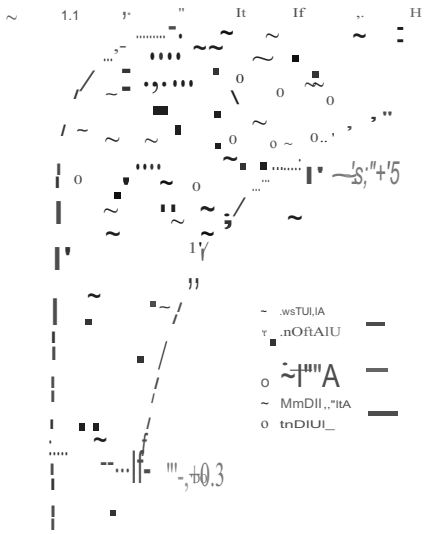

Figure 2.4a: Variation of *ko* with depth below surface *(Source: USACE,* 1997)

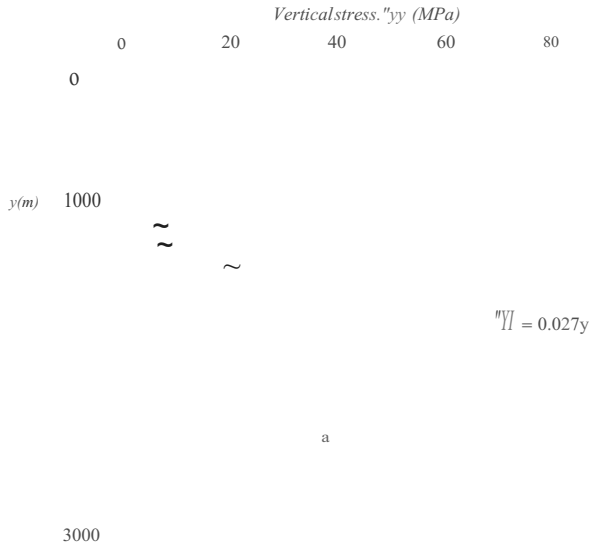

Figure 2.4b: vertical stress measurements around the world
(Source: Brown & Hoek, 1978, *and Hoek et al, 1998)*

However, *ko = v/(l - v)* in equation 2.10 is independent on the depth has been approved to be inaccurate by (Hoek et al, 1998 and USACE, 1997) as shown in figures *2.4a* and 2.4b.

It was found that *k.,* tends to be high in a shallow depth and decrease with depth which can be explained with geologically induced stresses in the lithosphere. In this regard, (Hoek, et al, 1998) recommends the simplified equation of obtaining the horizontal and vertical stress ratio proposed by Sheorey (figure 2.5). This equation is:

$$ko = 0.25 + 7Eh\ (0.001 + ;) \qquad (2.12)$$

Where *Eh* andy are deformation modulus and overburden depth respectively.

2.7.3 Non elastic material

A state of plastic is reached when the stresses in rock mass are sufficiently large that a failure zone develops around the tunnel. In that case, elasto-plastic analyses are required for stresses and strains analysis. However, the extent of the plastic zone surrounding around the opening is dependent on the rheology and the constitutive relationship of the surrounding rock mass (Sinha, 1989 and USACE, 1997). The plastic behavior of rock is characterized by irreversible deformations, meaning that the deformation remain after loading and unloading (Dimitrios, 2005). Figure 2.6 shows the fundamental of continuum-mechanical presentation of plastic behavior from one dimensional stress and strain point of view.

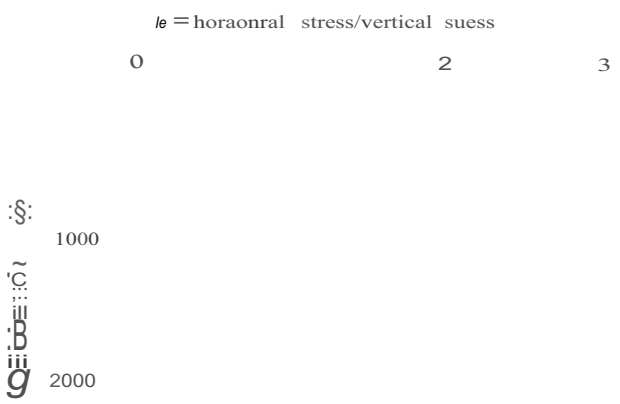

Figure 2.5: Ratio of horizontal to vertical stress for different modulii based on Sheorey's equation *(Source: Hoek et al, 1998).*

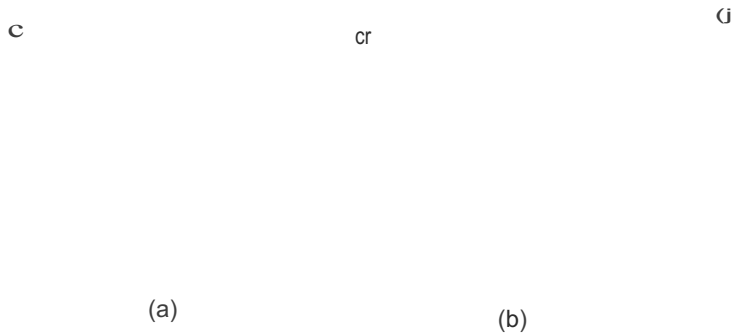

Figure 2.6: Rock material behaviours (a) linear elastic, (b) non linear elastic, (c) Plastic *(Source: Dimitrios, 2005).*

The concept of plastic behaviour in figure 2.6c can be distinguished as rigid elastic behaviour- as long as $\sigma < \sigma_e$. Ideal-plastic behaviour (figure 2.7 *a* and b) marked by plastic yield, smce deformation increases under constant stress. (Figure 2.7c) shows elastic - plastic hardening.

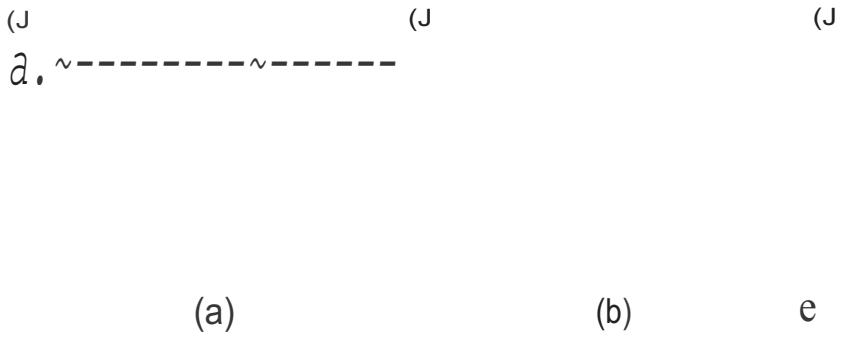

Figure 2.7: Various concepts of plastic behaviours *(Source: Dimitrios, 2005)*

2.7.4 Stress field around the tunnels

The usual encountered primary stress is $\sigma_{yy} = \gamma y$, $\sigma_{xx} = \sigma_{zz} = k_o \sigma_{yy}$. When an opening is created in the ground, the stress field is disturbed and there will be a redistribution of stresses in the rock surrounding the opening. The stress field around a tunnel has to fulfill the equations of equilibrium as well as the boundary condition at the ground surface ($y = 0$) and at the tunnel wall (Dimitrios, 2005). By simplifying the analytical solution with an assumption that the primary stress in the neighbourhood of tunnel (figure 2.8) as constant and not as linear increasing: $\sigma_y \sim \gamma y$, $\sigma_x \sim k\gamma y$. According to Dimitrios, (2005) the approximation is reasonable for deep tunnels ($y \gg r$).

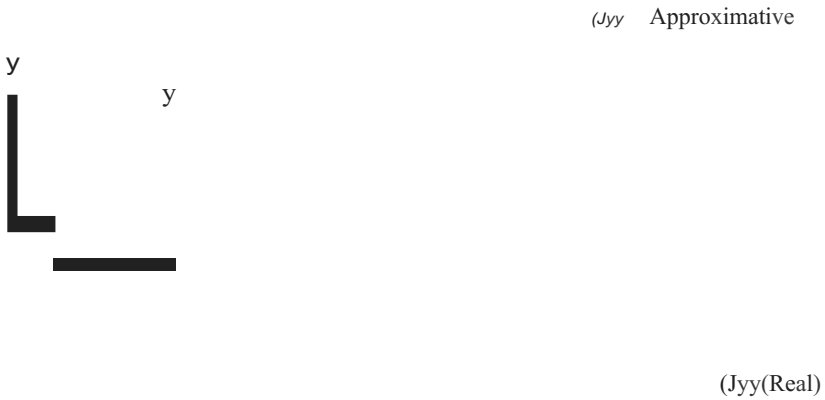

Figure 2.8: Distribution of vertical stress in the vicinity of a tunnel *(Dimitrios, 2005)*

The stress fields around the tunnel due to rock pressure and internal water pressure have been mathematically expressed by (Mosonyi, 1991 and Dimitrios, 2005) in polar form as follows:

$$arr = yH\left[\frac{1+ko}{2}\left(1-\frac{r_0^2}{r^2}\right)\right] + yH\left[\frac{1-ko}{2}\left(1+3\frac{r_0^4}{r^4}-4\frac{r_0^2}{r^2}\right)\cos 2\theta\right] \quad (2.13a)$$

$$a\theta\theta = yH\left[\frac{1+ko}{2}\left(1+\frac{r_0^2}{r^2}\right)\right] - yH\left[\frac{1-ko}{2}\left(1+3\frac{r_0^4}{r^4}\right)\cos 2\theta\right] \quad (2.13b)$$

$$ar\theta = -yH\frac{1-ko}{2}\left(1-3\frac{r_0^4}{r^4}+2\frac{r_0^2}{r^2}\right)\sin 2\theta \quad (2.13c)$$

where, a_{rr} is the radial stress

$a_{\theta\theta}$ is the circumferential (tangential) stress

$ar\theta$ is shear stress components

r_0 and r are radius of the tunnel and external radius to the rock zone respectively

Mosonyi (1991) showed that in the absence of internal load, the tangential stress is given by:

$$aee = \frac{1}{2}yH[2(1+ko) - 4(1-ko)\cos 2\theta] \quad (2.14)$$

At the crown or invert of the tunnel, $\theta = 0$ and π: Also at the sides of the tunnel, $\theta = \frac{\pi}{2}$ and $\frac{3\pi}{2}$

Therefore, the corresponding tangential stresses are:

$$aeeCcrestjinvert) = yH[3ko - 1] \quad (2.15)$$

and

$$aeeCside) = yH[3 - ko] \quad (2.16)$$

However, in the presence of internal pressure Pi, the tangential stress is a tension of magnitude equal to the internal pressure all along the perimeter of the tunnel and it is given by:

$$aeeCcrestorinvert) = yH[3ko - 1] - (Pi\ rofr \quad (2.17)$$

(2.18)

where (is a load factor.

2.8 Internal and external water pressure

The design of linings of pressure tunnels are based only on the internal pressure except for the steel linings which are also designed based on external pressure because of their imperviousness. The use of internal water pressure for lining calculation becomes more significant in rocks of good quality. However, the natural stresses in poor rock mass exerts load that counteract the internal pressure in the headrace tunnels. This is referred to as prestressing force or pressure relief (Seeber, 1985).

Figure 2.9: Static water pressure *(Source: Marence, 2010)*

The analysis and design of circular concrete lined rock tunnels based on internal pressure require consideration of rock-structure interaction as well as leakage control (USACE, 1997). The rock pressure must be absorbed by the primary lining (for example shotcrete) before the installation of the inner lining. The only external pressure that needs to be incorporated into the design of lining is the groundwater pressure. This is considered as a pressure relief but the seasonal variation must be taken into account especially where the groundwater pressure is found to be higher than the turbine water pressure (Seeber, 1985 and Mosonyi, 1991).
The internal pressure for design of power waterway must include surge pressure during operations and emergency shutdowns. The internal design pressure head may be in range of up to 200 percent of the normal static head (Sinha, 1989) and in usual cases up to maximum of 150 percent as shown in figure 2.9 and 2.10 for static and dynamic water pressure respectively.

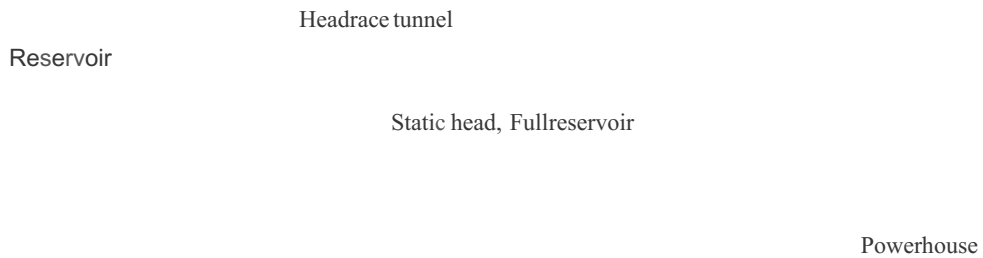

Figure 2.10: Dynamic water pressure *(Source: Marence, 2010)*

2.9 Grouting techniques

Grouting is performed to improve the engineering properties of rock. These properties are reduction in permeability and increase in stiffness and strength of rock mass (Seeber, 1984, Benson, 1989, Kazimierz, 1989, and Marence, 2005). According to (Seeber, 1984 and Schleiss, 1987), the cooling and shrinkage after concreting often result into stresses and deformation which produces contraction in concrete lining. The contraction, hence, detaches the lining from the rock mass and form a gap. A grout is required to fill on one hand the gap lining-rock and on the other hand fractures and large pores in the rock masses (Schleiss, 1986, Marence, 2005 and Marence et al, 2009).

Grouting is often performed in two steps: contact grouting and consolidation grouting (Seeber, 1984, Benson, 1989 and Marence, 2005). Contact grouting fills the contact between the lining and surrounding rock in the tunnel crown. The gap formation at the crown is as a result of self weight deformations and shrinkage of the concrete liner. The grout is usually performed with low pressure 2-3 bars in the crown (USACE, 1997 and Marence, 2005). With consolidation grouting, a continuous contact between the lining and surrounding rock mass is reconstituted after shrinkage of the lining by drying concrete and also cooling of the lining by water during filling of the system. Detail of consolidation grouting is explained by (Marence, 2005) and the injected grout results in the so-called pre-stressing effect on the lining (with pressure between 16-30bars). Consolidation grouting decreases rock mass permeability and increase shear strength and stiffness of the rock. Hence, increase the compressive strength of the concrete liner (Seeber, 1984, Benson, 1989, Kazimierz, 1989, and Marence, 2005).

2.10 Seepage in pressure tunnels

During loading operation of pressure tunnel, the internal water pressure results in expansion of the liner which then transfer part of the load to the surrounding rock. This is because of the compatibility of stresses and deformations between the lining and the ground provided there is a good connection at the contact between the liner and excavation (Seeber, 1984, Fernandez, 1994, Bobet and Nam, 2007).

Since the liner is pervious, there is seepage through the liner which can be neglected for technically tight tunnel (Marence, 2005). Seepage becomes more significant if cracks exist in the liner and water leak-out to the surrounding rock mass resulting in loss of energy (Hendron et al, 1987, Fernandez, 1994, Bobet and Nam, 2007, and Kang et al., 2009).

The respective equations for estimating the water pressure at any point in a cracked liner and the pressure gradient has given by (Kai Su and He-gao Wo, 2010) are:

$$P = \frac{Pl(R-rp)+P2(rp-r)}{R-r} \qquad (2.19)$$

$$\frac{dp}{dr} = \frac{P2-Pl}{R-r} \qquad (2.20)$$

Where P_J and $P2$ are inner and outer liner pressures respectively

and rand R are the corresponding radii (figure 2.11).

Figure 2.11: Loads on lining

After cracking, the concrete material become anisotropic whose permeability in the radial direction is much more than in the other direction (Kang, 2009). Kai Su and He-gao Wo, (2010) obtains the permeability of element with radial cracks from cubic law of percolation and it is given as:

$$Kc2 = \frac{JL}{127]} (0.5w\sim ax) \quad (2.21)$$

where g is acceleration due to gravity; n is kinematic viscosity of water and w_{max} is the max crack width in concrete.

According to Bobet and Nam, (2007), the leak -out or flow loss per unit length from the pressure tunnel into the ground through liner is given by:

$$Q_c = \frac{2n:r1Kc2}{d} (P! - Po) \quad (2.22)$$

The equation (2.22) is based under the assumptions that support takes the load from water pressure only; that the internal water pressure *(Pi)* is constant along the tunnel perimeter and that the hydraulic pressure *(Po)* build up behind the liner is constant along the perimeter of the liner-ground interface.

2.11 Numerical methods

Analytical solution are only possible under simplified boundary conditions (isotropic materials, hydrostatic state of stress, circular tunnel etc.) and therefore very restrictive. For this reason, numerical methods are used as they can handle large system of equations and complex conditions; for example non-linearity of materials, complicated geometries and loading that are common in engineering practice.

Numerical methods are techniques by which physical problems are formulated in mathematical manner so that they can be solved with arithmetic operation. They provide transition from the physical model to a mathematical algorithm that can be programmed to give solution to problems in the form of numbers or graphs (Kreyszig, 2006). According to (Gregoire, 2007), they are very useful because sometimes experiments are impossible. Additionally, numerical simulations are cheaper or faster. It allows us to calculate the solutions of these models on a computer by simulating different phenomena, and therefore to compare to physical reality. However, it should not be expected that simplified representation converts input to the exact output result, errors are inevitable and actual values of the output variables are uncertain (Popescu, 2010). Figure 2.12 shows the modified numerical methods and models for tunnel engineering. Each method involves a discretization of the problem domain, which is simplified by computer-aided analysis.

Numerical analysis (also known as numerical simulation) aims to predict or explains observed phenomena (Marence, 1996). By means of prediction, the analysis is used to assess the safety and to optimize the construction. It is tried to improve the understanding of system, to adjust the involved parameters and to analyze failures (Dimitrios, 2005). The analysis of stresses and strains, different geometrical shapes of tunnel openings and complex geological environment require discretization of elements and materials. ABAQUS, ADINA ANSYS, FLAC, PHASE2 and FINAL among many others are computer programs often used for numerical simulation of tunnel excavation and operational stages (Marence, 2008).

Figure 2.12 Numerical methods and models for tunnel engineering *(Modified Shina, 1989)*

2.12 Finite Element Method (FEM)

According to (Sinha, 1989, Dimitrios, 2005 and Marence, 2008) "the finite element method represent the most versatile and complex group of computational methods used for tunnel engineering and its application nowadays is becoming a standard in tunneling". FEM is a flexible and powerful method that allows the main body of a structure to discretize into an assemblage of elements of smaller dimensions. The small elements are connected to the neighbouring elements at the common points called nodes. The displacement under a system of loading determined at node points is used to find the displacements at any other point in the interior of the elements. The discretization allows coupling of different physical phenomena in one model. The use of numerical methods - FEM, seems promising solution for optimum and economic design of pressure tunnels (Ahmadi et. al, 2007). Finite element program PLAXIS-2D is selected as an experimental tool numerical design of pressure tunnels. The program will be put to test and its restriction highlighted as far as pressure tunnel design is concerned.

3 Design methods - Concrete lining

3.1 The plain, unreinforced concrete lining

Unreinforced concrete lining is the most economic fmal lining adapted only for tunnels where small tensile stresses in lining occurs during operation. The main loading for the pressure tunnel is the internal water pressure - hydrostatic and hydrodynamic loads caused by maintenance of turbines and valves. The internal water pressure causes tensile forces in the lining as a result of the low tensile strength of concrete. This loading is quite unfavourable and hence, a special treatment is required to reduce the tensile forces. Prestressing the rock mass has been found to increase the lining resistance based on experience and analytical solutions.

This chapter describes the analytical methods (such as Seeber, Singh and Schleiss and USACE theories) of analyzing stresses, strains and deformation in rock mass as well as deformation in lining under different loading conditions. The effect of seepage as a result of leak-out from cracked liner and the relief in tensile stress in the lining owing change in permeability of the liner and the effect on the surrounding rock mass is taken into consideration according to Schleiss.

3.2 Consideration of analytical methods used for concrete lining design

Most of the analytical methods used in the design of linings are based on practical experience on modes of failure pressure tunnels. The methods described below gives a simple design procedure for calculating lining requirements: the optimal wall thickness; the required prestressing and allowable injection pressure for a given natural rock and stress condition; an estimate of number of cracks in the lining; the maximum internal pressure that can result into cracking and the amount of water leaked from the tunnel.

3.2.1 Seeber - Lauffer Theory

Seeber (1984) defmes the design method for unreinforced fmal linings of the pressure tunnels. Under high pressure the grout is pumped into the contact between primary and fmal lining. The opened circumferential gap is filled with cement grout. With the grout pressure exerted in the circumferential gap, the concrete ring is prestressed against the rock and the deformations on both sides are fixed by the hardened cement grout. The prestressing should not exceed primary stress in the rock mass as it might otherwise be lost or can cause failure in the surrounding rock mass. The fmal lining and the surrounding rock mass take the internal water pressure depending on their stiffness. The lining can be left unreinforced if the prestressing by the injection is high enough that the lining remains in compression.

3.2.1.1 Assumptions:

- The circular tunnel is in homogenous rock mass with full all-round radial prestressing.
- The injection pressure is limited to concrete compressive strength as well as the minimum primary stress *(ax* or *ay,* whichever is lesser) in the rock mass during injection phase.
- Lining in operation (internal water pressure) is left in compression.

3.2.1.2 Input parameters:

Table 3.1: Input parameters

Geometry	*Rock mass*	*Concrete lining*	*Pressure loss:*
External radius, R (m)	Elastic modulus (Nzmnr')	Concrete quality C30	Pump, *Ppl* (%)
Internal radius, r (m)	Poisson's ratio, *vr (-)*	Elastic modulus, *Ee (N/mm2)*	Creep and shrinkage, Pes (%)
Overburden, H (m)	Unit weight *(kN/m3)*	Poisson's ratio, *V (-)*	
Groundwater height, hem)	Stress ratio.x, (-)	Thermal coefficient, *a (l/oe)*	Temperature *(OC)*
	Deformation modulus (Nzmm'')	Strength, *feu* (Nzmm')	
		Maximum allowable strain (-)	

Reduction and safety factors:

Concrete strength reduction, *CIs (-)*

Concrete strain reduction (-)

Internal pressure safety factor, *f.* s (-)

3.2.1.3 Calculations

Primary stresses in rock mass:

Vertical stress, $\sigma_v = \gamma H / 1000$ (3.1)

Horizontal stress, $\sigma_h = k.; \sigma_v$ (3.2)

Loading case - Empty tunnel:

Groundwater pressure, $P_{gw} = \gamma_w h_{jl} 000$ (3.3)

Knowing the magnitude of groundwater pressure, the strains in the internal and external wall of the lining are given as;

(3.4a)

(3.4b)

The corresponding thickness of the lining is obtained as;

Minimum thickness of lining, $tmin = f.$ s {R - (3.5)

Loading case - Injection:

The injection pressure definition is based on the following restrictions:

- ~ No tension stresses is allowed, meaning that during operation (internal water pressure) the fmallining must be in compression.
- ~ The minimal lining thickness is defined by the required thickness needed to take groundwater and the injection pressure acting on the lining.
- ~ The injection pressure acting on lining is limited by the minimal primary stress in the rock mass.

Pressure on pump, $Ppump$ = *variable*

Maximum allowable pressure on lining, $Pmax = C\mathbf{f}fcu$ {R:;~2} (3.6)

*The $Pmax$ < *the minimum* ofax *and* a_y

The injection pressure on the lining is given by:

$$Pinj - Ppump \left\{1 - \frac{ppump}{100}\right\} \times \frac{1000}{70} \quad (3.7)$$

Minimum thickness of lining, $tmin = \{R - (R2(1-2 \frac{Pinj}{Cfsxfcu})\}$ (3.8)

Strains in concrete, $cgut = - \frac{p..}{inj/Ee} \{\frac{R2+r2}{R2-r2} - v\}$ *(3.9a)*

(3.9b)

Loading case - Operation:

Injection pressure loss (due to creep), $I1Pes = - Ppump \times Pes/100$ (3.10)

Injection pressure loss (due to temperature,) $\hat{isp}, = - \{\frac{R2+r2}{R2-r2} - v\}$ (3.11)

The injection pressure remained in the gap *(Prem)* is the summation of equations 3.7, 3.10 and 3.11.

(3.12)

Remainder concrete strain, $c\sim ut,r = - Prem/Ee$ {:::~: - v} (3.13)

The pressure taken by rock (Pr) must be less than the minimum of the primary stresses in the rock.

$$\text{Pr} = \frac{\ldots\S:\_}{l+vr} \times (\_Eout,r) \quad (3.14)$$

Maximum allowable pressure in rock, $Pmax = \text{Prem} + \text{Pr}$ (3.15)

The calculated internal water pressure (i.e. internal pressure absorbed by the lining) during operation from the input Pi by applying a safety factor is given by,

(3.16)

The respective strains in concrete with contact to grout and the inner part of the concrete liner are given by equation 3.17 and 3.18.

(3.17)

(3.18)

The respective peripheral stresses can be obtained by multiplying equations 3.17 and 3.18 by the elasticity of the concrete lining.

(3.19)

Deformation modulus in rock is defmed in terms of elastic modulus and Poisson's ratio according to Lame and is given by:

$$D = \frac{\_E\_}{l+vr} \quad (3.20)$$

Rock mass characteristic line:

Since the minimum stress in the rock mass must not be exceeded by the injected pressure, the rock mass characteristic line can be obtained by plotting the strains against the corresponding rock mass pressure. The strain in the rock is given by:

$$E_r = \frac{a}{D} \quad (3.21)$$

System characteristic line:

This line is obtained by plotting the Prem and the minimum of the primary state of stresses or Prwith their corresponding strain values (see diagram of Seeber theory in appendix C4.8.12).

3.2.1.4 Limitation of Seeber theory

The theory assume that the concrete lining must be in compression, this follows the surface force theory according to the mechanism of internal water pressure acting on lining (Schleiss, 1986 and Kang, et al., 2009). This implies that the concrete lining is technically impermeable and the internal water force is treated as a surface load. This method, though simple but does not consider

seepage especially when crack is to occur in the lining and/or rock mass, and the stresses in rock mass are restricted to elasticity. The calculations are available in excel spreadsheet program.

3.2.2 Singh et al (1988)

The researchers agreed that plain concrete lining used in construction of power tunnels are susceptible to cracking and jointing as a result of construction process and loading due to internal water pressure. In case of TBM excavated tunnel lined with precast concrete segments the predefmed joints between segments exist and in case of the internal water pressure these joints can easily open (tensile stress in segments). Singh et al (1988), developed the design procedure for segment concrete lining used by TBM excavation where the six construction joints generally provided in are likely to be open up under internal pressure and the actual behaviour of the lining is expected to resemble that of the segment lining having six segments rather than seeing concrete lining as a monolithic structure. The disadvantage of cracked segment is that the flow of water may knock the segment out from the tunnel lining where example of a power waterway failure in Costa Rica is cited.

Singh et al (1988) stated that still a good, compact concrete that can withstand high velocities and abrasion is desirable for pressure tunnel, but reinforcements should be provided at the inlet and outlet ends, in distressed areas and in the plug area. A proposed simple method of analysis for preliminary study of a cracked segment lining by Singh et al (1988) is summarized below:

3.2.2.1Design assumptions

The following assumptions apply:

- The segment is assumed to behave approximately as thin shell.
- The lining is subjected to internal water pressure which also acts along the surface of the crack.
- The rock mass is replaced by normal and tangential/shear springs of stiffnesses KN and K_T.
- The rock mass is homogenous, isotropic and no radial fractures, the normal stiffness of the rock mass is given by:

$$KN = (1{:}V)T \qquad (3.22)$$

in which:

r: Internal radius of lining

- The modulus of deformation of the rock is small compared to that of the lining.
- No sliding occurs between the rock mass and lining.
- No radial cracking of the rock mass because the in-situ tangential stress around the opening is greater than the tangential tensile stress developed in the rock mass.

3.2.2.2 Method of Analysis (Singh et ai, 1988)

The radial deflection in the lining is given by:

(3.23)

Therefore, the crack opening of all the cracks and that of each crack are 2rrw and wl/J respectively.

In other words, the tangential displacement of each crack is:

(3.24)

The maximum shear stress occurs at the crack and is equal to:

$$(= KTu = \frac{Pil/J}{2} \times \frac{KT}{KN} \quad (3.25)$$

Figure 3.1: (a) Forces on segment oftunnellining (b) Variation of shear stress along the outer face of lining *(Source: Singh et al, 1988)*

The maximum hoop tension in the lining (at the centre line of the segment) is approximately equal to the resultant shear stresses at the base of the lining. Thus,

$$T = \frac{1}{2} KTu \frac{rl/J}{2} \quad p'_1$$

(3.26)

Also the maximum bending moment occur at the centre line of the segment (see figure 3.1a). The bending moment is given by:

$$M=-\frac{1}{2}Kru-x-\frac{rl./J}{2}\frac{d}{2} \qquad (3.27)$$

As the shear stiffuess of the rock mass increases, the more the tensile stress in the lining (see equation 3.26 and 3.27). The ratio *Kr/KN* depends inversely on the area of the loading surfaces. Thus, *Kr/KN* is proportional to 1/1/J (Singh et al, 1988). Since the contact shear stress is not uniformly distributed, the coefficient of proportionality seems difficult to obtain. Nevertheless, it is obtained by comparing the results of this method with a finite element analysis (Singh et al, 1988). Figure 3.lb suggests that the maximum ratio of shear stress to radial pressure is equal to 1.0 ± 0.20 and is independent on the modulii of deformation of the concrete and the rock mass and the number of segment.

The equation 3.25 yields:

(3.28)

The magnitudes of hoop tension and moment at the centre line are given by the following relationship:

$$T = \frac{rPi1./J}{4} - p.d. \qquad (3.29)$$

$$M = \frac{rPid1./J}{8} \qquad (3.30)$$

The maximum tensile stress at the outer periphery of the lining is given by:

(3.31)

If the crack is to occur the tangential stress exceeds the tensile strength of the concrete, the number of crack is formulated as:

(3.32)

The average crack opening *(2u)* is given by:

$$2u = \frac{2rrPi}{NKN} = \frac{(1+V)(ft+Pi)d}{E} \qquad (3.33)$$

3.2.2.3 Limitation:

The assumption of $E/Ee \sim 0.20$ and that number of cracks $(N < 36)$ shows that the method is valid for rock of poor quality. The method assumed that there is no gap between the lining and the rock mass. This implies that rock mass is exerting a load (called relief pressure) that counteracts internal pressure in the lining without artificial prestressing. This also confirms the behaviour of a weak rock.

3.2.3 Schleiss, (1986, 1987 and 1997)

The design of plain and reinforced concrete pressure tunnels that takes into accounts the seepage forces and secondary permeability in lining and rock is presented by Schleiss in 1986, 1987 and 1997, unlike the traditional design approach of structural theory whereby the inner surface of concrete-liner is considers as impervious, thereby treating the inner water pressure as surface force and neglecting the seepage pressure in lining and rock (figure *3.2a)*.

3.2.3.1 Design of pervious pressure tunnel

The design approach suggested by Schleiss, (1986 and 1987) design pressure tunnel as a pervious material and the inner water load are described based on body force theory (figure 3.2b). For permeable medium, water infiltrates cavities and exerts a surface pressure. The friction within the cavities reduces the water pressure and the water force on the liner is transmitted along the seepage line as body force.

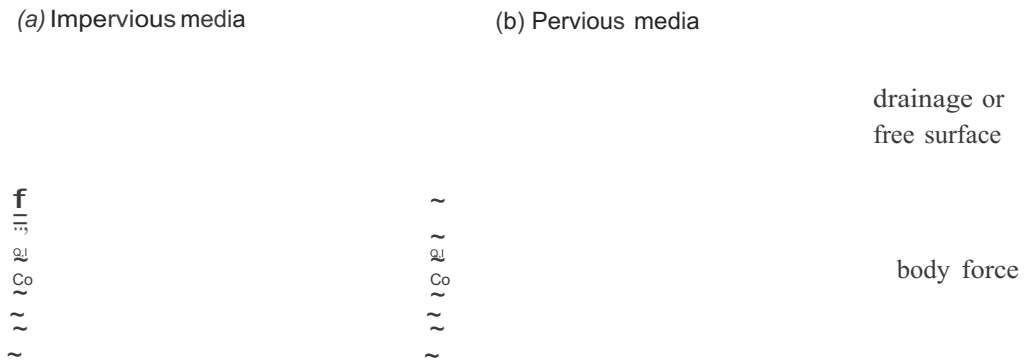

Figure 3.2: Effect of water pressure on liner media *(Source: Schleiss, 1986).*

According to Schleiss, as liner cracks, the internal pressure is displaced to the outside of the lining. In the fractures, a seepage flow is developed and the flow is dependent on the internal water pressure head and water level in the rock. The fractures and pores caused by water forces cause the permeability of rock to change and, this change, in turn, affect the seepage flow in rock and lining. Therefore, the seepage forces change and the chain continues. This mechanical-hydraulic coupling is schematized in figure 3.3.

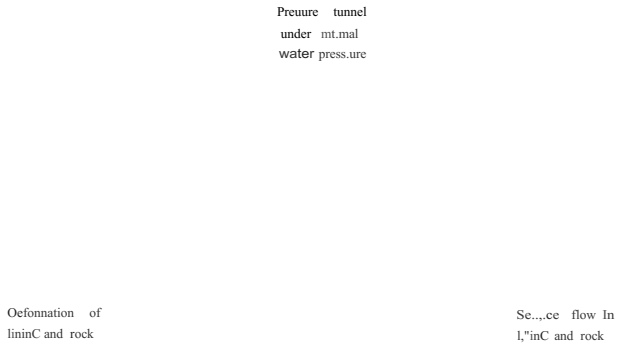

Figure 3.3: Mechanical-hydraulic coupling between deformation and seepage forces in lining and rock of power waterway with internal pressure *(Source: Schleiss, 1987)*

3.2.3.2 Pressure tunnel with uncracked concrete lining

For the computation of pervious pressure tunnels using thick-wall cylinder theory, four zones of different mechanical and permeability properties have been identified by the author namely: lining, grouted, cracked and fractured zones. The theory assumptions are that:

- ~ Zones are approximately radially symmetrical
- ~ Have homogenous isotropic material behaviour and,
- ~ The fractured rock mass behave mechanically and hydraulically like continuous media.

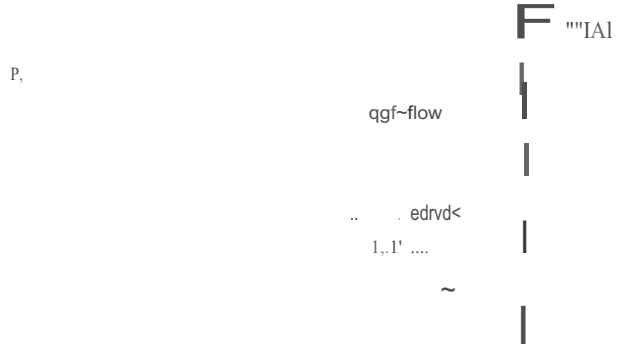

Figure 3.4: Distribution of seepage flow pressure in concrete lined pressure tunnel *(Source: Schleiss, 1987)*

Computation of deformations and stresses in that regard requires distinguishing for zones: concrete lining, grouted rock zone, rock mass inside and outside the reach of seepage flow path as shown in figure 3.4. The interaction of these zones is given unknown mechanical boundary stresses *PF (R), PF (Rg)and PF (Rs)* as well as unknown pressures *Pe* and *Pg* .

Parametric study of boundary pressure against lining thickness by varying the deformation ratio (with assumption that $K_i = K_r$) shows that the greater lining thickness and the poorer the rock quality will produce the higher boundary stress between lining and rock. For this reason, the lining tend to separate from the rock, this deformation of lining is dictated by rock mass (Schleiss, 1986). The effect seepage pressure is comparable to cooling of the lining.

The author shows further, the effect of varying the permeability ratio (assumingf', $= Er)$, results in tensile stress between lining and rock if Kc/Kr $::;$ 0.01. More so, for Kc/Kr 2:: 1 boundary stress is not affected. The natural tensile strength of the liner-rock boundary is usually small. Therefore, to transmit high tensile stresses to the rock the lining must be prestressed by grouting the gap between the lining and rock at high pressure.

3.2.3.3 Effect of cracks in lining and rock

Cracks occur if the tangential stresses in lining due to internal water pressure exceed the tensile strength of concrete (Schleiss, 1986 and 1997). The same limit in rock is given by the tensile strength and natural stresses. Therefore, in the cracked zones only the radial stresses and pressure gradient are linear. The head at the outside of cracked lining is given by continuity condition and usually negligible for plain concrete lining (Schleiss, 1986). The total with crack in lining is a function tangential displacement of the rock mass and it is estimated by:

(3.34)

The number of cracks (N) is governed by the weak zones in the lining and cracks are mostly found at roof of tunnel and transition floor-wall in a plain concrete lining.

If the crack width is known, and the assumption of lamina and parallel flow can be applied in the crack. The water losses through the liner can be calculated by equation 3.35:

(3.35)

The water loss through rock mass in a tunnel above groundwater level is obtained from equation 3.36:

$$\frac{\pi}{P_w\gamma} - \frac{(\sim r_a)}{4} = \frac{q}{2\pi K_r} \ln \frac{q}{\pi K_r r_a} \qquad (3.36)$$

where $P_a = f(2a)$ is the water pressure on the outer side of the liner.

(3.37)

where K; and K; are permeability of rock and concrete liner respectively;

ril ra and R are the respective internal radius of the lining, external radius of the lining and external radius of the rock zone affected by seepage.

According to Schleiss (1986), $R = 2r_a$ can be assumed for pervious rock $(K; 2:: 100Kc)$. For tight rock $(K; ::; Kc)$, $R = lOr_a$ give good result.

Based on the thick-walled cylinder theory, radial deformation of the rock zone influenced by seepage, $u(r_a)$, is calculated as follows (Schleiss, 1986):

(3.38)

The value ofR for tunnel above groundwater level can be obtained as follow Schleiss (1997):

$$R = qj_{tt.K;} \text{ in } 2 \quad (3.39)$$

Besides *Pa'* the mechanical boundary pressures at the inner and outer surface of the rock zone are influenced by seepage, *O'r(ra)* and *Pr(R),* have to be considered in equation 3.37. The radial stress transmitted to the rock mass by cracked concrete is calculated from equation 3.40 (Schleiss, 1986):

$$O'r(ra) = Pr(ra) = \sim(Pi - Pa)\left[1 + \sim\sim\right] \quad (3.40)$$

The boundary pressure, *Pr(R)* between rock zone affected by seepage and rock zone not affected is obtained as:

(3.41)

Where C_4 and C_5 are computed respectively from equation 3.42 and 3.43:

(3.42)

$$C_5 = (\sim)^2 \quad (3.43)$$

Water losses through concrete liner, grouted zone and rock mass zone are computed iteratively from equation 3.44.

$$\frac{Pi}{Pwg} \quad (3)_{4\,1;\,\vartheta} = \frac{q}{2\pi Ky} \ln \frac{q}{\pi Kyrg} \quad \frac{q}{2\pi}\left[\frac{1}{Kc} \ln \frac{(ra)}{ri} + \frac{1}{Kg} \ln \frac{(rg)}{r\alpha}\right] \quad (3.44)$$

where rg and Kg are the radius and permeability of the grouted zone respectively.

The crack of the grouted zone can be prevented by injecting pressure as high as the tensile stress generated by the internal water pressure at the outer surface of the liner (Schleiss, 1987).

3.2.3.4 Design criteria for pervious pressure tunnels

Schleiss suggested criteria for designing pressure tunnels are:

1. Avoid cracks in lining: This can be prevented either by reducing forces on lining or by increasing lining resistance. Increasing the thickness of the lining and rock grouting are among measures to reduce forces in lining. These methods are applicable for small internal pressure head *(Pi* < 20 *bar)* and good rock quality *(Eel E;* < 3). At high pressure heads cracks can be avoided by increasing the lining resistance through prestressing.
2. Limiting water losses: The water losses depend on alignment, depth under water table and type of lining. This can be limited by avoiding cracks in the concrete (see above) and to some extent reinforcing as well as grouting. And, if still found ineffective, special sealing such as plastic sheeting or thin steel tubes need to be used.
3. Bearing capacity of rock mass: The stress in rock due to internal water pressure should not exceed the natural stresses. Otherwise, the tunnel will probably fail as result of expansion of cracked zone which cannot be limited. The rule of thumb of using minimal overburden

is generally not applicable because of geological situation. The natural stresses are influenced indirectly by locating pressure tunnel deep enough underground.

3.2.3.5 Limitation

The solution is based on elastic theory, strength parameter of the rock mass are not taken into consideration. The reaches of horizontal and vertical flow are based on assumptions. These assumptions pose restrictions because the behaviour of rock is sometimes erratic most especially for deep tunnels. In addition, calculation of seepage flow requires many equations and the iteration is laborious.

3.2.4 USACE, (1997)

The technical criteria for the design and construction of tunnels among other contract and construction activities have been given by the department of the army, United State Corps of Engineers (USACE, 1997). The design oflinings as stated by the authors' is hereby presented.

The approach analyzed the structural interaction for radial loads using simplified thin-shell equations and compatibility of radial displacement between the lining and surrounding rock mass. The method analyzes the effect of internal water pressure by considering the rock-structure interaction as well as leakage control during cracking in the lining.

3.2.4.1 Material properties and assumptions

The material properties under consideration are modulus of elasticity *(Ee)* and Poisson's Ratio *(ve)* of the lining. The internal water pressure and the external pressure are considered as loads acting on the liner. The assumption for the analysis of stress and displacements is based on plane strain conditions.

3.2.4.2 Design approach

According to thin shell equation, the tangential stress *«(lee)* is computed from the relation:

(3.45)

where *Pi* and Pr are internal and external water pressures respectively and *Rav* is the average radius of the lining.

The relative displacement *(E)* in the lining is given as the product of the tangential stress and the deformation modulus:

$$E = \frac{u}{Rav} \quad \frac{I:J.R}{Rav} \quad (lee \times \frac{(I-\vee/)}{Ee}$$

(3.46)

$$E = (Pi - Pr)\ Le$$

At the rock interface, the relative displacement due to external pressure is given by:

$$E = \frac{u}{Rav} = \Pr \times \frac{(1+v)}{S;} r_{-} = PrLr \quad (3.47)$$

From equations (3.46) and (3.47) the external pressure from the rock is:

(3.48)

The net load in the lining is Pi _ Pr and the tangential stress in the lining is given by:

(3.49)

The relative radial displacement in the lining is calculated from:

$$E = \frac{u}{Rav} = CJeeEc$$

(3.50)

$$E = \frac{Pi\ Rav}{Ee\ d} \times \frac{Lr}{Le+Lr}$$

The quantity of water that flows through a cracked lining per unit length of tunnel is given by:

$$q = (N\,!ZTJ)\ (!1p/d)w_3 \quad (3.51)$$

where N is the number of crack (usually not more than two developed parallel to the plane of minimum in-situ stress.

w = ES and S = rrro (wand S are average crack width and cracking space in a plain concrete tunnel).

However, if the concrete is crack-free, the leakage through the lining is given by:

$$q = 2rrrkc!1pjYwd \quad (3.52)$$

$k;$ is the permeability of concrete.

3.2.4.3 Limitations

The method gives a quick estimate of the outward displacement due internal pressure as well as the tangential stress. However, theory elasticity is not a good approximation of behaviour of rocks. This is because, at great depths, the self weight of rock can cause the rock to behave as a plastic material. The behaviour of cracked liner changes, the permeability of the liner must change most especially in the radial direction from (isotropic to anisotropic).

4 Model Selection

4.1 Introduction

This chapter introduces PLAXIS 2D finite element program as a tunnel design tool and its salient features described in accordance with PLAXIS 2D material and reference manuals. The program can be used to study the influence of construction sequence and ground deformation on load transfer into support measures that cannot be accounted for using analytical methods. The program is readily available in the (UNESCO-IRE) menu folder, hence, can be put to test for the design of pressure tunnel.

4.2 PLAXIS 2D

"PLAXIS 2D 0'ersion 10.0) is a finite element package intended for the two-dimensional analysis of deformation and stability in geotechnical engineering. Geotechnical applications require advanced constitutive models for the simulation of the non-linear, time-dependent and anisotropic behavior of ground" (PLAXIS 2D, Material manual). Although the modelling of the ground itself is an important issue, tunnel projects involve the modelling of structures and the interaction between the structures and ground.

With PLAXIS 2D, material behaviours such as elastic and elasto-plastic ground/support interaction, identification of stress concentrations and study of modes of failure by simulation of different loading steps can be assessed. The problem of infinite boundaries can be handled in PLAXIS by generating meshes (i.e. to discretize) beyond the zone of influence of excavation and apply appropriate boundary conditions to the outer edges. The program incorporates material parameters that are well-known in geotechnical engineering. In addition, the program has graphical input of geometry models that are simple and easy to handle.

Although, PLAXIS 2D is a 2-dimensional program, stresses are based on the 3D Cartesian coordinate system. In the all output data, the tensile stresses and forces are taken as positive, whereas compressive stresses and forces are taken as negative. The program is adequate for the analysis of stresses and displacements in the rock surrounding of tunnel. This is because the length of the tunnel is much larger than the cross-sectional dimensions. In addition, since the ends are far away, the stresses and displacements in a plane, normal to the axis of the opening are not affected by the ends of the opening. Therefore, a plane strain model is used this research work.

4.3 Model

PLAXIS 2D is used to carry out two-dimensional finite element analyses. The fmite element models can be plane strain and its selection will result in a two dimensional finite element model with only two translational degrees of freedom per node *(x* andy directions).

r

Figure 4.1: A plane strain problem
(Source: PLAXIS Reference Manual)

4.3.1 A plane strain model

"The model is used for geometries with more or less uniform cross-sectional and the corresponding state of stress and loading scheme over a certain length perpendicular to the cross section *(z* - direction)" (PLAXIS 2D, Reference manual) as shown in figure 4.1. The displacement and strains are assumed to be zero in *z* - direction (that is $U_{zz} = \varepsilon_{zz} = \gamma_{xz} = \gamma_{yz} = 0$). Conversely, normal stresses in the z - direction are fully taken into consideration.

A plane strain model is adopted in this research work since the tunnel lining is very long compare to the cross sectional dimension. Therefore, the excavation of the tunnel can be idealized as a plane strain problem. Prior to the tunnel construction, the stress field along the axis of the tunnel will show no shear stress parallel to the tunnel axis. Therefore, the changes in stress and strain induced by excavation satisfy the plane strain conditions.

4.3.2 Model elements

In PLAXIS 2D, elements and material model are fully three-dimensional. The deformations and stresses in ground layer and structures are modelled using either 6- node or 15- node triangular elements. The latter is the default element, provides a 4th order interpolation for displacements and the numerical integration involves 12 stress points, whereas the former is mostly used for fast preliminary calculations, and provides a 2nd order interpolation with numerical integration of 3 stress points. This means that the power of 15- node element is four times that of the 6-node element. Therefore, the 15- node triangle is a very accurate element with high quality stress results for difficult problems (PLAXIS 2D: Reference Manual) and it is adopted as elements under the general settings throughout the simulation of the research work. Figure 4.2 shows the position of nodes and stress points in the ground elements.

5.3.3 Tunnel excavation

During excavation, the equilibrium state of in-situ stress is disturbed. Hence, the stresses in the ground change. The change is a variable which depend on the ground parameters: stiffness and strength of the lining. The excavation is simulated by deactivating the cluster excavation. Once the excavation is completed, the stresses around the opening are redistributed. The redistribution can overstress part of the rock mass and make it to yield; these parts of rock under yielding can be viewed in the output of the stress analysis as "plastic zone" in PLAXIS 2D. This implies that maximum allowable stress level in the rock has been exceeded. The difference between the allowable and new stress level is responsible for the additional stress redistribution in the surrounding rock mass and in the installed lining.

5.4.3.1 Two-dimensional simulation of excavation

Numerical model of tunnel with high overburden depth of 200m requires three dimensional simulation of excavation support to be simulated in 2D by stress relief in front of the face (3D arching effect). A load reduction method (otherwise known as beta *(f3)* - method) is adopted under plane strain condition. The idea is that the initial stress in the rock mass acting around the location where tunnel is to be constructed is divided into two parts: (1 - *f3)p* is applied to the surrounding rock mass (regarded as unsupported tunnel) and the remaining *f3p* is applied to the shotcrete lining (Figure 5.2). The value of *f3* depends on the tunnel dimension and shape, overburden, excavation method and phases, and rock mass characteristics. The *f3* - method is based upon controlling deformation processes in the excavation area in such a way that the excavation attains a secondary state of equilibrium.

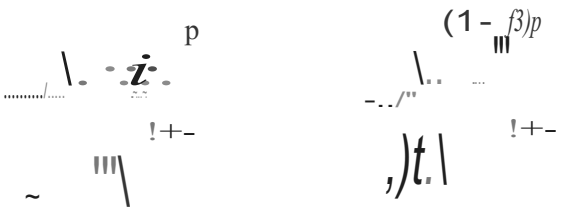

Figure 5.2: Schematic representation of *P - method* for analysis of tunnel
(Source: PLAXIS - Reference manual)

To determine the appropriate *f3 - value,* a parametric study has been carried out. The method has been used by many researchers in different names but referring to the same procedure to show 3D arching effect around tunnel face (Sinha, 1989 Marence, 1996, and Dimitrios, 2005). The load reduction factor, *f3* is varied in range between 0 and 1 for (0 ~ *f3* ~ 1).

5.3.4 Temperature and Shrinkage

The effect of temperature change not being taking into consideration can be said to be one of the limitations of the program. However, this can be compensated by modelling the shrinkage effect using the internal volumetric strain approach in the program. The negative volumetric strain (expressed percentage) which is a function of thermal coefficient of concrete and surrounding temperature has to be specified in order to simulate the contraction in the lining.

5.3.5 Shotcrete decay simulation

The mechanical properties of shotcrete usually vary with time due to ageing of the hardened concrete. This is normally taken into account with variable young modulus, E and compressive strengths, *feu* with time. Apart from this, shotcrete is a rate dependent material because its stiffuess depends on the time history and rate of loading. The decay will be simulated in this research by varying the E between 0.1 and 0.2 of the initial value. This is required to see the performance of PLAXIS 2D in that regard.

5.3.6 Grouting pressure

Gaps are caused by shrinkage and the feeling of the gap at low pressure is referred to as gap grouting. In order to increase the bearing resistance of the lining rock is injected with grout at high pressure- prestressing effect. Injection of grouting pressure (prestressing) is simulated by increasing the stiffuess of the surrounding rock mass say thickness equal to or twice the tunnel radius through positive volumetric expansion. *Calculation of % volumetric strain (Ev) in the rock mass is related to injection pressure:* To obtain the percentage volumetric strain for required prestressing of the rock mass, the allowable pressure on the lining and associated stress is calculated using *Seeber analytical theory.* The volumetric strain in the model is varied until comparable stress in the lining is found.

All simulation (from section 5.1.1 through 5.3.5) is carried out using plastic analysis. Plastic analysis is used to carry out an elastic - plastic deformation analysis according to the small deformation theory where undrained behaviour may be considered. It is appropriate in most practical engineering applications and does not take time effects into account (PLAXIS 2D Reference manual).

5.3.7 Internal water pressure

The operational loading of internal water pressure (IWP) is the most significant loading condition for the [mal lining. The internal pressure produces tensile stresses in the lining. The simulation of water losses or (seepage flow) is done using flow mode in groundwater analysis. In groundwater analysis, the effect of pore pressure and water conditions can be study with time. The pressures in bars are specified in the tunnel cluster and water pressure is generated. In addition, the stresses in the lining and rock mass due to internal water pressure are simulated using the consolidation analysis calculation type. Consolidation analysis is often conducted when analyzing the development and dissipation of excess pore pressure in ground as a function of time.

6 Modeling considerations

6.1 Introduction

Numerical design of deep tunnels consists of simulation of the construction and operational loading. In this study, the rock mass behaviour is approximated using non-linear Mohr-Coulomb model. Model parameters (for the rock mass and support measures) are obtained from Ermenek tunnel project, Turkey. The methodology flow chart is shown in figure 6.l.The geological and geotechnical assessment of the site is assumed to be adequate. The simulation phase is highlighted as:

- Model set up - ground simulation
- Modeling of excavation stage
- Installation of primary lining (shotcrete)
- Design of fmallining
- Shrinkage of fmal lining
- Shotcrete decay simulation
- Grout modelling - gap grouting and prestressing
- Operational loading modelling - internal water pressure
- Stress and seepage analysis

Model calibrationIParametric study

Correlation

Numerical Simulation of pressure tunnel

Figure 6.1: Methodology flow chart

6.2 Modell - Numerical Simulation of Pressure Tunnel

The modelling work is done using the Finite Element software Package-PLAXIS 2D. The simulation of construction of tunnel in rock and the influence on rock surrounding vis -a-vis the displacement and stress field around the tunnel is studied. The modeled tunnel is excavated in rock mass with overburden depth of 200m above the ground surface. The excavation is done using tunnel boring machine (TBM) and with installing the primary lining (shotcrete and rock bolts) behind it. The flow chart of numerical design of pressure tunnel in the study is shown in figure 6.2.

Figure 6.2: Flow chart for numerical analysis of pressure tunnels

6.2.1 Model set up

Two models have been set up: Full mesh generating model and distributed load model (figure 6.1). The former present modeling of real state of rock mass in terms of height while in the latter, part of model height is reduced to cater for the situations where model grid becomes too dense to display (see appendix A). The model simulates deep excavation thereby overcoming one of the shortcomings of PLAXIS 2D - shallow tunnel. The full mesh generating model area covers 250m height and 100m in width. For this research, a full mesh generating model has been used since the depth of overburden is 200m was found to be geometrically stable, no additional computations is required and is found not difficult to be modelled. The tunnel tube is circular with internal radius of 3.0m and the mesh is seven (7) times more than the tunnel diameter in all directions - the

deformations outside the specified area can be neglected and appropriate boundary conditions have been used.

6.2.1.1 Model Grid

The tunnel is situated in uniform rock mass and the basic geometry including one layer of rock is created. The input data for the geometry of the modeled region is defined as follows:

Dimensions of geometry:	Left	-50m
	Right	+50m
	Top	+200m
	Bottom	-50m

6.2.1.2 Model geometry

The tunnel geometry, rock and shotcrete parameters considered for the computational models are as follows:

Tunnel geometry:

The tunnel is excavated by the tunnel boring machine (TBM) with following main geometry data:

Overburden height (h)	200m
Internal tunnel radius (r)	3.00m
Groundwater height	below the tunnel

6.2.2 Material Properties

The materials are mainly rock mass and concrete structures.

6.2.2.1 Rock mass

In this study, the rock mass is defmed as elastoplastic material, with yield function defmed by Mohr - Coulomb model. Since long term deformation is of interest, the material behaviour is set to *drained condition.* The rock input parameters are presented in table 6.1.

Table 6.1: Material arameters

Parameters	Symbol	*Rock mass*	*Shotcrete*	*Final linin*	*Unit*
Young's modulus of elasticity	E	1~0 +- -=2~0 +- ~3~0			*GPa*
Poisson's ratio		0.20	0.22	0.22	
Unit weight		26	24	24	*kNlm³*
Frictional angle		40	40	40	°
Cohesion	C	1000	1000	1500	*kNlm²*
Thickness of lining	*d*		0.1	0.3	*m*
Weight	w		2.4	7.2	*kNlmlm*
Thermal coefficient	*a*		1.2 x 10-5		;oC

(Source: Ermenek Pressure Tunnel Project, Turkey, 2003)

6.2.2.2 Primary support (shotcrete)

In addition to the data set *Soil and interfaces,* the shotcrete lining is created as a *Plate* and from the shotcrete characteristics the input parameters for PLAXIS have been calculated (see table 6.2). The simple calculation of the input parameters is presented below.

Normal stiffness (EcA) = Ec x d x $lmetre\ strip$

$= 2 \times 10_7 \times 0.1 \times 1 = 2{,}OOO{,}OOOkN[m.$

Flexural rigidity (E, I) = $Ec \times \frac{bd_3}{12}$

$= 2 \times 10_7 \times 1 \times 0.13 \times \frac{2..}{12} = 1666.67kN \quad 1m2[m.$

Table 6.2: Material Properties of Shotcrete (calculated value)

6.2.3 Model Assumptions

- Rock mass behaviour is assumed to be in drained conditions.
- Lining material is elastic.
- The model is based on condition of plane strain.
- Rock mass is defined as elasto-plastic material, with yield functions defined by Mohr-Coulomb strength law.
- The stresses existing in the rock mass are related to the weight of the overlying strata and geological history. No geotechnical stresses are expected and the vertical stress is assumed as a weight of overburden. The horizontal stress is defined as a portion of the vertical stress for elastic solution with restrained horizontal movements.

6.3 Boundary conditions:

The schematized boundary conditions is shown in figure 6.3; standard fixity of boundary edges.

Horizontal displacement is prevented along the vertical edges of the mesh boundary (horizontal fixity $u_x = 0$).

The vertical edges of the whole area were fixed against horizontal displacement and bottom end was secured against vertical displacement (Vertical fixity $u_y = 0$).

Figure 6.3: Sketch of boundary conditions

6.4 Mesh generation

Mesh consists of 15-nodes as the basic element type. The global mesh is set to fine and, clusters and lines refined. The meshing of the model and boundary conditions as observed during model testing is shown in figure 6.4 below.

6.5 Initial conditions:

- Water weight is taken as *10kN* $1m_3$
- Coefficient earth pressure at rest (*ko* = 0.8)
- L M - *weight* = 1 (meaning that the full weight of the rock mass is used in the analysis before excavation).
- The water pressure is deactivated while the initial stress is generated.
- ~

Figure 6.4: Meshing of FEM model and boundary conditions.

6.6 Simulation processes

To simulate the excavation processes, the construction of tunnel and operational loading, stage calculation is needed. Loading 1 through 7 is simulated using *plastic analysis* calculation while loading 8 is simulated using *consolidation* and *ground flow analyses.* The calculation phases are described below:

Loading -0- Primary state of stresses *(k0* = 0.8)

Loading -1- Initial stress relief (,8 = 0.64)

Loading -2- *Excavation:* the cluster within the tunnel perimeter is deactivated and load reduction factor is applied using ,8- method. The 3D arching effect of the excavation face area and the description of the influence on the deformation in the tunnel is simulated using the load factor, ,8- method of loading on excavation and lining; this form the basis for the model calibration.

Loading -3- *Shotcrete lining:* the parameter is defined and the tunnel lining is activated and updated. The ground cluster in the tunnel section is deactivated and all forces caused by

excavation are in equilibrium. Figure 6.5 shows the loading simulation for initial state of stresses, excavation and shotcrete installation.

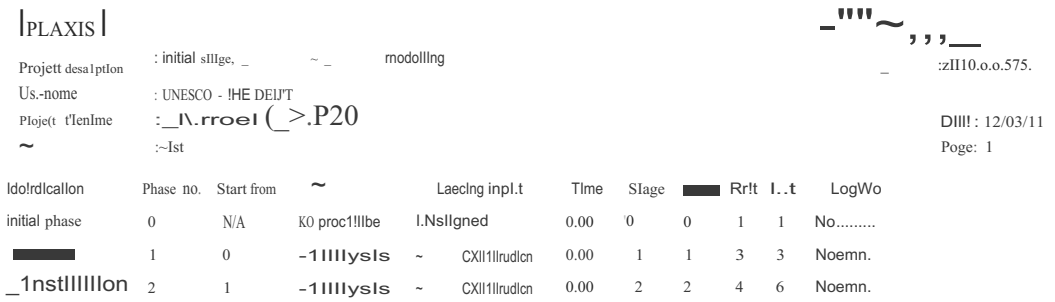

Figure 6.5: Calculation list for simulation of initial state, excavation and shotcrete

Loading -4- *Final lining:* the fmal together with the interface elements between the linings is installed by activating the dead weight of lining triangular element. The loading of simulation phase is show in figure 6.6.

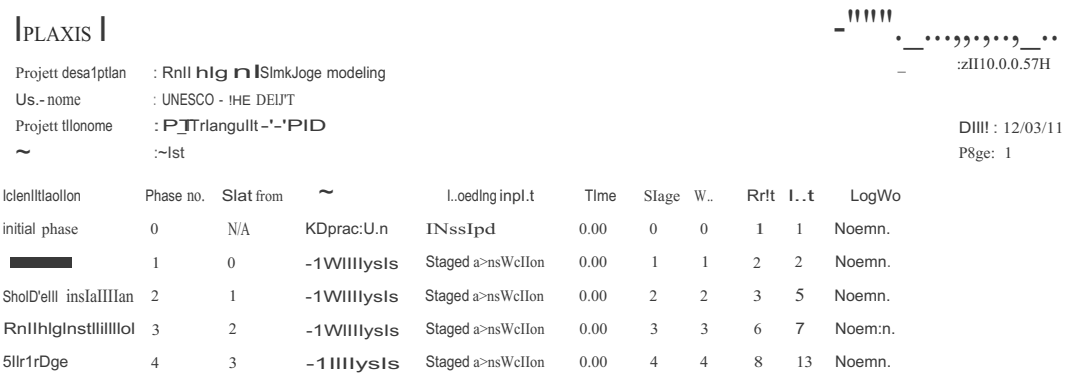

Figure 6.6: Loading -4- and -5- Final lining and shrinkage simulation

Loading -5- *Temperature and shrinkage effect:* The shrinkage and temperature effect are compensated for by applying volumetric strain to the fmal lining and activating its interface element.

Volumetric strain calculation:

The % volumetric strain *(cv)* = *al:!.T* x 100% = 0.022%

where a = 1.2 x 10-5 ;OC and *I:!.T= 18°C*

Loading -6- Shotcrete decay: The mechanical properties of shotcrete vary with time due to ageing of the hardened concrete. Therefore, strength of shotcrete lining due to long term effect is simulated by reducing modulus of elasticity of the shotcrete material. The parameters in the material set are modified and simulated. The calculation sheet for the simulation of shotcrete decay is shown figure 6.7.

PI'oject clesaWon : P'T..e«:avatlon
u.er nome : UNESCO ~ IHE DELFr
PI'oject IIenome : P'T_Sholtrele element dec;ay.P2D
OUtput : caJQUtlon1st

Veroion 101o.0.0.57St

Date : 01/04/11
Page: 1

IdentIlbtlon	Phase no.	5Iart fiom	caJQUtlon	I.Qodlr1gInput	11me	Stiga	W.tIr	Ant	list	IDjjWo
IIlItlal phase	0	NJA	I(D~,..	IlnMIIgned	0.00	0				NoIITOrI.
EiaVetIOn		0	Plastic anaiy>Is	~c:onstnJc:tICIl	0.00					Noemn.
SI'ooImtII_tlon	2		Plastic lnalysiS	~c:onstnJc:tICIl	0.00					Noemn.
IInaIlning			"'-Ie analysis	~_c:tIon	0.00				4	Noemn.
SI'ooImtIIdocly			Plastic ~nalysIs	staged consInJCtjon	0.00				11	Noemn.

Figure 6.7: Loading -6- shotcrete decay simulation

Loading -7- *Grout modelling:*

~ *Gap grouting simulation* The volumetric strain is applied radially to the about 2.5m thick rock mass behind the shotcrete. The output of the simulation is shown in section 7.3.6 (of chapter 7). Figure 6.8a and 6.8b show the calculation sheets for contact grouting and consolidation grouting simulation.

,!"LAXISi

PIoJoct"""- :c:ono.tt_
User"""",
PIoJoct_
~
: UNESCO ·IIiE 0EIF1'
: Gop -.. O.!'!b "" stroIn.P2D
: CIIcUatlon 1st

_:1010.0.0.'759

Dete: *29/03111*
Pogo: 1

	PIIose""	SIIIrtfrom	OIIcuIoUan	Loadng In""	I1me	stage	W_	Ant	Last	LogInIo
INt1al phase	O	N/A	kO proa<1Ure	UnassIgned	MD	0	0	1	1	Noemn.
EJay-'	1	0			0.00	1	1	2	2	Noemn.
	2	1	-1INIyoIs		0.00	2	2	3	5	Noerrors.
AoaIIIMg_	3	2			0.00	3	3	6	6	Noomn.
SI'orInoage	1	3			0.00	~	1	7	12	Noemn.
+.. — CO.1"")	5	4			0.00	5	5	13	17	No.....
0.125%	6	4			0.00	6	6	18	23	Noerrors.
0.175""	7	4	""		0.00	7	7	2.	29	No.....
O.2OO'!Io	8	1		consINc:tIon	0.00	8	8	30	35	No.....
0.22""	9	1	PlastIc analysis		0.00	9	9	36	12	No.....
0.2.""	10	~	PlastIc analysis		0.00	10	10	43	49	No .....
0.26'11>	11	4	PlastIc ana"",		0.00	11	11	50	56	No enors.
0.28'11>	12	4	PlastIc_Ioss		0.00	12	12	57	61	No.....
0.30'11>	13	1	Plastic_		0.00	13	13	64	70	No.....
0._	11	4	_IINt""		0.00	1.	14	71	78	No.""...

Figure 6.8a: loading - 7- Contact grouting simulation calculation sheet

~ *Consolidation grouting simulation*

Simple calculation:

Injection pressure *(Pinj)* = 15 *bars*
Remaining pressure after all losses = 5.3 *bars* (Seeber analytical solution)
Allowable pressure on lining *(Pc)* = *2340kN 1m2* (Seeber analytical solution see C4.8.9)
Stresses in lining *(ac)* = *5400kN 1m2* equations 3.13 and 3.19

Volumetric strain $\varepsilon_v = 0.2\%$ which is equivalent to 0.280m3/m volume change in the rock mass produce stresses of *(aFL) 5307kN 1m2* (side) and *4733kN 1m2* (crown) stresses in lining *(aFL)* is found from plastic analysis (PLAXIS 2D).

Figure 6.8b: Loading -7- Consolidation grouting simulation calculation sheet

Loading -8- *Internal waterpressure:*
The internal water pressure loading is the main loading in pressure tunnel, its operational loading starts after the installation of the final lining as a total loading. The respective calculation sheets for simulation of internal water pressure for consolidation analysis and groundwater analysis is shown in figure 6.9 and 6.10.

Case 1: *Simulation of the effect of water pressures on stresses in the liner (consolidation analysis)*

$$Pit < Pi2 < Pi3 < Pi4 < PiS \text{ and } KCl = KC2 < KC3 < KC4 < Kcs$$

Table 6.3 : Internal water

SIN	1	2	5
	10	20	

The internal water pressure and permeability input for the simulation is shown table 6.3.

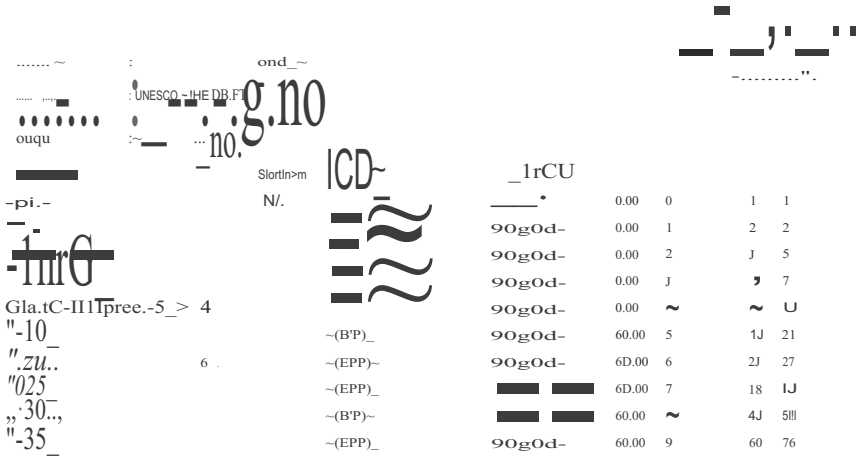

Figure 6.9: Loading -8- internal water pressure simulation (consolidation analysis)

Simulation of seepage flow in final lining due to high internal water pressure (groundwater flow analysis)

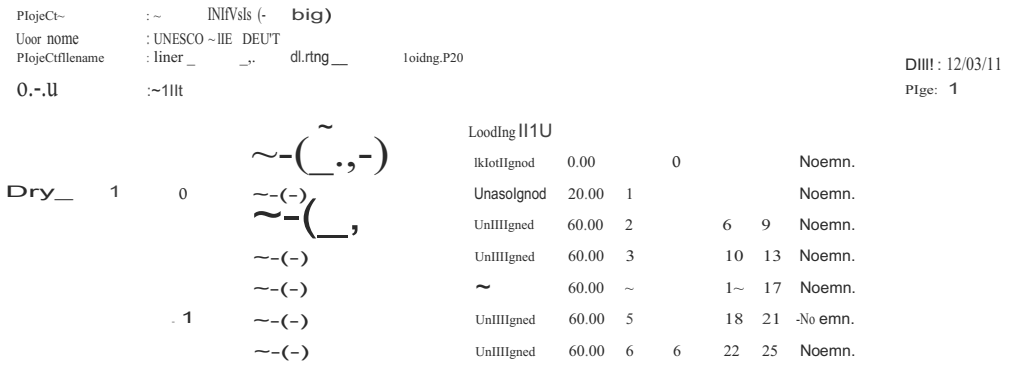

Figure 6.10: Loading -8- internal water pressure simulation (groundwater flow analysis)

Case 2: Simulation of seepage flow in final lining due to high internal water pressure (groundwaterflow analysis)

(Pi = 25 bars and K, = variable)

In this case, the internal water present is kept constant while the permeability of elements changes as shown in figure 6.1. The permeability values are presented in table 6.4.

Table 6.4 : Internal water ressure and rock

25

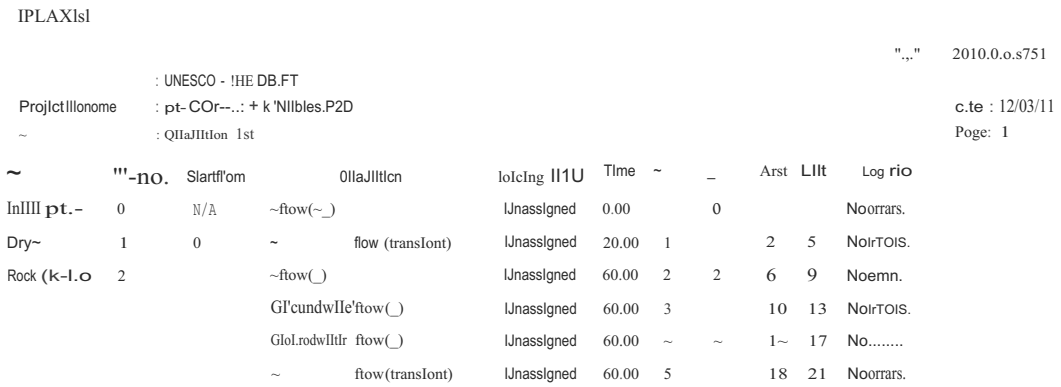

Figure 6.11: Loading -8- simulation of seepage losses through lining to the rock mass

The previous analysis showed cracks at 20 bars internal water pressure. The level of cracks confirmed that the cracks had occurred before 20 bars pressure. In order to get the point of initial of cracks due to high internal water pressure in the lining, the pressure is varied between 10 to 20 bars at 2 bars interval. The calculation sheet is shown in figure 6.12.

PLAXISI

Project deso1p11on : PT_Excavation
User """" : UNESCO~!HE DEIFT
Project "Iename : PllOto2O.P2D
OUtput : CalaJIaUon list

Venion 2010.0.i.i7H
Dale : 30/03/11
Page: 1

IdentIncatICJ1	Phase no.	StiIrt from	CIIIrulatIon	loading Input	Tome	Stage	Water	Am	Last
InItIaI phase	0	Nil.	K0 procedure	IJnassIgned	0.00	a	a	1	1
excavation	1	0	Plastic analysis	Staged CDOStructIon	0.00	1	1	2	2
SIIoIcrete Installation	2	1	PlastIc analysis	Staged CDOStructIon	0.00	2	2	3	5
Anal lining installation	3	2	Plastic analysis	Staged CDOStructIon	O.()()	3	3	6	7
Grout (RemaInder InJ pree. -5 bars)	4	3	PlastIc analysis	Staged oonstructIon	0.00	1	4	8	12
PI-I0 bars	5	4	Consolidation (EPP) analysis	Staged 0II15InJdjCJ1	60.00	5	5	13	21
PI~U bars	13	4	COnsoIIdatton (EPP) analysis	Staged construction	60.00	13	13	n	85
PI-14 bars	12	4	ConsolidatIon (EPP) analysis	Staged CDOStructIon	60.00	12	12	34	12
Plz16 bars	11	4	ConscHdatIon (EPP) analysis	Staged construction	60.00	11	11	86	94
PI-18 bars	10	1	ConsolidatIon (EPP) analysis	Staged CDOStructIon	60.00	10	10	95	103
PI-2Obars	6	4	ConsdIdatIon (EPP) analysis	Staged construction	60.00	6	6	23	27
PI-2S bars	7	1	consolidation (EPP) analysis	Staged construction	60.00	7	7	28	33
PI-3O bars	8	1	Consolidation (ePP) analysis	Staged construction	60.00	8	8	43	59
PI=35 bars	9	4	Consolidation (ePP) analysis	Staged construction	60.00	9	9	60	76

Figure 6.12: Detailed internal water pressure simulation (consolidation analysis)

Results of the simulation are presented in the next chapter.

7 Results, model calibration and analysis of results

7.1 Introduction

In the previous chapter, several numerical simulation of construction stages and operational loading of pressure tunnel were carried out. The results of numerical simulation are presented in two stages namely:

1) Model output before calibration (which defmed the tunnel as unsupported) and sensitivity study;
2) Model result after calibration using parametric study (which defmed the tunnel as supported), followed by secondary sensitivity analysis. Additionally, detail result of numerical analysis of the pressure tunnel is presented. Figure 7.1 shows the design flow chart.

Figure 7.1: Flow chart for results of numerical design of plain concrete pressure tunnels

7.2 Model result

The model results of the simulation of deep tunnel showing the initial state of stresses, excavation stage and shotcrete installation are presented below:

7.2.1 Loading -0- Initial State of stresses

The simulated results for initial state of stresses in vertical and horizontal directions are as shown in figures 7.2a and 7.2b respectively.

Figure 7.2a: Vertical stresses in rock mass (shading)

Figure 7.2b: Horizontal stresses in rock mass (shading)

7.2.2 Loading -2- Excavation stage

The simulation of excavation phase followed after the initial state of stresses in the rock mass has been determined, In this case, the total pressure exerted by the rock mass is simulated to be entirely carried by annulus of rock which surrounds the excavation. The results of rock mass stresses redistribution in vertical direction and horizontal direction due the pressure relief are shown in figure 7.3 while figure 7.4 respectively.

Figure 7.3: Redistribution vertical stresses in rock mass (shading)

Figure 7.4: Redistribution horizontal stresses in rock mass (shading)

The shear stress distribution in the vicinity of the excavation is shown in appendix B2.3

7.2.3 (Loading -3-) Shotcrete lining installation.

The shotcrete lining is modelled with *(f3* = 0) no rock load acting on it. This is done to have a feeling of the accuracy of the model set up. The deformation in the mesh before and after the shotcrete installation is shown in figure 7.5.

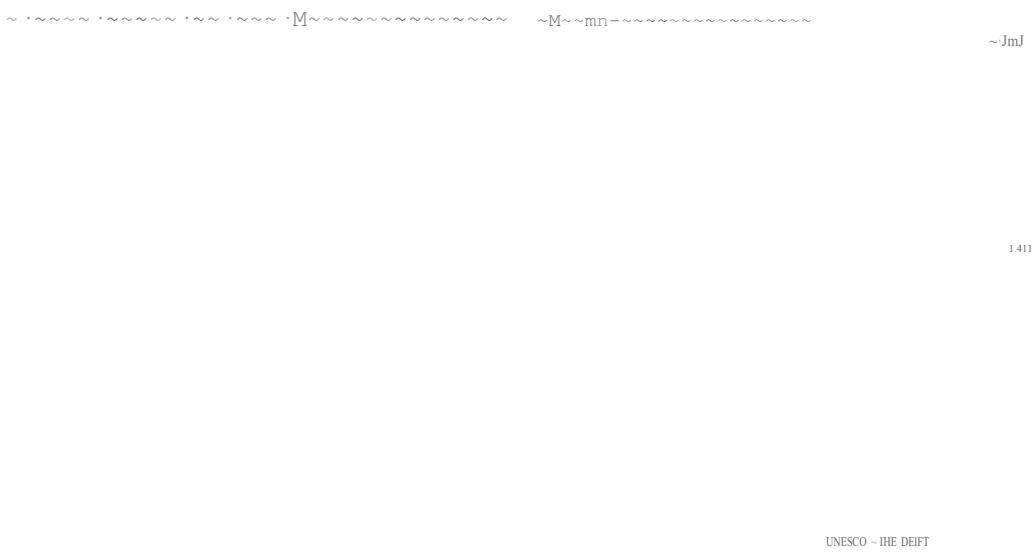

Figure 7.5: Deformations before and after shotcrete installation

7.2.3.1 Sensitivity study

In order to ascertain the accuracy of the set-up as well as understanding the internal forces in the lining, a sensitivity analysis has been carried out on the shotcrete lining. This is done by keeping the subsurface parameters constant while the thickness of the shotcrete lining is varied. The tunnel thickness is varied between 0 and 200mm at 25mm interval. The result is presented in appendix B4.

7.3 Model results after calibration

The results of (loading -0-) initial state of stresses is still valid as before after calibration. This is because the calibration is done at the excavation stage. The first stage (loading -1-) is the relief stress using load factor which have to be determined through parametric study in order to simulate the 3D arching effect of the excavation support. This stage forms the basis for the model calibration.

7.3.1 Parametric study/Calibration result

In order to simulate the stress relief around the excavation boundary, parametric study has been carried out to determine load reduction factor, *f3*. The load reduction factor is varied in range between 0 and 1 (i.e. 0 :::;*f3* :::; 1) and suitable value of *f3* = 0.64 for the selected case have been found. A calibration is performed by the normal stresses in the shotcrete lining, that in the Ermenek project have been measured and in the geological conditions similar to the selected rock mass parameters (list of rock mass properties and their values) the normal compressive force in range of 1000 kN has been observed.

The result of axial forces in the lining for simulated $f3$ values is shown in appendix C1. An approximate uniform normal compressive stress in the range of 1000kN has been observed. The Axial force envelopes and their corresponding load reduction factors are shown in appendix C2.

7.3.1.1 Performance of the models

After the calibration, the performance of the two models is compared in terms of axial forces in the lining and total deformation of the tunnel.

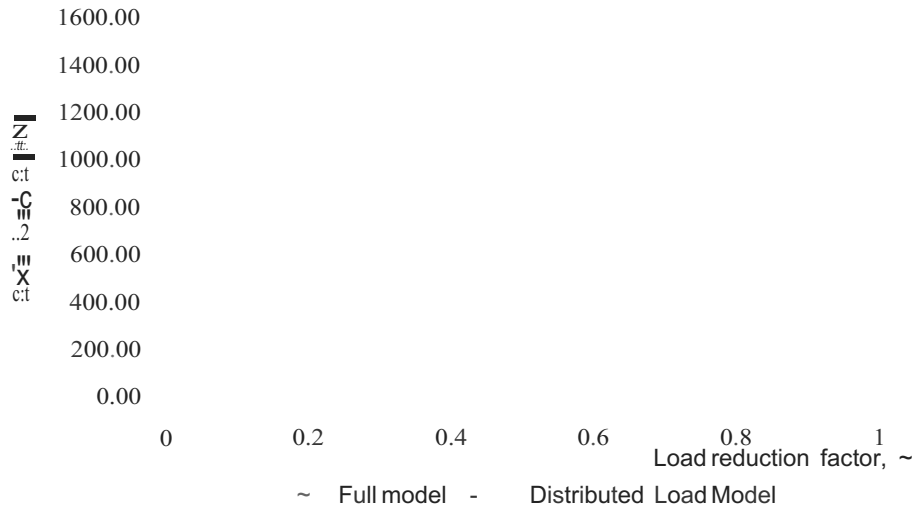

Figure 7.6: Effect ofload reduction factor on the internal forces in the lining

Figure 7.6 and figure 7.7 shows the effect of load reduction factor on the internal forces in the lining and on the total deformation respectively for the two models. The table of values is shown in (appendix C1).

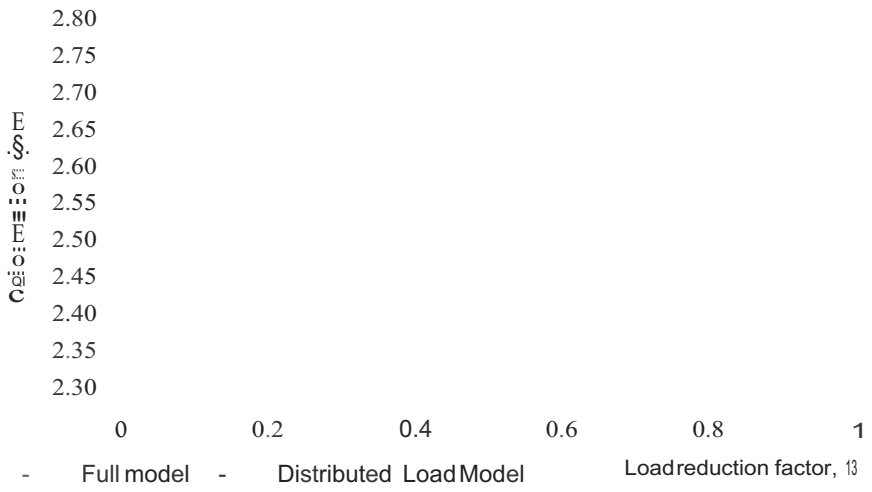

Figure 7.7: Effect of load reduction factor on total deformation.

The result of significance of load reduction factor on relationship between axial forces in the shotcrete and total deformation for the models is presented in figure 7.8.

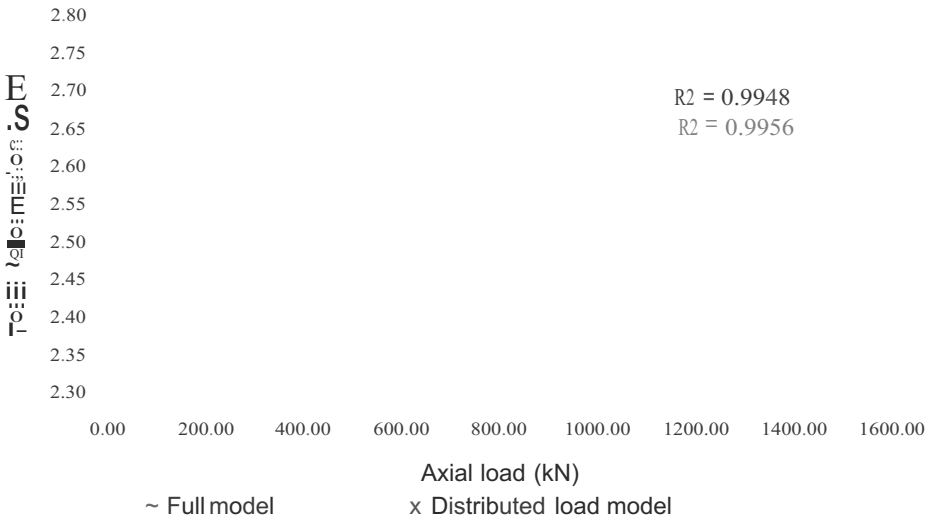

Figure 7.8: correlation between internal force and deformation

7.3.2 Loading -2- Excavation stage

The simulation of excavation is carried out after calibration using $f3 = 0.64$. The stresses in the vicinity of excavation are shown in appendices C4.2.1, C4.2.2 and C4.2.3.

7.3.3 Loading -3- Shotcrete lining installation

The simulation of the shotcrete lining followed a simulated sequence of rock excavation. Appendices C4.3.2, C4.3.3 show the respective vertical and horizontal distribution of stresses around the shotcrete while the deformed mesh is shown in appendix C4.3.1.

7.3.3.1 Result of sensitivity Analysis on the calibrated model

Having obtained the value of $f3 = 0.64$, load reduction factor for model calibration, that gives equilibrium position of the pressure distribution after excavation of the opening and installation of the shotcrete lining of the tunnel.

The tunnel thickness is varied intervals by holding the $f3$ and subsurface parameters constant (see appendix C3). This leads to understanding of internal forces in the lining. The results of the effect of variation of shotcrete lining thickness on internal forces and deformation are shown in figure 7.9 and figure 7.10 respectively.

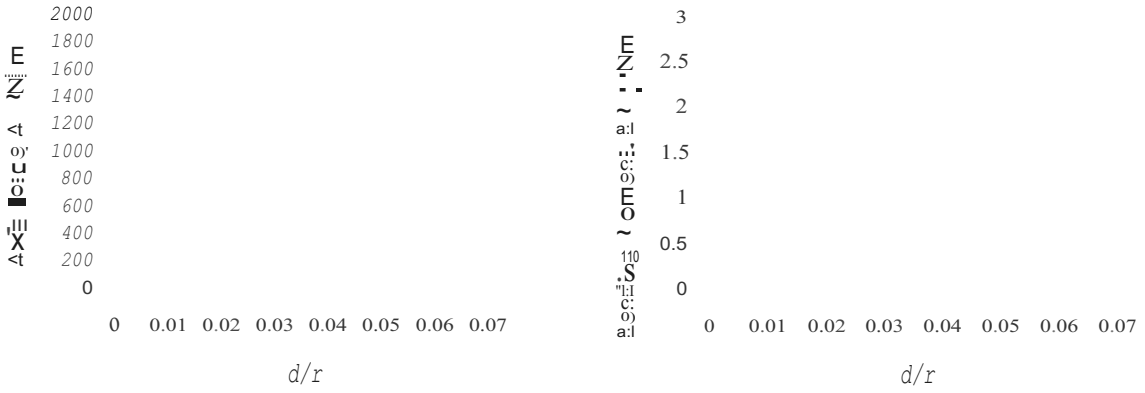

Figure 7.9: Effect of thickness variation on axial forces and bending moment in the lining

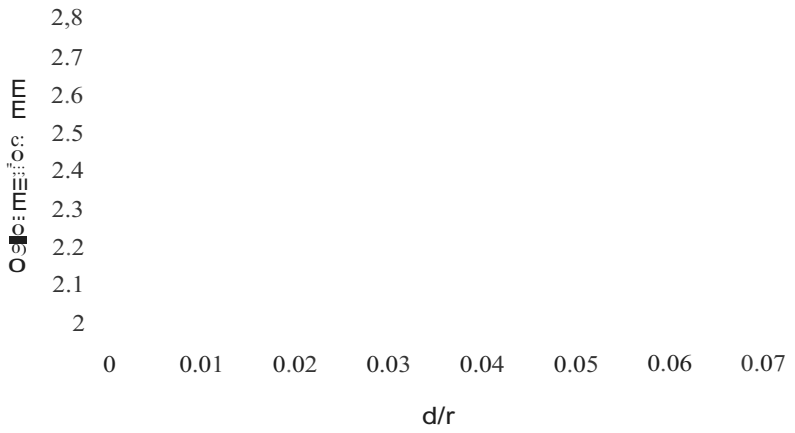

Figure 7.10: Effect of varying thickness of lining on the Liner deformation (P = 0.64)

7.3.4 Loading- 4- Final lining installation

A step-by-step analysis has been performed in order to describe the interaction among rock mass, shotcrete lining and fmallining. The fmallining simulation followed a simulated sequence of rock excavation and shotcrete lining installation with consideration to load reduction factor. The fmal lining is simulated and the result showed the stresses and deformation in fmal is presented in appendices *C4.4.2* and *C4.4.4* respectively.

7.3.4.1 Shotcrete decay simulation

In order to get more feeling of relevant results concerning the final lining, further analysis has been carried out which represents the tunnel condition by assuming loss of strength in shotcrete after a long term. The analysis simulates the shotcrete element decay by reducing the bearing contribution of the shotcrete from *EelEr* = 2 *to EelEr* = 0.2.

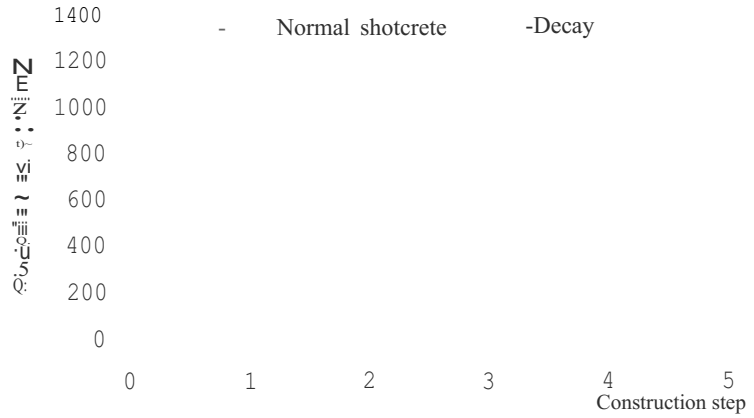

Figure 7.11a: Stresses in fmallining (shotcrete decay effect)

The simulation results showing the change in stress level in the lining and corresponding deformations at the tunnel crown due to shotcrete decay are shown in figure 7.11a and figure 7.11b respectively. The effect of the simulation on principal stresses and total deformations is presented (see appendix C4.6).

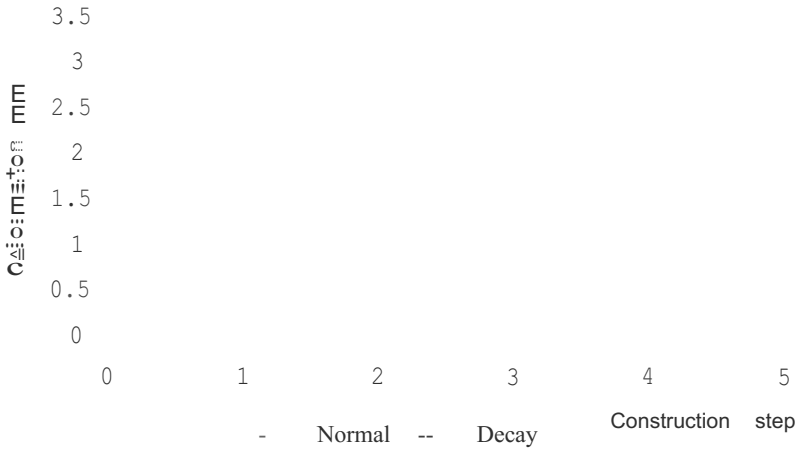

Figure 7.11b: Effect of shotcrete decay on final lining

7.3.4.2 (Loading step -5-) Temperature and shrinkage effect (Gap modelling)

Furtherance to the simulation of fmallining, modelling of the gap due to shrinkage of the linings is carried out by activating the fmal lining interface and introducing volumetric strain into the lining

element. A percentage volumetric strain of (-0.02%) which correspond to 0.001m3/m volume change of concrete is found to have activated the gap. The regular gap is more visible under a scale factor of250. However, the visibility is impaired at the invert.

Figure 7.12: Decoupling of shotcrete and final lining

The results show a clear gap formation under 250 scale factor magnifications Figure 7.12. The normal stresses at the interface of lining before and after shrinkage are shown in (appendices C4.4.5 and C4.4.6) respectively. The respective compressive stresses, deformation and shear stresses in the lining element numbers are shown in (appendices C4.4.3, C4.4.4 and C4.4.5).

7.3.5 Grouting

7.3.5.1 Modelling of contact grouting

Before this loading case, gap is formed between the shotcrete and the fmal lining due to shrinkage effect. The gap is reconstituted with 0.3% volumetric strain prestressing effect on rock mass behind the shotcrete.

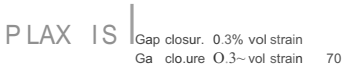

Figure 7.13: Gap reconstitution with 0.3% volumetric strain

The result of grouting the rock mass to reconstitute the gap between the shotcrete and fmal lining is shown in figure 7.l3. Figure 7.14 shows the variation of normal stresses in the rock mass due to positive volumetric strain. The variation is contrary to expectation because the normal stress in the lining is expected to be constant before the closure of the gap and, then, increased after gap is

closed. However, the stress increased with volumetric strain. Based on this, it can be assumed that PLAXIS 2D cannot model the contact grouting.

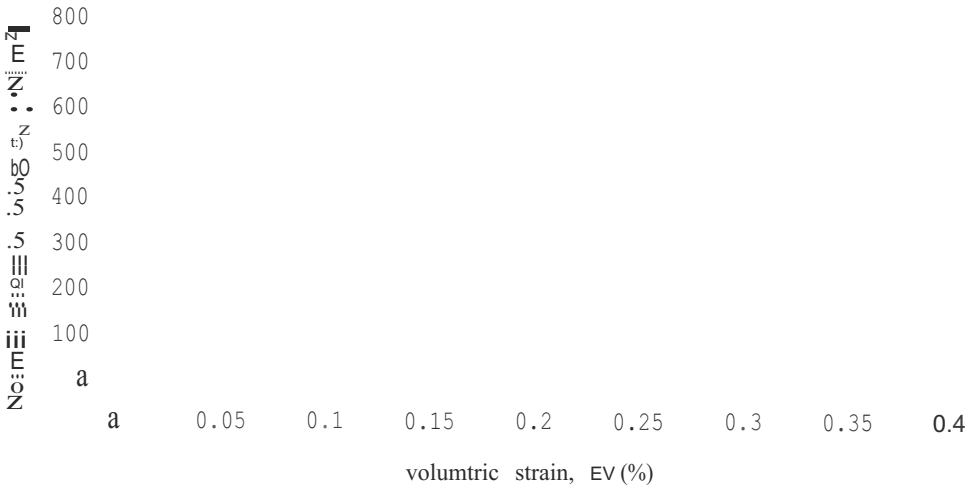

Figure 7.14: Normal stresses in lining due to positive volumetric strain

7.3.5.2 Modelling of prestressing

The result of simulation of the prestressing effect of the rock mass with 5 bars of pressure (after all losses) is presented in (appendices C4.7.3 and C4.7.4). The significant of grouting on the bearing capacity of the rock is shown in figure 7. 15.

(a) With grouting (b) Without grouting

Figure 7.15: Increase in load bearing capacity of lining

7.3.6 Internal water pressure

7.3.6.1 Consolidation analysis

Case 1: *Simulation of seepageflow in lining due to high internal waterpressure*

$P_{i1} < P_{i2} < P_{i3} < P_{i4} < P_{iS}$ and $K_{C1} = K_{C2} < K_{C3} < K_{C4} < K_{cs}$

The result change of internal water pressure on stresses in the lining, grouted zone and rock mass zone is presented in table 7.1 and the [mite element result sheet is shown in appendix C4.8.19.

Table 7.1: Stresses (13 *(kN 1m2)* in the elements (crown)

SIN	Pressure (bars)	Stress in Lining (Element 2715)		Grouted zone (Element 1650)		Rock zone (Element 120)	
		(J1	(J3	(J1	(J::1	(J1	(J::1
1	10	1678	605.00	9042	1572	6283	2324
2	20	1758	20.130*	9022	2160	6367	2230
3	25	2194	3.671*	9024	2548	6424	2172
4	30	2577	1.026*	9024	2927	6484	2112
5	35	2980	0.213*	9026	3310	6545	2053

*- cracks in concrete (tensile strength of concrete is exceeded)

Appendix C4.8.1 present the tension crack developed in the lining during loading operation.
The [mite element result sheets for the prestressing effect, the loading operation for the simulated internal water pressure is available in appendices C4.8.4 through C4.8.9. The water force in the tunnel is shown in figure 7.16.

(a) Pi = 20 bars (b) Pi =35 bars

Figure 7.16a: Water force in the tunnel

7.3.6.2 Groundwater flow analysis

The corresponding seepage through the lining is simulated using groundwater flow analysis. The detailed [mite element results are provided in appendices C4.8.11 through C4.8.15. The numerical result is compared with analytical solution ofSchleiss using equation 3.44. The analytical iteration

Figure 7.16 b: Flow pattern of seepage out of tunnel above groundwater table.

assumed $K; = Kg$ as applied to the numerical simulation. The water loss in the tunnel can be computed as follow:

Water losses = q x rrDd x 10_6 *llslkmlbar*

Where D= tunnel internal diameter and d =equivalent thickness of the lining

The reach of seepage flow through liner by inner pressure increment and the amount of leakage calculated is shown in table 7.2.

For 10 bars of pressure (numerical values) of $q = 1.6 \times 10\text{-}6$ *m] s:*

Water losses, $Q_{wl} = 1.6 \times 10\text{-}6 \times rr \times 6 \times 0.3 \times 10_{6/10} = 091$ *llslkmlbar*

Similarly the corresponding water losses for different internal water pressure are as shown in table 7.2.

Table 7.2: Seenaze through lining (Element number 1422) - side element

SIN	Pressure (bars)	Numerical result Seepage, q ex 1O-6m/s)			Water loss *l/sjkmjbar*	Analytical result Seepage, q x *10-6m/s*
		qx	qy	q		q
1	10	1.600	0.034	1.600	0.91	2.175
2	12	1.949	0.043	1.949	0.92	2.629
3	14	2.298	0.052	2.299	0.93	3.052
4	16	2.647	0.061	2.649	0.94	3.449
5	18	2.996	0.070	2.997	0.94	3.851
6	20	3.350	0.079	3.350	0.95	4.220
7	25	6.250	0.067	6.250	1.40	6.680
8	30	7.460	0.646	7.500	1.42	7.950
9	35	8.770	3.093	9.500	1.50	8.970

Figure 7.17 show the seepage flow through the liner to the grouted zone of the rock mass. Computation of seepage flow for analytical solution is shown in appendix C4.9.

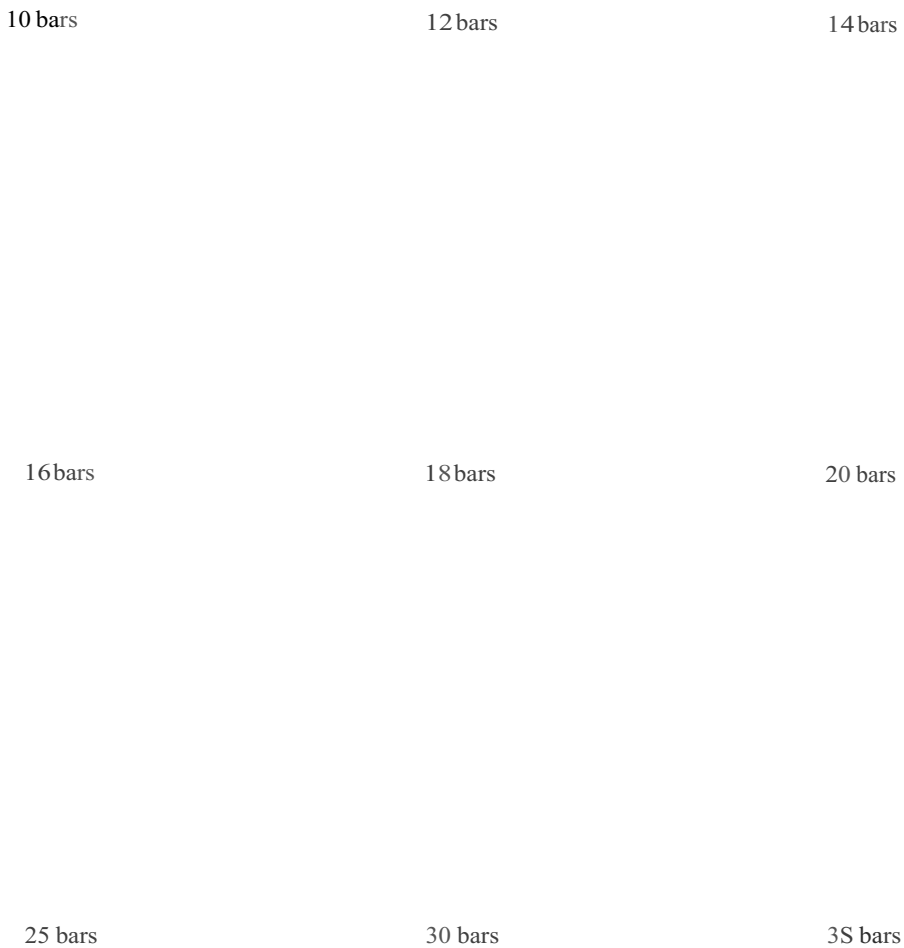

Figure 7.17 Seepage flow through the liner with different internal water pressure.

7.3.6.3 Groundwater flow analysis

Case 2: *Simulation of seepageflow in lining due to high internal waterpressure*
(Pi = 25 bars and K, = variable)

The result change of rock mass permeability on seepage flow through lining, grouted zone and rock mass zone is presented in table 7.3. The detail fmite element results are provided in appendices C4.8.18.

Table 7.3: Seepage through lining, grouted zone and rock mass (tunnel side elements)

SIN	Kc/ K;	Seepage, q x lO-6m/s Lining (Element 1137)	Grouted zone (Element 893}	Rock zone (_(_Element108~
1	1.000	6.162	2.96	5.735
2	0.100	9.474	8.261	10.077
3	0.020	9.329	10.318	12.140
4	0.002	8.821	56.280	66.977

The simulation result of seepage flow through the lining with different rock permeability is shown in figure 7.18.

Krl = 1 x 10-7

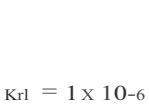

Krl = 1 x 10-6

Figure 7.18: Reach of Seepage flow through lining, through the grouted zone into rock mass of higher permeability (Pi = constant).

Figure7.19 shows extend of the reach of the seepage outside the grouted zone for rock of higher permeability.

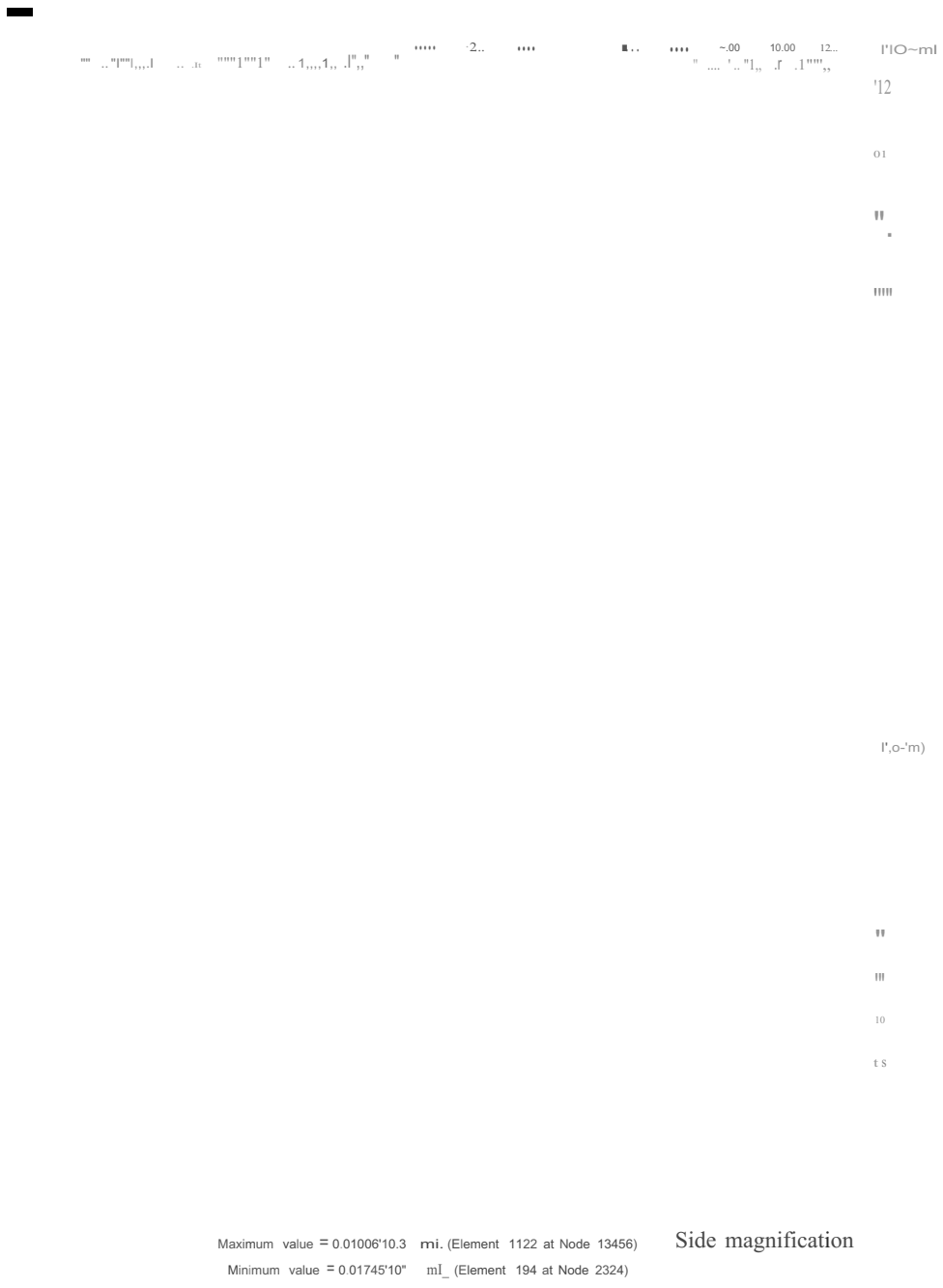

Figure 7.19: Reach of seepage out of grouted zone of tunnel above groundwater table.

8 Discussion of results

8.1 Introduction

The result of numerical simulation of pressure tunnel using PLAXIS 2D fmite element program is discussed herein. The discussion is based on results obtained from simulation of construction stages and different loading cases in high head pressure tunnel. Further results of sensitivity and parametric studies are explained. The results of seepage flow and water losses in the tunnel through cracked concrete lining are compared with analytical solution.

8.2 Full model: discussion of results

The discussion of fmdings on how excavation stage and installation of the shotcrete lining affect the equilibrium state of the rock mass is explained in the following sub-sections:

8.2.1 Initial stage

At this stage, there is no deformation, strain and shear stresses in the ground indicating that the full overburden depth is assumed not cause any settlement. The initial state of stresses defmed by the overburden depth in vertical, horizontal and out-of-plane directions are about 5200 kN/m_2, 4200 kN/m_2 and 4200 kN/m_2 respectively. These stresses give the initial equilibrium state of the ground before intervention (see figure 7.2a and 7.2b).

8.2.2 Excavation phase $(p = 0)$

The modelling of excavation work shows deformation of the rock mass as a result settlement due to relative movement of the overlying rock mass strata. This led to generation of shear stresses. The equilibrium state of the ground is disturbed due to deformations resulting from removal of rock mass is the excavated area. The deformation is gradual, resulting in redistribution of stresses in all directions until a new (secondary) state of equilibrium is attained. The redistribution of stresses is concentrated in the rock close to the tunnel and, at a distance of about three times the radius from the centre of the hole; the disturbance in in-situ stress field is negligible (see figure 7.3 and figure 7.4). The shear stress concentration is high around the tunnel surrounding rock mass but decreases outwards. Observation shows that the excavation stage brought about stress relief at the boundary of excavated tunnel.

8.3 Discussion of model result after calibration and sensitivity analysis

The step-by-step removal of ground elements and installation of tunnel lining is a 3D settlement analysis simulated from 2D point of view using load reduction factor method. Discussion of fmdings on the appropriate $f3$ value which form the basis for model calibration as related to the project site range of values for normal compressive forces in the lining is discussed below. The results of the two models set up are highly correlated and further sensitivity study is discussed herein.

8.3.1 Discussion of parametric analysis result

From figure 8.1, before excavation, initial radial stress is the same as the initial state of stress in the rock mass. Immediately the excavation starts, the reduction factor applies because the natural

equilibrium of the rock is disturbed. The load reduction factor defines the degree to which the lining is unloaded due to rock mass being allowed to converge. The reduction factor increases as the excavation progresses leading to decrease in deformation around the opening as the shotcrete takes part of the rock pressure. This implies that the shotcrete lining partly confmes the convergence and reduces deformation.

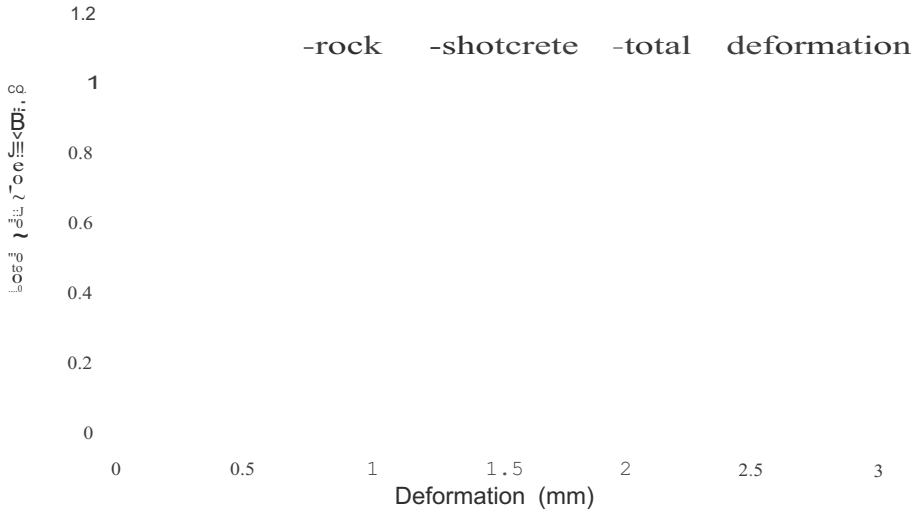

Figure 8.1: Rock mass -lining characteristic curve (Element 7, Node 2873, Crown).

Since the installation of the lining does not immediately stop the deformation of the rock mass, the effect continues until a stage where the rock mass - support system attains a state of fmal equilibrium. At this point, a load reduction factor of 0.64 gives approximated uniform normal compressive forces in the range of 1000kN in the lining (see appendix C2 and FE result sheet C4.3.7).

8.3.2 Performance results of full model and distributed load model

The models give approximate results in terms of axial forces and total deformation in the tunnel (see figures 7.8 and 7.9) during calibration. The load reduction factor, $f3 = 0.64$ gives the almost the same values for the inner force and total deformation at the secondary equilibrium state. The result in figure 7.10 shows a perfect correlation between the two models. Hence, both models are found adequate for further analysis.

8.3.3 Stress level around excavated tunnel $(JJ = 0.64)$

The deformation as a result of excavated rock mass reduces because part of the support pressure is transferred to the shotcrete lining. Additionally, principal stresses and shear stresses decrease as well at the excavation phase. After the installation of lining, the stress concentration increases due to confmement of the rock material (see appendix C4.3.5). The stress concentration becomes negligible sideways at approximate distance about three times the tunnel radius. Stresses become normalized at the distance about four times the radius of the tunnel (see appendices C4.3.3 and C4.3.4).

The installation of shotcrete brought about 12% reductions in total deformation when compared to an unsupported tunnel in the initial model set-up. The 2D simulation of 3D effect resulted into about 25% transfer of the rock pressure to the support lining. The redistribution overstresses part of the rock around the tunnel and makes it yield (see appendix C4.3.6).

8.3.4 Discussion of result of sensitivity study $(p = 0.64)$

With load reduction factor of 0.64, part of support pressure is transferred to the shotcrete. The shotcrete becomes loading bearing member. Increase in lining thickness result to increase in axial force because the stiffness of the member is equally increasing as (E constant). Since the forces acting in the lining are getting bigger, the moment of resistance tend to increase. This agreed with the fmding of Carter and Booker, (1984). The increase in forces in relation to stiffness distribution between the rock mass and shotcrete result in decrease in deformation in the liner (figure 7.9). The liner forces reduce the impact of the pressure from the rock mass. The thickness of the shotcrete lining is proportional to tunnel deformation (figure 7.10). Therefore, increase in the thickness of the shotcrete lining resulted in an increase in compressive stress in the shotcrete lining. Part of 3D arching effect produces deformation and stresses in the shotcrete, hence total deformations is smaller than by unsupported tunnel.

8.4 Discussion of result of numerical study of tunnel final lining

The results of the step-by-step analysis shows that fmal lining is not subjected to significant stresses because most of the load has been carried by the shotcrete lining (appendix C4.4.2). The stresses found in the lining are attributed to the self weight of the fmal lining. This is because much of the support pressure has been taken by the shotcrete. The maximum stresses are found at the extrados of the lining while the minimum stresses are observed at the intrados. The normal stresses and the shear stresses at the interface boundary of the lining are very negligible (order of $6kN/m^2$) when compared to the loads on the shotcrete (appendix C4.4.5).

8.4.1 Shotcrete decay

The results show increase stresses in the final lining as deformations as seen in the finite element result sheet, appendices C4.6.1, C4.6.4 (crown elements) and C4.6.2, C4.6.6 (side elements). The deformations in the lining increased to about three times the initial value, ever though, it is small due to the quality of rock material. The deformation resulted into transfer of about 30 % of force from shotcrete and the force is distributed in 30cm thick fmallining and gives approximately 10% stresses in shotcrete. This shows that bearing of external loads in the long term will be partly taken by the final lining.

8.4.2 Gap formation

The results show gap formation under 250 scale factors (figure 7.12). The normal stresses at both crown and sides of the lining interface are zero values indicating that no external force is acting on the lining. Nonetheless, compressive normal stresses in the maximum range of $6kN/m^2$ have been found at the invert of the lining and shear stresses are negligible (appendices C4.4.5 and C4.4.6). The gap indicates decoupling of the fmallining from the shotcrete. This is usual in practice during concrete curing and initial filling due to temperature change in the lining. The activation of interface of the lining represent the spraying of white wash (in practice) which acts as bond breaker and facilitate gap opening during loading operation.

8.5 Grouting

8.5.1 Contact grouting

The application of volumetric strain to shotcrete and/or [mal lining is found impossible to reconstitute the gap formed between the support measures as the elements body collapsed during simulation. However, prestressing the rock mass with 0.3% volumetric strain was found adequate for the closure of the gap (figure 7.13). However, the result contradicts expectation. It is expected that before the closure of the gap, the stresses in the lining be constant and increase after the gap is closed (see figure 7.14). Based on this fact, it can be inferred that PLAXIS 2D program cannot model contact grouting.

8.5.2 Consolidation grouting

The result from appendices 4.7 shows that prestressing of the rock mass increase the bearing resistance in the lining from say 100 kN/m^2 to about 4000 kN/m^2. The prestressing effect provides external pressure acting upon lining increases the stiffness of the rock mass and reduces rock permeability.

8.6 Internal water pressure

8.6.1 Consolidation analysis

The lining is found to be compression with 10 bars internal water pressure and (no crack is visible). Further increase of water pressure in the tunnel results in tension crack (appendix C4.8.1). This implies that the tensile strength of the lining is exceeded. As the inner pressure in the tunnel is increased, the stiffness matrix of the element will change as soon as concrete cracks. In order to understand the transition of concrete stresses from compression to tension and obtain the point of initiation of cracks, the internal water pressure is gradually increased from (10, 12, 16, 18,20,25,30 and 35 bars). The result is analyzed in figure 8.2 and 18 bars of internal water pressure was found to initiate the cracks. Increase in pressure increase the number of cracks as well as sizes thereby changing stress field. The change in permeability is introduced for each simulation to reflect reality because change in crack width corresponds to change in permeability of the medium. The prestressing effect increases the bearing capacity of the rock mass which reduce the tensile stresses in the lining (figure 7.15). Increase in tensile stresses by water pressure lead to decrease in compressive stresses in the lining.

The porewater pressure in the grouted zone increase with increase in inner pressure and attain its peak value at 20 bars pressure correspondence (Figure 8.2). The different between the internal water pressure and pore pressure at the contact of the lining - surrounding rock mass decrease leading to decrease in tensile stress in the lining while the suction pressure is constant. Based on continuity of flow, increase in the magnitude of hydraulic pressure at the liner - rock boundary will tend to attain equilibrium. This is because the rate at which water is leaking through the cracked lining is more than the rate at which it seeps into the surrounding rock mass due to prestressing effect. The prestressed rock provides the lining good resistance to the inner water pressure by reducing the rock permeability and increasing the compressive strength of the concrete. This explains why there is no significant difference in tensile stress in the lining under such high internal water pressures of30 and 35bars.

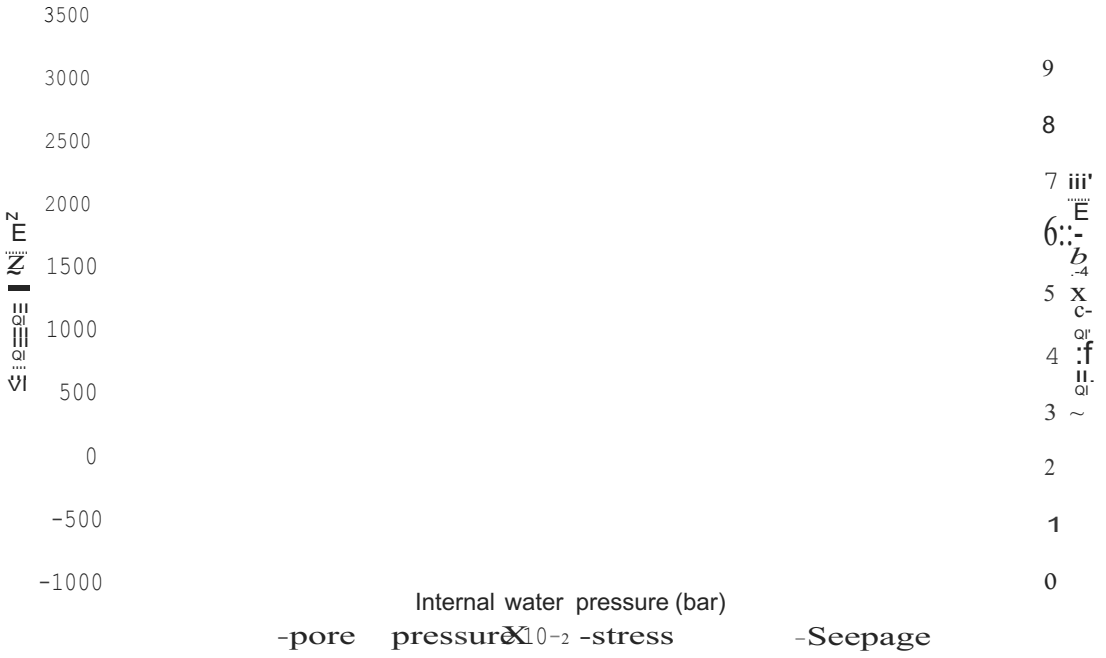

Figure 8.2: Pore pressure, Stress -seepage transformation in lining and internal water pressure

8.6.2 Groundwater flow analysis

Even though, it has been established that the lining is fully in compression for *(Pi = 10 bars),* seepage of water is seen through the liner which confirms concrete liner as permeable (figure 7.17). This result supports the body force theory of Schleiss, (1986, 1987), Kang et al, (2009) and Kai Su and He-gao Wu, (2010).The increase in internal water pressure *(Pi = 18 bars)* cracked the concrete. This results to increased seepage flow through the liner to the grouted zone. The change in permeability is introduced for each simulation to reflect reality because change in seepage flow corresponds to change in permeability of the liner due cracking.

It can be observed that at such high inner pressure of25, 30 and 35 bars, the seepage losses are not significantly different. This is an indication that a steady state of flow because all leaked out water are confined within the grouted zone with concentration at the liner - rock boundary (see figure 7.17). The result showed less difference in seepage losses through the lining at high inner pressure. This confirm the effect of prestressing in plain concrete pressure tunnel even though the rock mass is stable.

Superimposing the consolidation and groundwater flow analyses showed that change in internal water pressure (of cracked lining) result to change in stress field, which, in turn, result to change in permeability of the lining and seepage flow. The performance and accuracy of the model results tested by carrying out seepage analysis using Schleiss analytical solution confirm the validity of the numerical results. The seepage losses from Numerical result and analytical results gave approximate values and the trend is similar. The water losses or leakage in the tunnel are found to be in range of values specified by Schleiss irrespective of the internal pressure (figure 8.4).

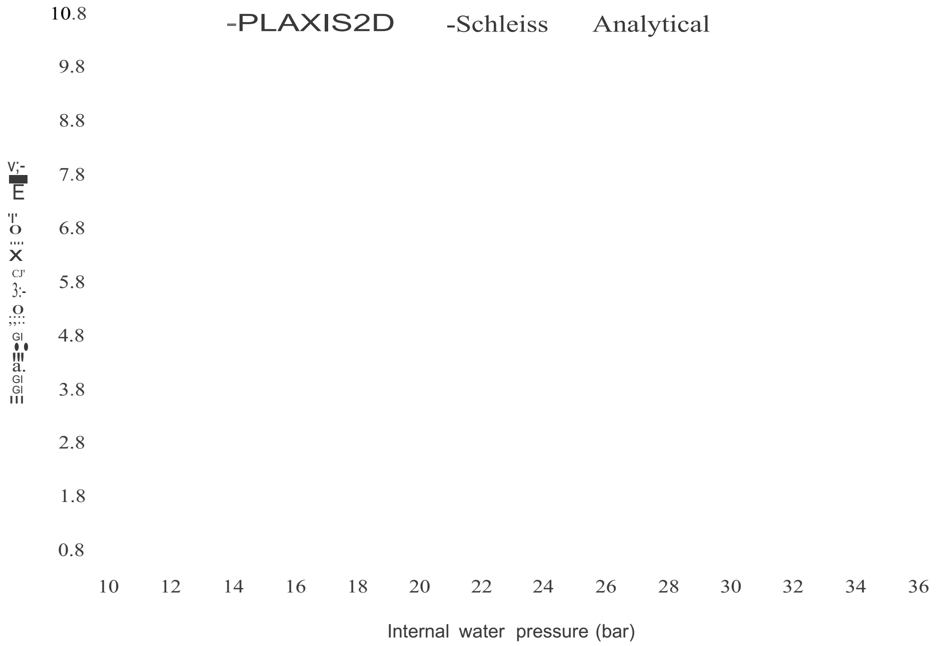

Figure 8.3: Internal water pressure and seepage flow in pressure tunnel

8.6.3 Groundwater flow analysis

V« = *constant* and $K_{r1} < K_{r2} < K_{r3} < K_{r4}$

The result showed that the efficiency of grouting is dependent on the permeability coefficient of the rock mass. The more permeable the ground material the more the reach of seepage flow in the rock. However, the seepage through the lining is reduced by prestressing of the lining even though the rock permeability is increased (see table 7.3). Since the prestressing reduced the rock permeability by increasing its strength, hydraulic pressure is built up behind the concrete lining. Hence, seepage through the rock tends to reduce gradually, this account for drop in seepage flow (table 7.3). The reduction in seepage flow through rock increases the hydraulic pressure and result into strain relief in the lining. However, the reach of seepage flow extends beyond the grouted zone into the un-grouted rock mass (figure 7.18). This may be due to high permeability assigned to the rock mass during simulation, showing the effect of rock permeability on grouting.

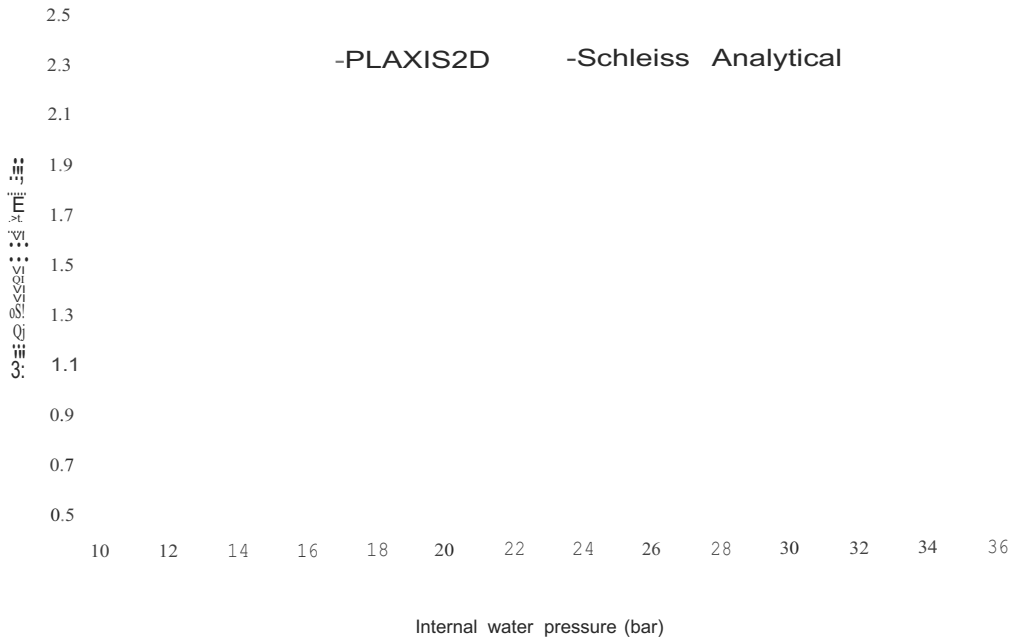

Figure 8.4: Water losses in the pressure tunnel

8.7 Overall assessment ofPLAXIS 2D FE Program as a tool for numerical design of pressure tunnels

Table 8.1: Assessment of PLAXIS 2D Finite Element Program as a tool for design of pressure tunnels

Loading step	Result from PLAXIS 20	Observation	Performance evaluation	Remark
Initial state of stresses	At h=O, $u_x = u_y = 0$,< = O,$CTx\bar{x} = c_{Tyy} = c_{TZZ} = 0$; @ depth $h = hi$ $c_{Tyy} = Y\,hi$ and $CTx\bar{x} = KoY\,hi$ (Geostatic).	The result agreed with literature and expectation.	Satisfactory	
Excavation	Stress relief at the tunnel boundary, decrease in rock pressure, shear stress increase, redistribution of stresses and large deformation.	The result agreed with literature and expectation.	Satisfactory	Deformations and stresses found adequate.
Shotcrete	With P - 0.64, 25% of rock pressure is taken by shotcrete, principal stresses increased at outer vicinity of shotcrete. Lower deformation. Shotcrete become a load bearing member due to arching effect with approximately uniform normal compressive forces.	The result agreed with literature and expectation.	Satisfactory	Deformations and stresses found adequate.
Final lining, temperature and shrinkage effect	The lining is not subjected to any significant stresses. Stresses are maximum at extrados and minimum at intrados of the tunnel. Normal and shear stresses at the boundary of the interface are negligible. The shrinkage resulted in gap formation between the sbotcrete and the final lining,	The result agreed with literature and expectation.	Satisfactory	PLAXIS 2D is found adequate for the simulation of temperature and shrinkage effect.
Decay simulation	Deformations and stresses in final lining increases and tbe lining became a load bearing member	Tbe result gives a good prediction of expectation	ok	Stresses in the sbotcrete after decay seem high.
Grouting	Contact grouting: Gap closure, stress in tbe lining increased before and after grouting.	Contrary to expectation	Un-satisfactory	PLAXIS 20 cannot simulate the phenomenon. Further investigation is required.
	Consolidation grouting: Reduce rock mass permeability, increase compressive strength of lining. Increase the stiffness of rock mass.	Principle of grouting justified as well as its engineerin~ reguirement.	Satisfactory	Performance depends on imported output from analytical solution
Operational loading (IWP)	Cracks are visible under bigb inner water pressure. Stress transformation, seepage flow and hydraulic pressure behind the liner can be linked to stress relief in the liner. The seepage flow due to cracking cbanges the stress field and tbe increased external pressure reduces the gradient between internal and external pressures, thereby reducing seepage and losses.	Tbe result agreed witb expection and literature but technically difficult to explain.	Satisfactory	The analyses would bave been easier if result of one calculation can be imported to another for furtber analysis.

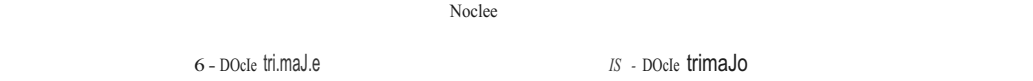

Figure 4.2: Position of nodes and stress point in ground elements
(Source: PLAXIS Reference Manual)

4.4 Geometry model description

4.4.1 Two-dimensional cluster

The production of fmite element model starts with the creation of a geometry model. It is a representation of the problem of interest and consists of three basic components: lines, points and clusters. Points and lines are specified by users, whereas PLAXIS program generates clusters automatically. For example a closed geometric line forms a cluster which represents a ground layer while the points on the edges of the cluster indicate the boundary.

4.4.2 Plates

Plates are structural objects used to model structures (such as tunnel linings, shells and other slender structures) in the ground. In PLAXIS, a distinction can be made between elastic and elastoplastic behaviour of plates. The behaviour of these elements is defmed using flexural rigidity, (bending stiffness) *E1* and a normal stiffness, *EA*. The material properties of plates such as *E1* and *EA* are entered in material data sets.

4.5 Material properties

In PLAXIS 2D, ground properties (modulus of elasticity, Poisson's ratio, cohesion, friction angle and dilatancy) and material properties (unit weight of concrete, Poison's ratio, EA, EI, weight of lining, equivalent thickness, and permeability coefficients) of structures are stored in material data sets. The material data sets consist of four different types: Soil and interfaces, plates, geogrids and anchors. For the research work, the soil and interfaces, and plates are mainly used. The rock parameters are stored in the soil and interfaces data set while the shotcrete and lining parameters are stored in plate data set. However, shotcrete and lining parameters can be stored in soil and interfaces data when modelled as triangular element.

4.5.1 Modelling of ground behavior

In most cases, ground behaves in a highly non-linear way under load. PLAXIS 2D supports nine (9) different material models to simulate ground behaviour under different conditions that are close to reality. These models and their parameters are explicitly discussed in the Material Models

Manual. Among these material models, a robust and simple non-linear (Mohr-Coulomb) model is selected for this research work.

4.5.2 Mohr-Coulomb model and Parameters

A well-known (elasto-plastic) Mohr Coulomb model involves five parameters namely: Young modulus, E, Poisson's ratio, *v,* for rock elasticity; cohesion, c, and friction angle, *cp* for plastic analysis, and dilatancy, I/J. The model is considered as first order approximation of ground behaviour. It works on the principle of a constant average stiffness for layers of ground. The constant stiffness makes computation to be relatively fast and a first estimate of deformation is obtained. More so, increase in stiffness with depth can be taken into account using the model. In general, the states of stress at failure are well described using the Mohr-Coulomb failure criterion with effective strength parameters.

4.5.3 Material type

In principle, all model parameters in PLAXIS are represented in terms of effective ground response, that is, the relationship between stresses and strains is a function of ground skeleton. However, the pore water is taken care of, as PLAXIS offers choices of three types of behaviour: Drained, undrained and non-porous behaviours (Material Models Manual).

The drained behaviour setting is used for the research work, meaning no excess pore pressures are generated under plastic analysis. This is a case of dry ground and/or low rate of loading. This option allows the simulation of long term behaviour without the exact history of undrained loading and consolidation.

4.5.4 Constitutive equations

The constitutive equations for Mohr-Coulomb model are available in (PLAXIS 2D, Material model manual). The basic equations of continuum deformations, water flow (seepage) and consolidation including the finite element discretisation can be found in PLAXIS 2D, Scientific manual).

4.5.5 Interface behaviour and parameters

Interfaces are joint element available to model ground-structure interaction. For example, these elements are can be used to simulate the zone of shearing material at the contact between a shotcrete and the fmallining. The values of interface friction angle and cohesion are defined by an associated strength reduction factor for interface *(Rinter).* The *Rinter* is a Coulomb criterion used to distinguish between elastic and plastic behaviour of interface. The interface properties are calculated from the ground properties in the associated data set as follows:

(4.1)

$$tancpi = Rintertancpground \sim tancpground \quad (4.2)$$

9 Conclusions and Recommendations

The main goal of this research is to test and verify the use of PLAXIS 2D finite element program as a suitable tool for modeling of the pressure tunnels. Basically, the program is a geotechnical tool and meant for soft soil analysis and not for pressure tunnel. It is approximated in this research as a tool for rock engineering and design of pressure tunnels in rock mass. All salient features of the model (as mentioned in chapter 4) were studied and manipulated to serve the intended purpose as research shown certain level of possibility of using the program for the design of pressure tunnel. In this research, the whole construction stages and loading operation in pressure tunnel is simulated. These tasks were performed in order to study the behaviour of the model. Based on comparison and analysis presented above, the results can be used to observe and/or predict phenomena. However, further research is needed as identified in this study.

9.1 Conclusions

Based on the 2D elasto plastic finite element method, a coupled stress - seepage numerical design of pressure tunnel is studied to simulate the cracking process in the lining of plain concrete pressure tunnel. It must be kept in mind that, with the output results from excavation phase, shotcrete installation and final lining, the mechanical behavior of rock mass is very important in the stability of tunnel because the linings support almost all the distress due to excavation of the opening by the redistribution of stresses around the opening. More so, the shotcrete has provided a confinement by preventing further deformation of materials and enhanced the realization of secondary equilibrium.

The coupling of stress - seepage in pressure tunnel is complex because of the changes in behaviour of material. The effect of internal water pressure on the lining has been studied. The cracks encountered from high internal water pressure are simulated. The hydraulic-mechanical interaction due to change in stress in cracked liner change permeability which results to change seepage flow in the rock zone. The stress field and seepage field affect each other while trying to attain a state of equilibrium. The water flowing out of cracked concrete changed the material behaviour of concrete, the leaked out water were found to be in the usual and accepted range when compared with analytical solution.

The overall assessment of PLAXIS 2D showed that the program is capable of evaluating the rock mass behaviour around pressure tunnels in terms of stresses and deformation, a tool for faster simulation of 3D arching effect, assessing the performance of lining, predicting the effect of internal pressure on the lining, reach of seepage through lining to the surrounding rock mass as well as estimating the leakage in pressure tunnels. However, the package remained not independent in the modeling of prestressing as the injection pressure needs to be related to the volumetric strain using analytical method.

9.2 Recommendations

Based on this research work, the following recommendations for further study are presented:

- Numerical design of pressure tunnels using other material model such as Hoek - Brown model (from PLAXIS 2D Finite Element Program) need to be carried out and results compared, most especially the strength of the materials. For example, the effect of stress level on stiffness of rock can be neglected. On the other hand, the shear strength of the rock mass depend on stress level, a model like Hoek-Brown with non - linear stress dependency

will give a better approximation of the strength of rock at very high stress level because it involves shear strength and tensile strength in its formulation. It is obvious that the tensile strength of rock in this study has been underestimated.

- The effects of groundwater as external pressure on the lining during loading operation and dewatering (during maintenance) in pressure tunnel using PLAXIS 2D needs to be investigated and compare with analytical solution. This will provide a good performance judgement on the program.
- Possibility of modeling contact grouting using PLAXIS 2D should be investigated.
- The research suggest the inclusion of PLAXIS 2D program as additional package for summer courses in Water Science Engineering (WSE) programme most especially for Hydraulic Engineering River Basin Development (HERBD) and, Land and Water Development (LWD) specialization. Additionally, if schedule permits should be incorporated into elective module courses such geotechnical engineering and, storage and hydropower. This will provide a better understanding of other material models that are yet to be exploited.
- New version of the program needs to consider the effect of temperature variation on the properties of materials. More so, a medium for importing results of one analysis to the other needs to be incorporated. For example, importing results of plastic calculation or consolidation analysis to flow mode for groundwater analysis. This may be available in the package, but as the time of reporting this research work, it has not been discovered.
- The research suggests that fewer expectations should be posed on the computability of the model because the model does not guarantee uniqueness of results. Consequently, the practical experience needs to complement model results.

Above all, this research work recommends PLAXIS 2D finite element program as a tool for observing and/or predicting phenomena in pressure tunnels while further research using more real life cases and validation of results with existing methods is recommended for the purpose of justification.

References

Ahmadi, H., Soltani, A and Fahimifar, A., (2007) A [mite element model for the stability analysis and optimum design of pressure tunnels. Taylor and Francis Group, London, United Kingdom.

Alun, T. (2009) Sprayed Concrete Lined Tunnels: An Introduction. Published by Taylor and Francis, Oxon.

Benson, R.P. (1989) Design of Unlined and Lined Pressure Tunnels. Journal of Tunnelling and Underground Space Technology. Volume 4, No 2, pp. 155-170.

Bobet, A and Nam, S.W., (2007) Stresses around pressure tunnels with semi-permeable liners. Rock Mechanics and Rock Engineering. Volume 40(3), pp 287-315.

Brekke, T.L and Ripley, B.D. (1986) Design Strategies for Pressure Tunnels and Shafts. Electrical Power Research Institute Contract No. RP-1745-17

Brown, E.T. and Hoek, E. (1978) Trends in relationships between measured rock in situ stresses and depth ". Int. J. Rock Mech. Min. Sci. & Geomech. Abstract. 15, 211-215.

Carter, J.P., and Booker, J.R, (1984) Elastic consolidation around a lined circular tunnel. International journal of Solids structures Vol. 20 No.6, pp. 589-608.

Craig, R.F. (1992) Soil Mechanics. 5th Edition, Published by Chapman and Hall, London, UK.

Dahlo,T., Evans, K., Halvorsen, A., and Myrvang, A. (2003) Adverse effect of pore-pressure drainage on stress measurements performed in deep tunnels: An example from the Lower Kihansi hydroelectric power project, Tanzania. Journal of Tunnelling and Underground Space Technology.

Dimitrios, K., (2005) Tunnelling and Tunnel Mechanics. Springer- Verlang Berling, Heidelberg, Germany.

Fernandez, G., (1994) Behaviour of pressure tunnels and guidelines for liner design. In. Journal of Geotechnical engineering, Volume 120.

Gregoire, (2007) Numerical analysis and optimization: An Introduction to mathematical modelling and numerical simulation. Oxford University Press, Oxford.

Hartmaier, H.H., Doe, T.W. and Dixon, G. (1998) Evaluation of Hydrojacking Tests for an Unlined Pressure Tunnel. Journal of Tunnelling and Underground Space Technology. Volume 13, No 4, pp. 339-401.

Hendron, A. J., Fernandez, G., Lenzini, P., and Hendron, M. A. (1987) Design of pressure tunnels. The art and Science of Geotechnical Engineering at the dawn of the twenty first century, Prentice-Hall, Englewood Cliffs, N.J., 161-192.

Hoek,E., Kaiser, P.K. and Bawden, W.F. (1998) Support of underground excavation in hard rock. Published by A. A. Balkema, Rotherdam, Netherlands.

Huangfu, M., Wang, M., Tan, Z and Wang, X, (2010) Analytical solutions for steady seepage into an underwater circular tunnel. Tunnelling and Underground Space Technology.

Hudson, J. A. and Harrison, J. P.. (1997) Engineering Rock Mechanics: An Introduction to the Principles. Published by Elsevier Science Limited, Oxford, UK.

Hudson, J. A. and Harrison, J. P.. (2000) Engineering Rock Mechanics: Part 2. Published by Elsevier Science Limited, Oxford, UK.

In-Mo Lee and Seo-Woo Nam (2004) Effect of tunnel advance rate on seepage forces acting on the underwater tunnel face. Tunnelling and Underground Space Technology.

Kai Su and He-gao Wu, (2010) Analysis of mechanical hydraulic interaction to pervious pressure tunnel. Journal of Power and Energy Engineering Conference (APPEEC) Asia-Pacific, pp1-4.

Kang, B., Ming, X. and Juntao, C. (2009) Study on coupled seepage and stress fields in the concrete lining of the underground pipe with high water pressure. Tunnelling and Underground Space Technology.

Kazimierz, T. (1989) Rock mechanics in Hydro-engineering. Elsevier Science Publishers, Amsterdam, The Netherlands. Page 29-61.

Kocbay,A. Marence, M. and Linortner, J. (2009) Hydropower Plant Ermenek, Turkey Pressure tunnel- Design and Construction.

Kreyszig, E. (2006) Advanced Engineering Mathematics. 8th edition. John Wiley and Sons, Inc.

Marence, M (1996) Finite Element Modelling of Pressure Tunnel. Computational Methods in Applied Sciences. Published by John Wiley and Sons Ltd.

Marence, M (2009) Geotechnical design of Underground Structures. In. Underground Construction, pp 563-572, London Hemming Group.

Marence, M and Oberladstatter, A (2005) Design of pressure hydropower plant Ermenek. In ITA 2005, Istambul, Turkey.

Marence, M. (2008) Numerical Modelling and Design of Pressure Tunnels. In. Hydro 2008, Ljubljana, Slovenia.

Marence, M. (2010) Storage and Hydropower Courseware, Module 8, UNESCO-IHE, Delft, The Netherlands.

Mosonyi, E, (1991) Water Power Development - High Head Power Plant. Volume Two/A. Third Edition. Published by Akademiai Kiado, Budapest.

Pietro, L (2008) Design and Construction of Tunnels. Springer-Verlang Berling, Heidelberg, Germany.

PLAXIS 2D Material Manual, 2010

PLAXIS 2D Reference Manual, 2010

PLAXIS 2D Tutorial Manual, 2010

Ponl~,:ich, A, Jae-Hyeung, 1., Chang-Yong, K. and Kyung-Ho, P., (2009) Effect of drainage conditions on porewater pressure distributions and lining stresses in drained tunnels. Tunnelling and Underground Space Technology.

Popescu, I, (2010) Modeling and Numerical Methods Courseware, Module 11, UNESCO-IHE, Delft, The Netherlands.

Schleiss, AJ. (1986) Design of pervious pressure tunnels. Water Power and Dam construction, May, pp21-26,29.

Schleiss, A.J. (1987) Design criteria for pervious and unlined pressure tunnels. Underground Hydropower Plants, Oslo, June 22-25.

Schleiss, A.J. (1997) Design of reinforced concrete linings of pressure tunnels and shafts. Hydropower and Dams, Volume 3, pp88-94.

Seeber, G. (1984) Recent Developments in the Design and Construction of Power Conduits for Storage power stations. Semina Idraulica Del Territorio Montano, Bressanone, Italy.

Seeber, G. (1985) Power conduits for high-head plants - Partl. Water Power and Dam Construction, June 1985.

Seeber, G. (1985) Power conduits for high-head plants - Part2. Water Power and Dam Construction, July 1985.

Shetty, M.S, (2005) Concrete Technology, Theory and practice. Revised edition. Published by S.Chand and Company limited, New Delhi, India.

Seok-Won, L., Jong-Won, 1., Seok-Woo, N, and In-Mo Lee (2006) The influence of seepage forces on ground reaction curve of circular opening. Tunnelling and Underground Space Technology.

Singh, B., Nayak, G.C.,Kumar, R. and Chandra, G. (1988) Design Criteria for Plain Concrete Lining in water and Power tunnels. Journal of Tunnelling and Underground Space Technology. Volume 3, No 2, pp. 201-208.

Sinha, R.S, (1989) Underground Structures - Design and Instrumentation. Elsevier Science Publishing Company Inc. New York, U.S.A

US Army Corps of Engineers (USACE, 1997) Engineering and Design Tunnels and Shafts in Rock", - Engineering manual EM 1110-2-2901, Washington DC.

Verruijt,A (2010) Soil mechanics. Delft University of Technology, 2001,2010

Vahid Galavi, 2010 Groundwater flow, fully coupled flow deformation and undrained analyses in PLAXIS 2D and 3D.

Appendices

A: Short Note on Numerical Simulation of Deep Tunnel Excavation (Model rr- Distributed Load Model)

PLAXIS 2D is designed for shallow tunnel but can be use for model up to 200m height as found in the full model approach of this research work. When the model becomes too high (say above 200m) and the grid is too dense to display, the upper part of the model can be omitted. The weight of the soil that makes the upper part must be compensated for to avoid the generation of unrealistic stresses.

Since the pressure in the rock is proportional to the depth of the overlying strata. A thin layer of thickness says $h_{virtual} = 1$ is created on top of the model to cater for the omitted part. The soil weight in the thin layer is modified as $Y_{virtual}$ and is given by:

$$Y_{vIrtual} = Y_{real} \times h_{realj} \; {}_{hvirtual} = 26 \times 100_j \; {}_1 = 2600kN \; 1m_3$$

Theory of deep tunnel simulation (Source: PLAXIS BULLETIN, 2001)

This approach has been used in the research and found to produce approximate result with the full model. However, the thin layer behaves like a beam element. Priority is given to the full model approach because the 200m is found to be modelled without any approximation. The distributed load theory is adopted for comparison and modelled in PLAXIS 2Das shown below.

II

Distributed Load Model (PLAXIS 2D)

B- Model set-up

Bl- Initial stresses

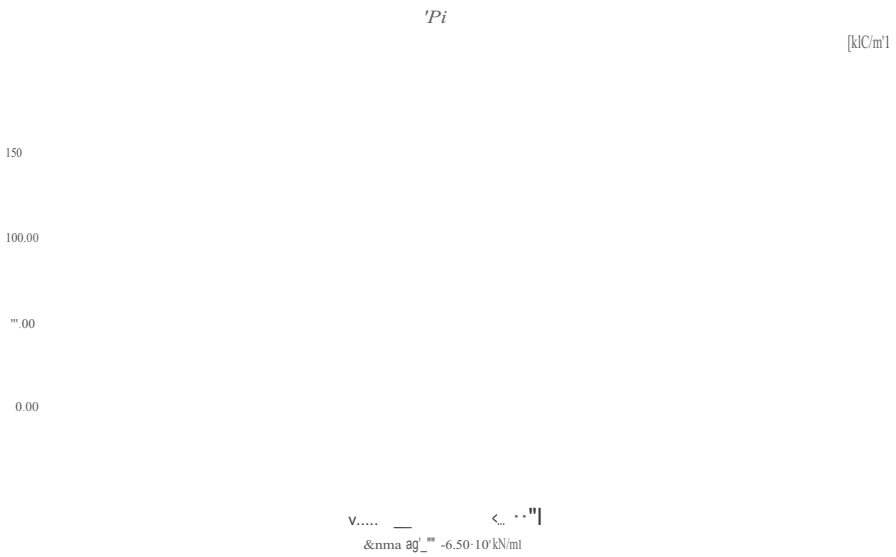

B1.1: Vertical stresses in rock mass (shading)

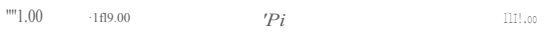

B1.2: Horizontal stresses in rock mass (shading)

B1.3: Shear stresses in rock mass

B2- Excavation phase

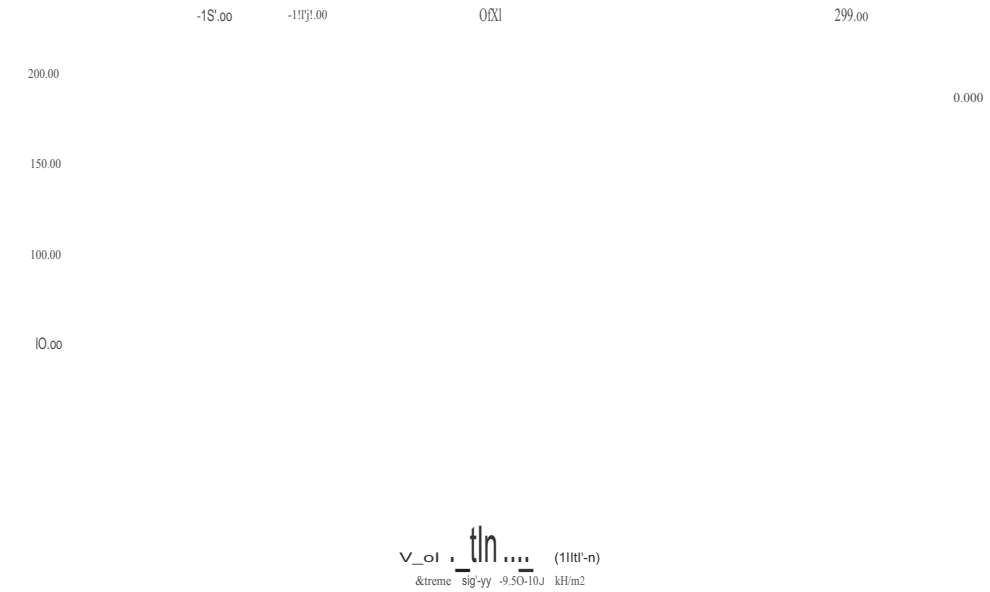

B2.1: Redistribution vertical stresses during excavation (shading)

B2.2: Redistribution horizontal stresses during excavation (shading)

B2.3: Shear stresses during excavation (shading)

Full model

UNESCO· IHE OELFT

B2.3.1: Details ofB2.3

B3- Shotcrete installation

UNESCO· (HE DELFT

B3.1: Deformation around shotcrete

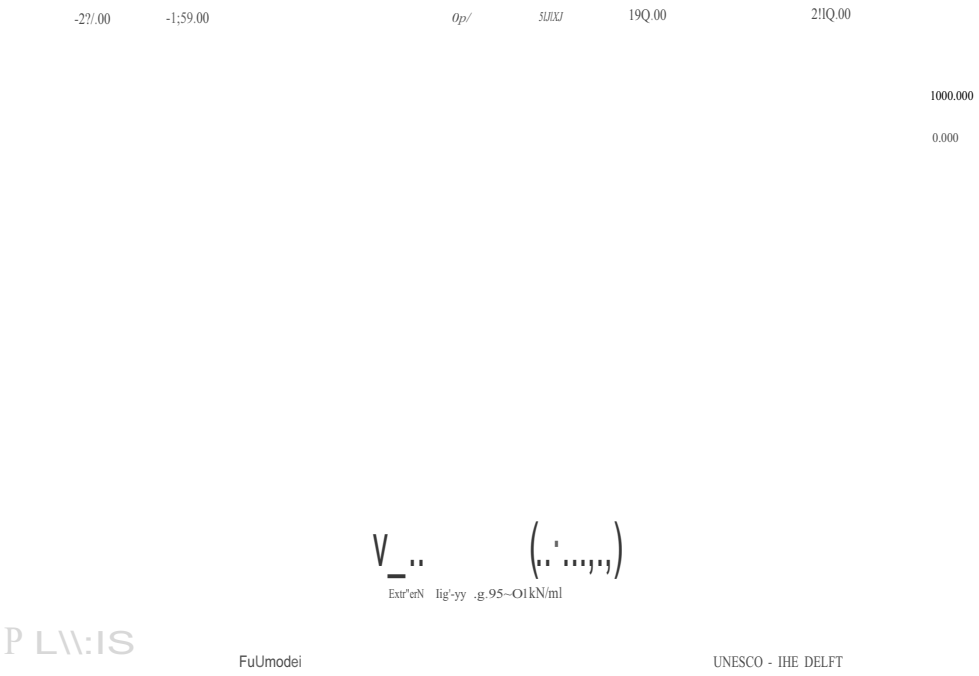

B3.2: Redistribution of vertical stresses after shotcrete installation (shading)

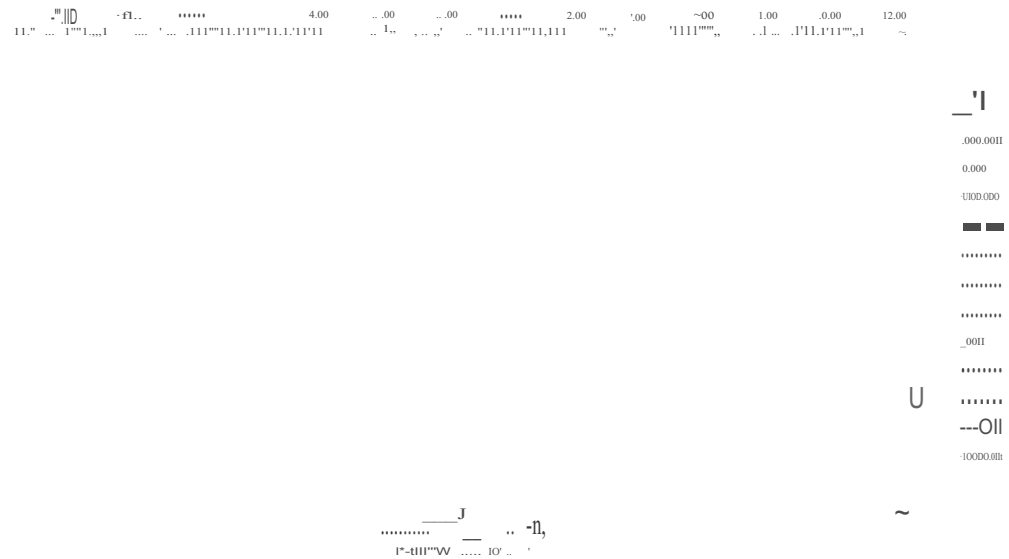

B3.2.1: Details ofB3.2

B3.3: Redistribution of horizontal stresses after shotcrete installation (shading)

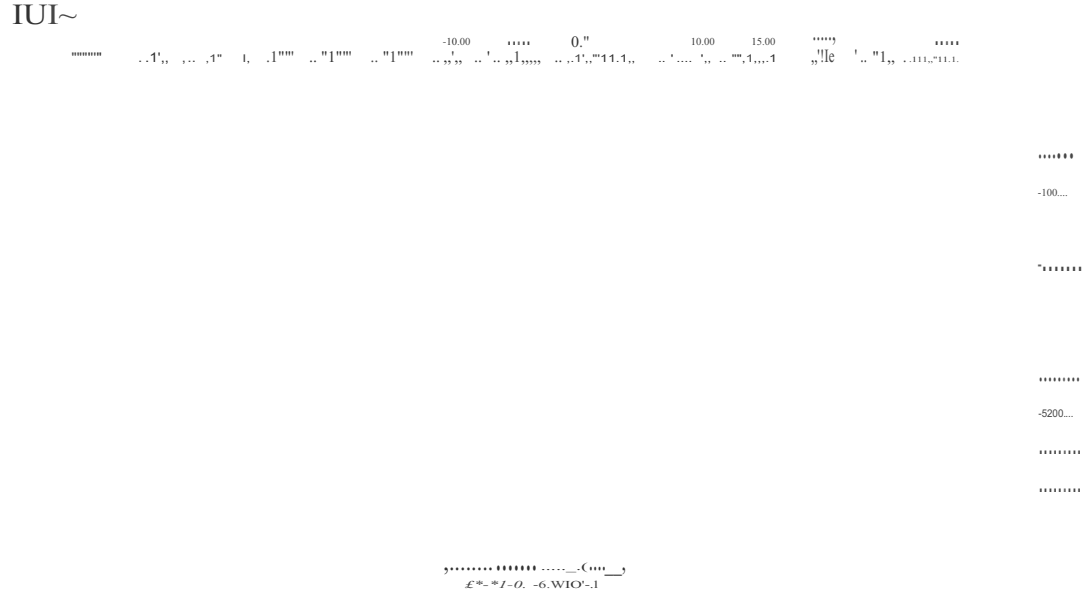

B3.3.1: Details of B3.3

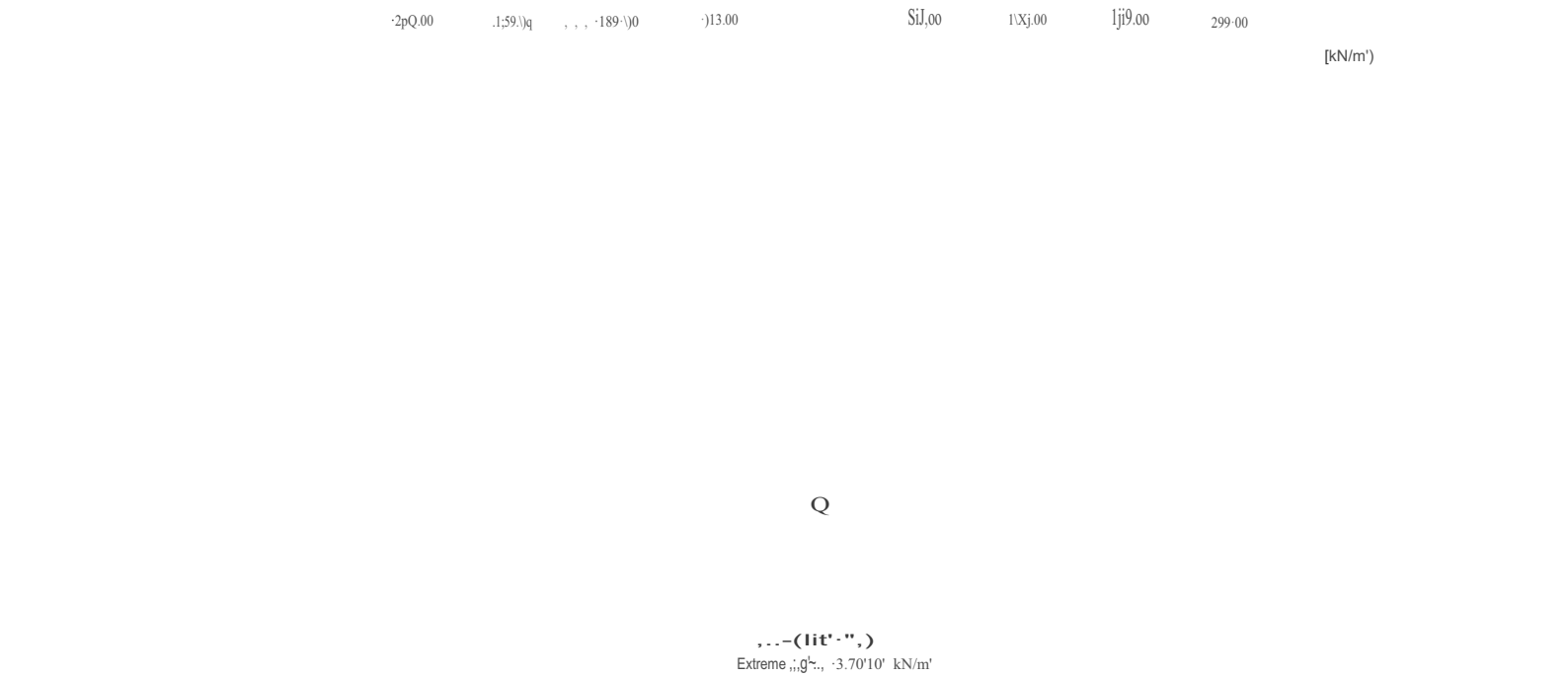

B3.4: Shear stresses around tunnel after shotcrete installation

B3.4.1: Details ofB3.4

B4 - Inner forces in the lining and deformations before and after lining installation

Full model set up
Tunnel radius = 3.00m
p=0

SIN	d (mm)	Axial force, N (kN)	Shear force, Q(kN)	Moment, M (kNm)	Displacement (mm)	Displacement (mm)
1	Unsupported (0)	0.00	0.00	0.000	2.76	2.76
2	25	6.79	1.17	0.048	2.76	2.76
3	50	10.2	2.4	0.123	2.76	2.76
4	75	12.69	3.00	0.196	2.76	2.76
5	100	14.74	3.17	0.270	2.76	2.76
6	125	16.43	3.04	0.327	2.76	2.76
7	150	17.93	2.78	0.382	2.76	2.76
8	175	18.37	2.93	0.431	2.76	2.76
9	200	19.33	2.93	0.444	2.76	2.76
		Forces in compression			after exc.	with Lining

C-Model Calibration

Cl: Parametric study

C1.1: Distributed load Model Results

Parametric study

Dl model (d=100mm)

Sin	/3	*A (kNlm)*	*M(kNm)*	*Displacement (mm)*
1	0	7.89	0.073	2.76
2	0.1	341.75	0.500	2.65
3	0.2	548.11	0.535	2.59
4	0.3	677.32	0.436	2.56
5	0.4	772.25	0.363	2.52
6	0.5	885.42	0.407	2.49
7	0.6	1000.00	0.453	2.46
8	0.64	1050.00	0.461	2.45
9	0.7	1120.00	0.495	2.43
10	0.8	1240.00	0.534	2.40
11	0.9	1360.00	0.56	2.37
12	1	1480.00	0.581	2.35

C1.2: Full Model Approach Results

Parametric study

Full model (d=100mm)

Sin	/3	*A (kNlm)*	*M(kNm)*	*Displacement(mm)*
1	0	14.74	0.270	2.76
2	0.1	341.97	0.580	2.66
3	0.2	552.50	0.424	2.60
4	0.3	691.37	0.454	2.57
5	0.4	781.83	0.474	2.53
6	0.5	895.09	0.443	2.49
7	0.6	1010.00	0.426	2.46
8	0.64	1050.00	0.442	2.45
9	0.7	1120.00	0.484	2.43
10	0.8	1240.00	0.555	2.40
11	0.9	1360.00	0.625	2.37
12	1	1480.00	0.687	2.35

5 Material and loading modeling

5.1 Introduction

The construction of pressure tunnel represents a system that consists of ground with excavation, and support. The support system includes shotcrete, concrete linings, rock bolts and steel ribs. The behaviors and function of these systems is very essential in the design and construction of pressure tunnels. The numerical modeling of pressure tunnel in the research work is divided into two: materials and loading modeling. The former provides simple description of how ground, lining and grout are modeled, whereas the latter gives detail description of how the loading during construction and operation are simulated. A simple schematization of modeling of pressure tunnel for this study is shown in figure 5.1.

Figure 5.1: Schematic diagram for pressure tunnel numerical modelling

5.2 Material modeling

5.2.1 Modeling of ground

In this study, rock mass is modeled as a continuum, The fmite Element describing the rock mass is selected from a two-dimensional plain strain fmite element PLAXIS 2D program, The rock behavior is approximately represented by a non-linear elastoplastic Mohr-Coulomb model with geotechnical parameters to form rock cluster. The rock parameters defming the enclosed line-cluster represent the elastic and plastic properties of the rock-cluster. The infmity boundary of the ground is modelled by providing enclosed area that is beyond the zone of influence of the excavation and applying appropriate boundary conditions to the outer edges,

5.2.2 Modeling of lining

The lining of tunnel is made of concrete; this concrete will take a part of the deformation caused by excavation. The deformation depends on the axial, shear and bending stiffness. For the shotcrete, an elastic element of 10cm defmed as plate or triangular element is used. Shortly after installation, the shotcrete is loaded by ground deformation and the 3D arching effect of excavation is simulated using load reduction factor. This will form the basis of comparison with the normal forces in the prototype - Ermenek pressure tunnel project lining. After which a fmal lining is simulated.

The fmal lining support is modelled using the same material type of triangular element as used for rock mass but the material models and properties are that that correspond to the support material. The behaviour of the lining after loading will be related to its stress level, but the bending behaviour will be neglected. The dead weight of the fmallining becomes significant and has to be activated during simulation.

5.2.3 Modeling of gap and grout

Gap formed between the fmal lining and shotcrete can be simulated by activating the lining interface element. The interface allows interaction between the two lining materials. The shrinkage and temperature variation which is responsible for gap formation is modelled by introducingnegative volumetric stain into the liner element. A grout in form of positive volumetric strain which depend on the stiffness of material is imposed in the rock cluster to simulate the prestressing effect - mechanical processes of reducing the permeability of the surrounding mass during loading operation.

5.3 Loading modeling

It is expected that during the construction stages and operation time, a lining has to take loading. Loading for construction stage is different from that encounter during operation time. These loadings need to be included in the modelling as a close representation of reality.

5.3.1 Primary state of stress

The initial state of stress (otherwise known as in-situ stress) is defmed as the stress condition in the ground under equilibrium (undisturbed) condition. For the modelling, the vertical stresses are estimated based on the overburden weight of the overlying strata. The automatic calculated coefficient of earth pressure (k_o) using gravity loading approach in PLAXIS is disregarded and user defmed option is adopted. The rock is not an elastic material and the history of the rock development is often more significant than the condition of zero lateral deformation. Therefore, k_o value (different from zero lateral deformation) obtained from field or assumed based on geological conditions is specified in the generation window (for k_o procedure).

5.3.2 Surface loadings

In figure 5.1, simulation of surface loadings is not considered because the effect of building and traffic on the total stress for deep excavation (such as 200m below ground level under consideration) is negligible.

C2: Uniformity envelope of internal forces

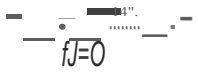

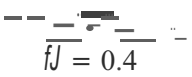

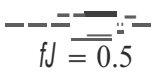

fJ = 0.6

fJ = 0.64

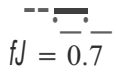

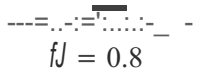

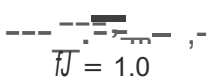

Note: Axial forces not the same scale

C3- Sensitivity Analysis Results

Full model set up

Tunnel radius = 3.00m

β= 0.64

SIN	d (mm)	Axial force, N (kN)	Shear force, Q(kN)	Moment, M (kNm)	Displacement (mm)
1	0	0	0	0	2.76
2	25	326.81	2.18	0.08	2.65
3	50	599.98	4.99	0.167	2.57
4	75	840.64	5.99	0.264	2.51
5	100	1050	5.82	0.442	2.46
6	125	1250	7.93	0.885	2.4
7	150	1430	11.49	1.4	2.36
8	175	1590	12.85	1.99	2.32
9	200	1750	11.15	2.73	2.28

C4 - Simulation of loadings

The load reduction factor of p= 0.64 takes effect from excavation phase in order to simulate the 3D arching effect of excavation supports.

C4.1 - Initial stresses

The initial state of stresses remain the same as in Bl

C4.2 - Excavation phase

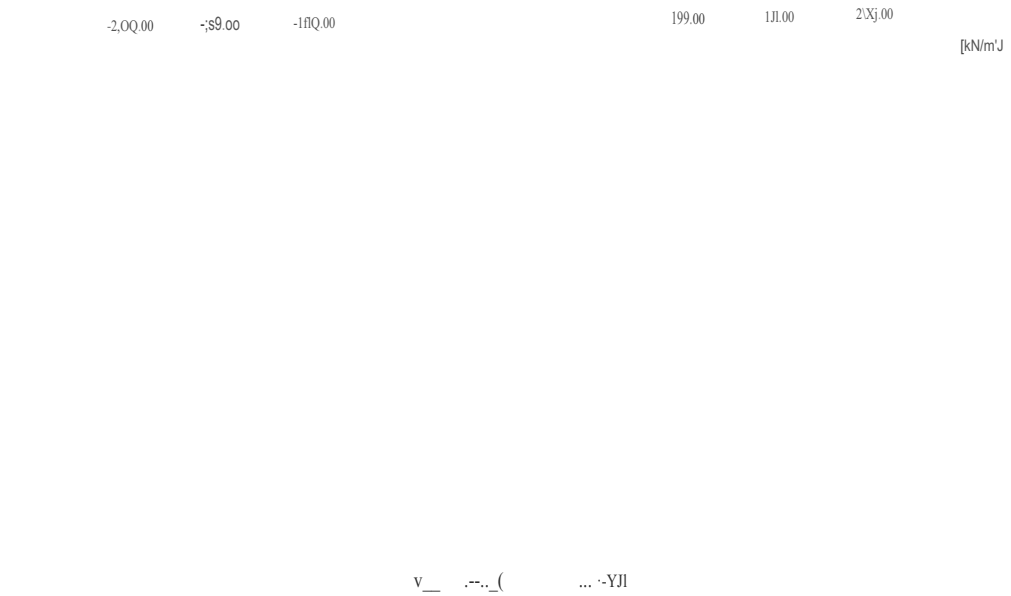

C4.2.1: Redistribution of vertical stresses after excavation

C4.2.2: Redistribution of horizontal stresses after excavation

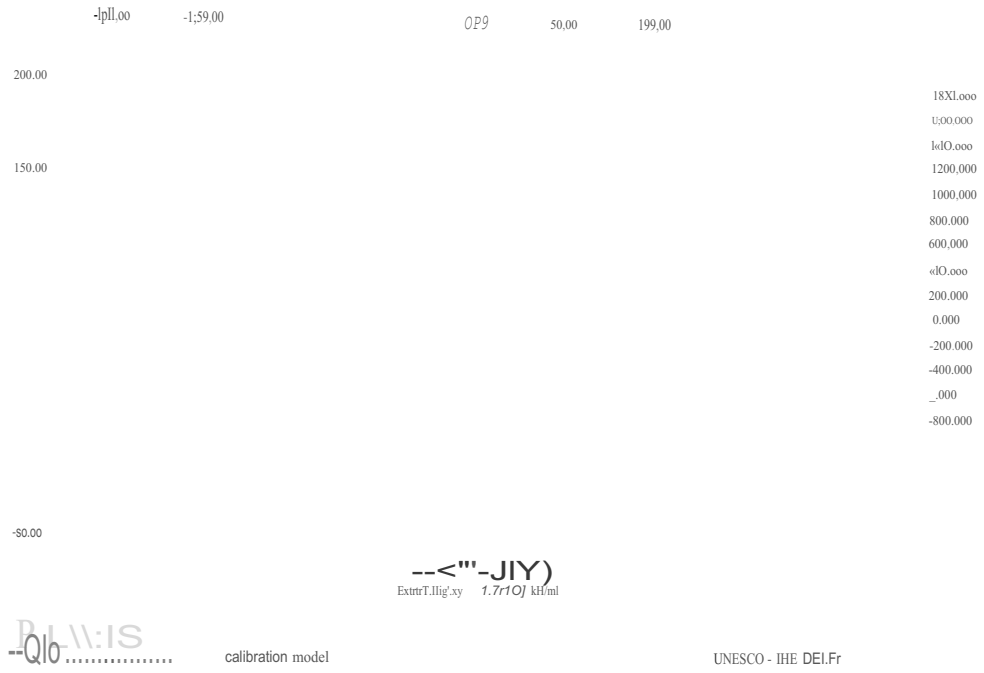

C4.2.1: Shear stresses around the vicinity of excavated tunnel

C4.3 - Shotcrete installation

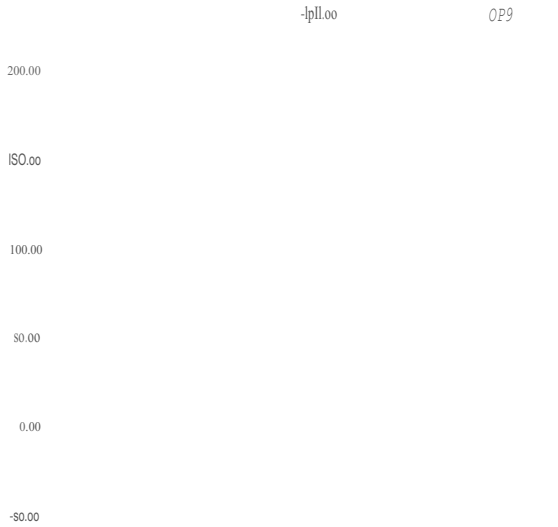

C4_3_1:Deformation after shotcrete installation

C4.3.1.1: Details ofC4.3.1

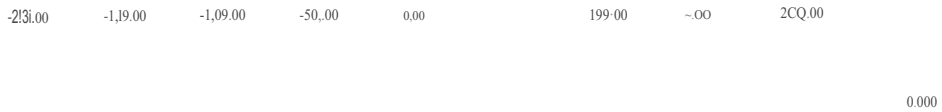

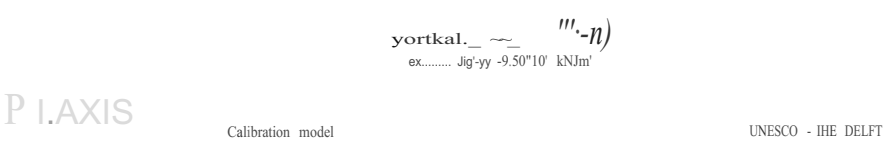

C4.3.2: Redistribution of vertical stresses after shotcrete installation

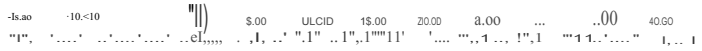

C4.3.2.1: Details ofC4.3.2

C4.3.3: Redistribution of horizontal stresses after shotcrete installation

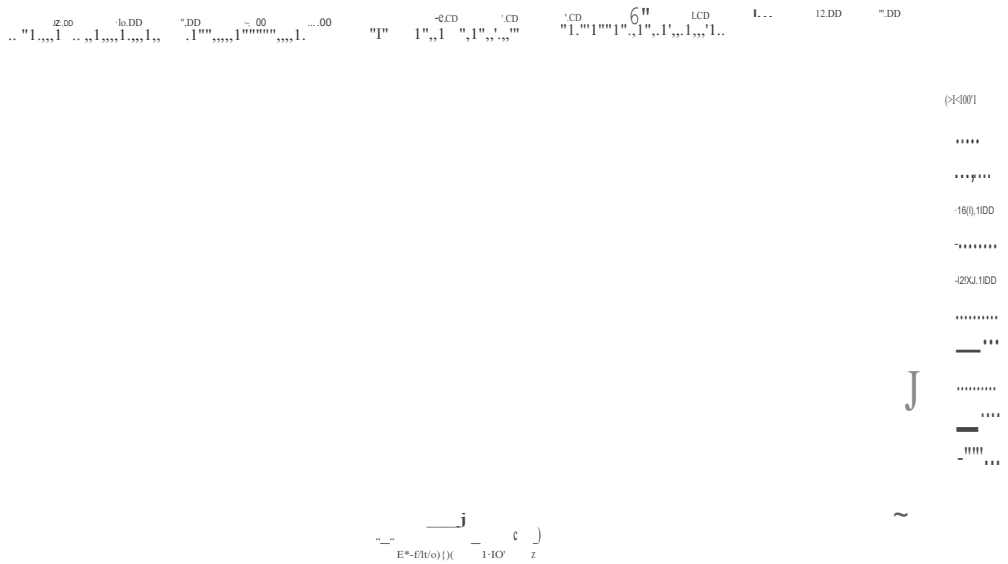

C4.3.3.1: Details ofC4.3.3

C4.3.4: Redistribution of stresses in out-of-plane direction after shotcrete installation

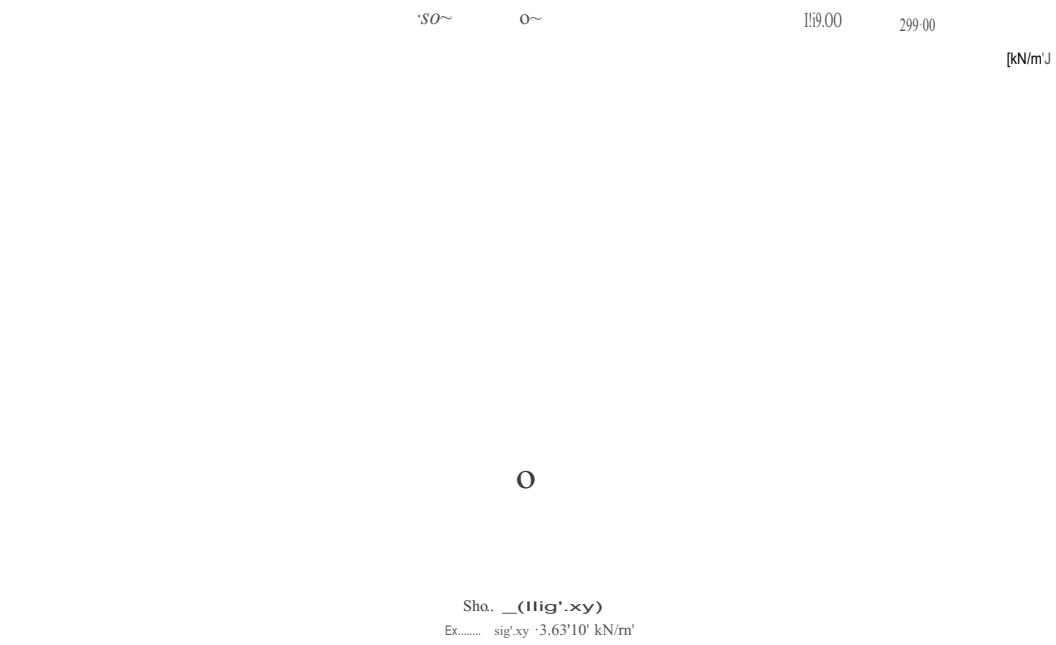

C4.3.5: Shear stresses around the vicinity of excavated tunnel after shotcrete installation

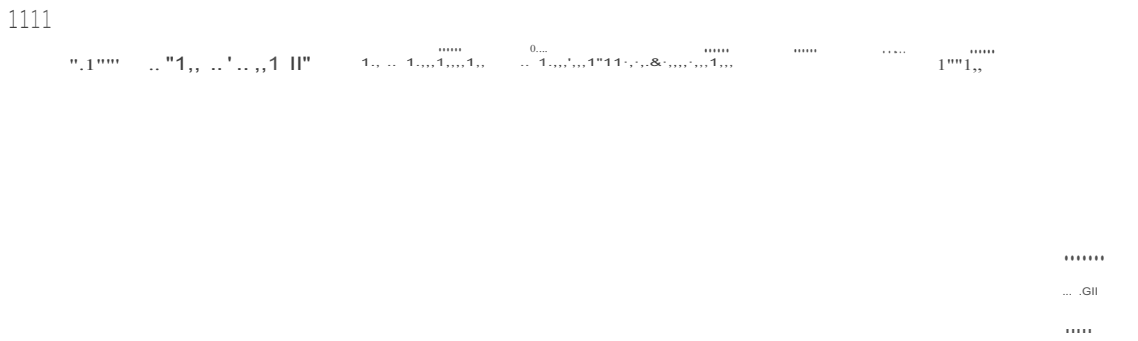

C4.3.5.1: Details ofC4.3.5

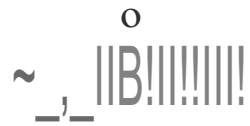

C4.3.6: Plastic zone around the shotcrete lining

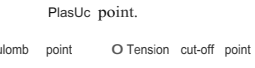

C4.3.6.1: Plastic zone details

C4.3.7: Axial (inner) forces envelope in shotcrete lining ($f3 = 0.64$)

Structural element	Node	Local number	X [mJ	Y [mJ	N [kN/mJ	N_min [kN/mJ	N_max [kN/mJ
(shotcrete)	2163	2	2.64	-1.89	-932.72	-932.72	0.00
	2164	3	2.70	-1.81	-949.95	-949.95	0.00
	2165	4	2.76	-1.72	-967.50	-967.50	0.00
	2166	5	2.81	-1.63	-985.51	-985.51	0.00
Plate 1-9	2166	1	2.81	-1.63	-985.56	-985.56	0.00
(shotcrete)	2103	2	2.87	-1.53	-999.79	-999.79	0.00
	2104	3	2.91	-1.44	-1014.37	-1014.37	0.00
	2105	4	2.96	-1.34	-1029.41	-1029.41	0.00
	2137	5	3.00	-1.24	-1045.03	-1045.03	0.00
Plate 1-10	2137	1	3.00	-1.24	-1045.07	-1045.07	0.00
(shotcrete)	2138	2	3.04	-1.14	-1055.36	-1055.36	0.00
	2139	3	3.08	-1.04	-1066.20	-1066.20	0.00
	2140	4	3.11	-0.94	-1077.67	-1077.67	0.00
	2136	5	3.14	-0.84	-1089.88	-1089.88	0.00
Plate 1-11	2136	1	3.14	-0.84	-1089.90	-1089.90	0.00
(shotcrete)	2122	2	3.17	-0.74	-1095.60	-1095.60	0.00
	2123	3	3.19	-0.63	-1102.00	-1102.00	0.00
	2124	4	3.21	-0.53	-1109.17	-1109.17	0.00
	2125	5	3.22	-0.42	-1117.16	-1117.16	0.00
Plate 1-12	2125	1	3.22	-0.42	-1117.17	-1117.17	0.00
(shotcrete)	2078	2	3.23	-0.32	-1117.93	-1117.93	0.00
	2079	3	3.24	-0.21	-1119.50	-1119.50	0.00
	2080	4	3.25	-0.11	-1121.91	-1121.91	0.00
	2077	5	3.25	0.00	-1125.16	-1125.16	0.00
Plate 1-13	2077	1	3.25	0.00	-1125.14	-1125.14	0.00
(shotcrete)	2064	2	3.25	0.11	-1120.93	-1120.93	0.00
	2065	3	3.24	0.21	-1117.58	-1117.58	0.00
	2066	4	3.23	0.32	-1115.06	-1115.06	0.00
	2063	5	3.22	0.42	-1113.35	-1113.35	0.00
Plate 1-14	2063	1	3.22	0.42	-1113.31	-1113.31	0.00
(shotcrete)	2037	2	3.21	0.53	-1104.43	-1104.43	0.00
	2038	3	3.19	0.63	-1096.38	-1096.38	0.00
	2039	4	3.17	0.74	-1089.09	-1089.09	0.00
	2040	5	3.14	0.84	-1082.51	-1082.51	0.00
Plate 1-15	2040	1	3.14	0.84	-1082.46	-1082.46	0.00
(shotcrete)	1986	2	3.11	0.94	-1069.48	-1069.48	0.00
	1987	3	3.08	1.04	-1057.23	-1057.23	0.00
	1988	4	3.04	1.14	-1045.63	-1045.63	0.00
	1985	5	3.00	1.24	-1034.59	-1034.59	0.00
Plate 1-16	1985	1	3.00	1.24	-1034.53	-1034.53	0.00
(shotcrete)	1972	2	2.96	1.34	-1018.26	-1018.26	0.00

C4.3.8: Shotcrete lining bending moment envelope

C4.4 - Final lining instaUation

MIDchufl" .... _ 2.669-10') m(a.n.t47S2 _ ... 3769

CAA.I: Deformation in rock mass after final lining installation

C4.4.2: Stresses in the fmallining before shrinkage

Soil element	Stress point	Local number	X[m]	Y[m]	0, [kN/m2]	02 [kN/m2]	0, [kN/m2]	{o,+o,)/2 [kN/m2]	{o,-o,)/2 [kN/m2]
Clus. 3 - El. 4745	56929	1	-2.34	2.27	-0.36	-0.08	0.00	-0.18	-0.18
Concrete	56930	2	-2.22	2.04	-20.48	-4.50	0.00	-10.24	-10.24
	56931	3	-2.04	2.22	-7.94	-1.75	0.00	-3.97	-3.97
	56932	4	-2.24	2.21	-6.01	-1.32	0.00	-3.00	-3.00
	56933	5	-2.21	2.14	-10.59	-2.33	0.00	-5.29	-5.29
	56934	6	-2.15	2.19	-9.01	-1.98	0.00	-4.51	-4.51
	56935	7	-2.31	2.20	-4.72	-1.04	0.00	-2.36	-2.36
	56936	8	-2.26	2.11	-10.89	-2.39	0.00	-5.44	-5.44
	56937	9	-2.17	2.09	-17.39	-3.83	0.00	-8.69	-8.70
	56938	10	-2.10	2.17	-11.18	-2.46	0.00	-5.59	-5.59
	56939	11	-2.13	2.24	-7.00	-1.54	0.00	-3.50	-3.50
	56940	12	-2.25	2.26	-3.63	-0.80	0.00	-1.81	-1.81
Clus. 3 - El. 4746	56941	1	-2.05	2.54	-1.45	-0.32	0.00	-0.73	-0.73
Concrete	56942	2	-2.00	2.26	-5.77	-1.27	0.00	-2.88	-2.88
	56943	3	-1.80	2.42	-0.14	-0.03	0.00	-0.07	-0.07
	56944	4	-1.98	2.45	-1.12	-0.25	0.00	-0.56	-0.56
	56945	5	-1.96	2.37	-2.85	-0.63	0.00	-1.42	-1.42
	56946	6	-1.90	2.42	-1.33	-0.29	0.00	-0.67	-0.67
	56947	7	-2.03	2.46	-0.62	-0.14	0.00	-0.31	-0.31
	56948	8	-2.01	2.35	-3.74	-0.82	0.00	-1.87	-1.87
	56949	9	-1.94	2.31	-3.61	-0.79	0.00	-1.80	-1.80
	56950	10	-1.86	2.38	-1.04	-0.23	0.00	-0.52	-0.52
	56951	11	-1.87	2.46	-1.08	-0.24	0.00	-0.54	-0.54
	56952	12	-1.97	2.51	-1.33	-0.29	0.00	-0.67	-0.67
Clus. 3 - El. 4747	56953	1	-1.72	2.77	-1.97	-0.43	0.00	-0.98	-0.98
Concrete	56954	2	-1.75	2.46	0.00	0.00	0.00	0.00	0.00
	56955	3	-1.53	2.60	0.00	0.00	0.00	0.00	0.00
	56956	4	-1.68	2.66	-1.31	-0.29	0.00	-0.65	-0.65
	56957	5	-1.69	2.57	-0.64	-0.14	0.00	-0.32	-0.32
	56958	6	-1.63	2.61	-0.28	-0.06	0.00	-0.14	-0.14
	56959	7	-1.73	2.68	-1.87	-0.41	0.00	-0.93	-0.93
	56960	8	-1.74	2.55	-1.12	-0.25	0.00	-0.56	-0.56
	56961	9	-1.68	2.50	0.00	0.00	0.00	0.00	0.00
	56962	10	-1.60	2.56	0.00	0.00	0.00	0.00	0.00
	56963	11	-1.59	2.65	-0.16	-0.03	0.00	-0.08	-0.08
	56964	12	-1.66	2.72	-1.37	-0.30	0.00	-0.68	-0.69

C4.4.3: Stresses in the final lining (crown) with shrinkage effect

Soil element	Stress point	Local number	X[m]	Y[m]	σ_1 [kN/m²]	σ_3 [kN/m²]	σ_3 [kN/m²]	$(\sigma_1+\sigma_3)/2$ [kN/m²]	$(\sigma_1-\sigma_3)/2$ [kN/m²]
Clus. 3 - EI.4745	56929	1	-2.34	2.27	0.00	0.00	0.00	0.00	0.00
Concrete	56930	2	-2.22	2.04	0.00	0.00	0.00	0.00	0.00
	56931	3	-2.04	2.22	0.00	0.00	0.00	0.00	0.00
	56932	4	-2.24	2.21	0.00	0.00	0.00	0.00	0.00
	56933	5	-2.21	2.14	0.00	0.00	0.00	0.00	0.00
	56934	6	-2.15	2.19	0.00	0.00	0.00	0.00	0.00
	56935	7	-2.31	2.20	0.00	0.00	0.00	0.00	0.00
	56936	8	-2.26	2.11	0.00	0.00	0.00	0.00	0.00
	56937	9	-2.17	2.09	0.00	0.00	0.00	0.00	0.00
	56938	10	-2.10	2.17	0.00	0.00	0.00	0.00	0.00
	56939	11	-2.13	2.24	0.00	0.00	0.00	0.00	0.00
	56940	12	-2.25	2.26	0.00	0.00	0.00	0.00	0.00
Clus. 3 - EI.4746	56941	1	-2.05	2.54	0.00	0.00	0.00	0.00	0.00
Concrete	56942	2	-2.00	2.26	0.00	0.00	0.00	0.00	0.00
	56943	3	-1.80	2.42	0.00	0.00	0.00	0.00	0.00
	56944	4	-1.98	2.45	0.00	0.00	0.00	0.00	0.00
	56945	5	-1.96	2.37	0.00	0.00	0.00	0.00	0.00
	56946	6	-1.90	2.42	0.00	0.00	0.00	0.00	0.00
	56947	7	-2.03	2.46	0.00	0.00	0.00	0.00	0.00
	56948	8	-2.01	2.35	0.00	0.00	0.00	0.00	0.00
	56949	9	-1.94	2.31	0.00	0.00	0.00	0.00	0.00
	56950	10	-1.86	2.38	0.00	0.00	0.00	0.00	0.00
	56951	11	-1.87	2.46	0.00	0.00	0.00	0.00	0.00
	56952	12	-1.97	2.51	0.00	0.00	0.00	0.00	0.00
Clus. 3 - EI.4747	56953	1	-1.72	2.77	0.00	0.00	0.00	0.00	0.00
Concrete	56954	2	-1.75	2.46	0.00	0.00	0.00	0.00	0.00
	56955	3	-1.53	2.60	0.00	0.00	0.00	0.00	0.00
	56956	4	-1.68	2.66	0.00	0.00	0.00	0.00	0.00
	56957	5	-1.69	2.57	0.00	0.00	0.00	0.00	0.00
	56958	6	-1.63	2.61	0.00	0.00	0.00	0.00	0.00
	56959	7	-1.73	2.68	0.00	0.00	0.00	0.00	0.00
	56960	8	-1.74	2.55	0.00	0.00	0.00	0.00	0.00
	56961	9	-1.68	2.50	0.00	0.00	0.00	0.00	0.00
	56962	10	-1.60	2.56	0.00	0.00	0.00	0.00	0.00
	56963	11	-1.59	2.65	0.00	0.00	0.00	0.00	0.00
	56964	12	-1.66	2.72	0.00	0.00	0.00	0.00	0.00

C4.4.4: Deformation in the lining

					Before shrinkage effect			With shrinkage effect		
Soil element	Node	Local number	X[m]	Y[m]	u,[m)	u, [m)	lui [m)	u, [m)	uy[m)	lui [m)
Clus. 3 - EI.4745	8707	1	-2.23	2.01	1.10E-03	-1.97E-03	2.25E-03	1.08E-03	-1.98E-03	2.26E-03
Concrete	8840	2	-2.01	2.23	9.74E-04	-2.13E-03	2.35E-03	9.54E-04	-2.15E-03	2.35E-03
	8850	3	-2.37	2.30	1.03E-03	-1.99E-03	2.24E-03	1.04E-03	-2.01E-03	2.26E-03
	8520	4	-2.12	2.12	1.04E-03	-2.05E-03	2.30E-03	1.02E-03	-2.07E-03	2.30E-03
	8842	5	-2.19	2.26	1.01E-03	-2.06E-03	2.29E-03	9.97E-04	-2.08E-03	2.30E-03
	8709	6	-2.30	2.15	1.07E-03	-1.97E-03	2.24E-03	1.05E-03	-2.00E-03	2.26E-03
	8521	7	-2.18	2.07	1.07E-03	-2.01E-03	2.28E-03	1.05E-03	-2.03E-03	2.28E-03
	8519	8	-2.07	2.18	1.01E-03	-2.09E-03	2.32E-03	9.86E-04	-2.11E-03	2.33E-03
	8841	9	-2.10	2.25	9.92E-04	-2.09E-03	2.32E-03	9.76E-04	-2.11E-03	2.32E-03
	8843	10	-2.28	2.28	1.02E-03	-2.02E-03	2.26E-03	1.02E-03	-2.04E-03	2.28E-03
	8708	11	-2.33	2.22	1.05E-03	-1.98E-03	2.24E-03	1.04E-03	-2.00E-03	2.26E-03
	8710	12	-2.26	2.08	1.08E-03	-1.97E-03	2.25E-03	1.07E-03	-1.99E-03	2.26E-03
	8522	13	-2.21	2.14	1.05E-03	-2.01E-03	2.27E-03	1.04E-03	-2.03E-03	2.28E-03
	8523	14	-2.15	2.19	1.02E-03	-2.05E-03	2.29E-03	1.01E-03	-2.07E-03	2.30E-03
	8524	15	-2.24	2.21	1.04E-03	-2.02E-03	2.27E-03	1.03E-03	-2.04E-03	2.28E-03
Clus. 3 - EI.4746	8840	1	-2.01	2.23	9.74E-04	-2.13E-03	2.35E-03	9.54E-04	-2.15E-03	2.35E-03
Concrete	8447	2	-1.76	2.43	8.41E-04	-2.28E-03	2.43E-03	8.25E-04	-2.28E-03	2.43E-03
	8836	3	-2.07	2.57	8.89E-04	-2.17E-03	2.35E-03	8.91E-04	-2.19E-03	2.37E-03
	8442	4	-1.89	2.33	9.08E-04	-2.21E-03	2.39E-03	8.90E-04	-2.22E-03	2.39E-03
	8449	5	-1.92	2.50	8.68E-04	-2.22E-03	2.38E-03	8.60E-04	-2.23E-03	2.39E-03
	8831	6	-2.04	2.40	9.30E-04	-2.15E-03	2.34E-03	9.20E-04	-2.17E-03	2.36E-03
	8443	7	-1.95	2.28	9.41E-04	-2.17E-03	2.37E-03	9.22E-04	-2.18E-03	2.37E-03
	8441	8	-1.83	2.38	8.75E-04	-2.24E-03	2.41E-03	8.58E-04	-2.25E-03	2.4IE-03
	8448	9	-1.84	2.46	8.56E-04	-2.25E-03	2.40E-03	8.43E-04	-2.26E-03	2.41E-03
	8450	10	-1.99	2.53	8.79E-04	-2.19E-03	2.36E-03	8.76E-04	-2.21E-03	2.38E-03
	8830	11	-2.05	2.49	9.09E-04	-2.16E-03	2.34E-03	9.06E-04	-2.18E-03	2.36E-03
	8832	12	-2.02	2.31	9.51E-04	-2.14E-03	2.34E-03	9.36E-04	-2.16E-03	2.35E-03
	8444	13	-1.96	2.37	9.20E-04	-2.18E-03	2.36E-03	9.05E-04	-2.19E-03	2.37E-03
	8445	14	-1.90	2.42	8.88E-04	-2.21E-03	2.39E-03	8.74E-04	-2.23E-03	2.39E-03
	8446	15	-1.98	2.45	8.99E-04	-2.19E-03	2.36E-03	8.90E-04	-2.20E-03	2.38E-03
Clus. 3 - EI.4747	8447	1	-1.76	2.43	8.41E-04	-2.28E-03	2.43E-03	8.25E-04	-2.28E-03	2.43E-03
Concrete	7531	2	-1.50	2.60	7.05E-04	-2.40E-03	2.50E-03	6.91E-04	-2.40E-03	2.50E-03
	7781	3	-1.74	2.81	7.37E-04	-2.33E-03	2.44E-03	7.38E-04	-2.34E-03	2.46E-03
	7533	4	-1.63	2.52	7.73E-04	-2.34E-03	2.47E-03	7.59E-04	-2.34E-03	2.46E-03
	7536	5	-1.62	2.70	7.23E-04	-2.36E-03	2.47E-03	7.16E-04	-2.37E-03	2.47E-03
	7776	6	-1.75	2.62	7.87E-04	-2.30E-03	2.43E-03	7.79E-04	-2.31E-03	2.44E-03
	7534	7	-1.70	2.47	8.07E-04	-2.31E-03	2.45E-03	7.92E-04	-2.31E-03	2.44E-03
	7532	8	-1.57	2.56	7.39E-04	-2.37E-03	2.48E-03	7.25E-04	-2.37E-03	2.48E-03
	7535	9	-1.56	2.65	7.15E-04	-2.38E-03	2.48E-03	7.04E-04	-2.38E-03	2.48E-03
	7537	10	-1.68	2.75	7.31E-04	-2.34E-03	2.45E-03	7.27E-04	-2.36E-03	2.46E-03
	7775	11	-1.74	2.71	7.62E-04	-2.31E-03	2.44E-03	7.58E-04	-2.33E-03	2.45E-03
	7777	12	-1.76	2.52	8.14E-04	-2.29E-03	2.43E-03	8.01E-04	-2.30E-03	2.43E-03
	7538	13	-1.69	2.57	7.81E-04	-2.32E-03	2.45E-03	7.69E-04	-2.33E-03	2.45E-03
	7539	14	-1.63	2.61	7.48E-04	-2.35E-03	2.47E-03	7.37E-04	-2.36E-03	2.47E-03
	7540	15	-1.68	2.66	7.55E-04	-2.33E-03	2.45E-03	7.47E-04	-2.34E-03	2.46E-03

C4.4.5: Normal stresses at the interface of the lining before shrinkage

Structural element	Node	Wall node	Local number	X[m]	У [m]	cr'N [kN/m2l	crN [kN/m2l	'1 [kN/m2]	'2 [kN/m2]	'rei	'max [kN/m2]
Interfacel-26	5801	4546	1	3.30	0.10	-5.14	-5.14	-6.27	0.00	4.16E-03	1.51E+03
(Shotcrete)	5795	3851	2	3.30	0.05	-5.07	-5.07	-6.77	0.00	4.50E-03	1.51E+03
	5796	3850	3	3.30	0.00	-5.20	-5.20	-7.20	0.00	4.78E-03	1.51E+03
	5797	3849	4	3.30	-0.05	-5.10	-5.10	-7.63	0.00	5.07E-03	1.51E+03
	5827	4483	5	3.30	-0.10	-4.96	-4.96	-8.11	0.00	5.39E-03	1.50E+03
Interface 1-27	5827	4483	I	3.30	-0.10	-4.96	-4.96	-8.11	0.00	5.39E-03	1.50E+03
(Shotcrete)	5811	4486	2	3.30	-0.15	-5.38	-5.38	-8.67	0.00	5.76E-03	1.51E+03
	5812	4485	3	3.29	-0.20	-5.57	-5.57	-9.17	0.00	6.09E-03	1.51E+03
	5813	4484	4	3.29	-0.25	-5.91	-5.91	-9.64	0.00	6.40E-03	1.51E+03
	5817	4501	5	3.29	-0.30	-5.81	-5.81	-10.14	0.00	6.73E-03	1.51E+03
Interface 1-28	5817	4501	1	3.29	-0.30	-5.81	-5.81	-10.14	0.00	6.73E-03	1.51E+03
(Shotcrete)	5717	4500	2	3.28	-0.36	-6.19	-6.18	-10.51	0.00	6.98E-03	1.51E+03
	5718	4499	3	3.27	-0.41	-6.15	-6.14	-10.79	0.00	7. 17E-03	1.51E+03
	5719	4498	4	3.27	-0.46	-5.86	-5.86	-11.08	0.00	7.36E-03	1.51E+03
	5723	4497	5	3.26	-0.51	-5.86	-5.86	-11.45	0.00	7.60E-03	1.51E+03
Interface 1-29	5723	4497	I	3.26	-0.51	-5.86	-5.86	-11.45	0.00	7.60E-03	1.51E+03
(Shotcrete)	5724	4476	2	3.25	-0.56	-5.89	-5.89	-11.87	0.00	7.88E-03	1.51E+03
	5725	4475	3	3.24	-0.61	-5.83	-5.83	-12.31	0.00	8.18E-03	1.51E+03
	5726	4474	4	3.23	-0.66	-5.96	-5.96	-12.74	0.00	8.46E-03	1.51E+03
	5733	4473	5	3.22	-0.71	-6.95	-6.95	-13.01	0.00	8.64E-03	1.51E+03
Interfacel-30	5733	4473	1	3.22	-0.71	-6.95	-6.95	-13.01	0.00	8.64E-03	1.51E+03
(Shotcrete)	5701	4462	2	3.21	-0.76	-6.68	-6.68	-13.32	0.00	8.84E-03	1.51E+03
	5702	4461	3	3.20	-0.80	-6.30	-6.30	-13.51	0.00	8.97E-03	1.51E+03
	5703	4460	4	3.19	-0.85	-6.00	-6.00	-13.74	0.00	9.12E-03	1.5IE+03
	5707	4459	5	3.17	-0.90	-5.87	-5.87	-14.06	0.00	9.34E-03	1.51E+03
Interfacel-31	5707	4459	1	3.17	-0.90	-5.87	-5.87	-14.06	0.00	9.34E-03	1.51E+03
(Shotcrete)	5708	4408	2	3.16	-0.95	-5.68	-5.68	-14.42	0.00	9.58E-03	1.51E+03
	5709	4407	3	3.14	-1.00	-5.36	-5.36	-14.79	0.00	9.83E-03	1.51E+03
	5710	4406	4	3.13	-1.05	-5.50	-5.50	-15.11	0.00	1.00E-02	1.51E+03
	5759	4425	5	3.11	-1.10	-6.70	-6.70	-15.22	0.00	1.01E-02	1.51E+03
Interface 1-32	5759	4425	I	3.11	-1.10	-6.70	-6.70	-15.22	0.00	1.01E-02	1.51E+03
_(Shotcrete)	5750	4428	2	3.10	-1.14	-6.21	-6.20	-15.36	0.00	1.02E-02	1.51E+03
	5751	4427	3	3.08	-1.19	-5.94	-5.94	-15.47	0.00	1.03E-02	1.51E+03
	5752	4426	4	3.06	-1.24	-5.81	-5.80	-15.65	0.00	1.04E-02	1.51E+03
	5749	4452	5	3.04	-1.29	-5.63	-5.63	-15.89	0.00	1.06E-02	1.51E+03
Interface 1-33	5749	4452	1	3.04	-1.29	-5.63	-5.63	-15.89	0.00	1.06E-02	1.51E+03
(Shotcrete)	5743	4451	2	3.02	-1.33	-5.39	-5.39	-16.18	0.00	1.07E-02	1.51E+03
	5744	4450	3	3.00	-1.38	-5.06	-5.05	-16.46	0.00	1.09E-02	1.51E+03
	5745	4449	4	2.98	-1.43	-5.53	-5.53	-16.65	0.00	1.11E-02	1.51E+03
	5775	4719	5	2.95	-1.47	-6.80	-6.80	-16.66	0.00	1.11E-02	1.51E+03

C4.4.6: Normal stresses at the interface of the lining after shrinkage

Structural element	Node	Wall node	Local number	Xfml	Y[mJ	O'N fkN/m2	ON _lkN/mj	'| _lkN/mj	'2 _lkN/mj	'trel	'mu [kN/m2]
Interface 126	5801	4546	I	3.30	0.10	0.00	0.00	-8.88	0.00	5.92E-03	1.50E+{)3
(Shotcrete)	5795	3851	2	3.30	0.05	0.00	0.00	-8.56	0.00	5.71E-03	1.50E+{)3
	5796	3850	3	3.30	0.00	0.00	0.00	-7.19	0.00	4.79E-03	1.50E+{)3
	5797	3849	4	3.30	-0.05	0.00	0.00	-6.18	0.00	4.12E-03	1.50E+{)3
	5827	4483	5	3.30	-0.10	0.00	0.00	-5.08	0.00	3.38E-03	1.50E+{)3
Interface 1-27	5827	4483	I	3.30	-0.10	0.00	0.00	-5.08	0.00	3.38E-03	1.50E+{)3
(Shotcrete)	5811	4486	2	3.30	-0.15	0.00	0.00	-5.92	0.00	3.95E-03	1.5OE+{)3
	5812	4485	3	3.29	-0.20	0.00	0.00	-6.71	0.00	4.47E-03	1.50E+{)3
	5813	4484	4	3.29	-0.25	0.00	0.00	-7.52	0.00	5.01E-03	1.50E+{)3
	5817	4501	5	3.29	-0.30	0.00	0.00	-8.91	0.00	5.94E-03	1.50E+{)3
Interface 1-28	5817	4501	1	3.29	-0.30	0.00	0.00	-8.91	0.00	5.94E-03	1.50E+{)3
(Shotcrete)	5717	4500	2	3.28	-0.36	0.00	0.00	-7.78	0.00	5.19E-03	1.50E+{)3
	5718	4499	3	3.27	-0.41	0.00	0.00	-6.43	0.00	4.29E-03	1.50E+{)3
	5719	4498	4	3.27	-0.46	0.00	0.00	-4.89	0.00	3.26E-03	1.50E+{)3
	5723	4497	5	3.26	-0.51	0.00	0.00	-4.49	0.00	2.99E-03	l.50E+{)3
Interface 1-29	5723	4497	I	3.26	-0.51	0.00	0.00	-4.49	0.00	2.99E-03	1.50E+{)3
(Shotcrete)	5724	4476	2	3.25	-0.56	0.00	0.00	-4.56	0.00	3.04E-03	1.50E+{)3
	5725	4475	3	3.24	-0.61	0.00	0.00	-4.82	0.00	3.2IE-03	1.50E+{)3
	5726	4474	4	3.23	-0.66	0.00	0.00	-5.39	0.00	3.59E-03	1.50E+{)3
	5733	4473	5	3.22	-0.71	0.00	0.00	-5.35	0.00	3.57E-03	1.5OE+{)3
Interface 1-30	5733	4473	1	3.22	-0.71	0.00	0.00	-5.35	0.00	3.57E-03	1.5OE+{)3
(Shotcrete)	5701	4462	2	3.21	-0.76	0.00	0.00	-6.01	0.00	4.00E-03	1.5OE+{)3
	5702	4461	3	3.20	-0.80	-l.l9	-l.l9	-5.51	0.00	3.67E-03	1.50E+{)3
	5703	4460	4	3.19	-0.85	-0.85	-0.84	-4.86	0.00	3.24E-03	1.5OE+{)3
	5707	4459	5	3.17	-0.90	-l.l9	-l.l9	-4.44	0.00	2.96E-03	1.50E+{)3
Interface 1-31	5707	4459	1	3.17	-0.90	-l.l9	-l.l9	-4.44	0.00	2.96E-03	1.50E+03
(Shotcrete)	5708	4408	2	3.16	-0.95	-l.l6	-l.l6	-3.95	0.00	2.63E-03	1.5OE+{)3
	5709	4407	3	3.14	-1.00	-0.55	-0.55	-3.73	0.00	2.49E-03	1.5OE+{)3
	5710	4406	4	3.13	-1.05	-1.69	-1.69	-3.78	0.00	2.52E-03	1.50E+{)3
	5759	4425	5	3.11	-l.l0	-4.34	-4.34	-3.74	0.00	2.49E-03	1.5OE+{)3
Interface 1-32	5759	4425	1	3.11	-l.l0	-4.34	-4.34	-3.74	0.00	2.49E-03	1.50E+03
(Shotcrete)	5750	4428	2	3.10	-1.14	-4.99	-4.99	-3.22	0.00	2.14E-03	1.50E+{)3
	5751	4427	3	3.08	-1.19	-5.00	-5.00	-2.52	0.00	1.67E-03	1.51E+{)3
	5752	4426	4	3.06	-1.24	-5.83	-5.83	-1.98	0.00	1.32E-03	1.51E+{)3
	5749	4452	5	3.04	-1.29	-5.93	-5.93	-1.44	0.00	9.58E-04	1.5 IE+{)3
Interface 1-33	5749	4452	I	3.04	-1.29	-5.93	-5.93	-1.44	0.00	9.58E-04	1.5 IE+{)3
(Shotcrete)	5743	4451	2	3.02	-1.33	-4.49	-4.48	-l.l9	0.00	7.9IE-04	1.50E+{)3
	5744	4450	3	3.00	-1.38	-0.84	-0.84	-1.06	0.00	7.08E-04	1.5OE+{)3
	5745	4449	4	2.98	-1.43	-1.08	-1.08	-0.78	0.00	5.17E-04	1.5OE+{)3
	5775	4719	5	2.95	-1.47	-2.47	-2.47	-0.93	0.00	6.21E-04	1.5OE+{)3

C4.5 -Temperature and Shrinkage effect (Gap modelling)

C4.S.1 Final lining before shrinkage (shading)

C4.S.2 Final lining after shrinkage (shading)

C4.6 - Shotcrete decay simulation

	Simulation stage (Deformation, rrun)				Simulation stage (Stress, kN/m_2)			
Element	Excavation	shotcrete	F/Lining	Decay	Excavation	shotcrete	F/Lining	Decay
Rock (150)	0.845	2.416	2.430	2.424	5123.28	6732.154	6729.318	6624.721
Shotcrete (6062)	-	0.201	0.201	0.159	-	5445.168	5427.272	703.423
Final lining (6166)	-	-	0.009	0.139	-	-	50.300	1151.609

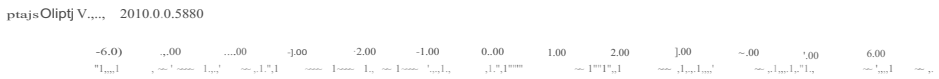

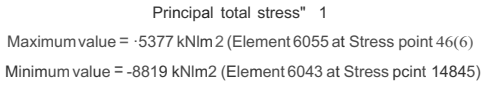

C4.6.1 Shotcrete before decay

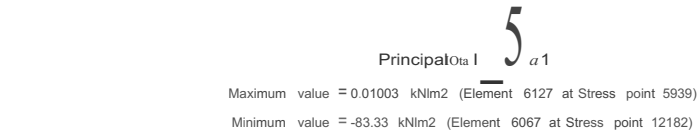

C4.6.2 Final lining before decay

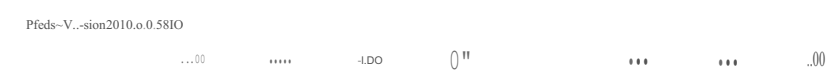

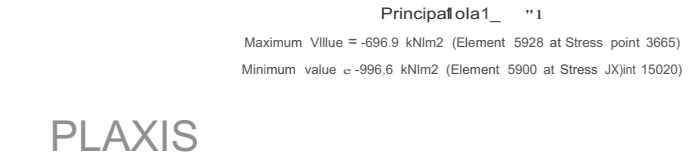

C4.6.3 Shotcrete after decay

Principal total stress <f1

Maximum value: -674.8 kN/m2 (Element 6166 at Stress point 3055)

Minimum value: -1358 kN/m2 (Element 6097 at Stress point 3173)

PLAXIS

!:::~otcrete elementdecay 02/04/11

PT_Shotcrete element decay UNESCO - IHE DELFT

C4_6A Final lining after decay

C4.7 - Grout injection

C4.7.1: Compressive stresses in final lining (lJFL)before prestressing (crown)

Soil element	Stress point	Local number	X[m]	Y[m]	°1 [kN/m2)	°2 [kN/m2)	03 [kN/m2)
Clus. 4 - EI. 2714	32557	1	-0.02	3.26	0.00	0.00	0.00
Concrete	32558	2	-0.27	3.01	-0.04	-0.01	0.00
	32559	3	-0.02	3.02	0.00	0.00	0.00
	32560	4	-0.08	3.15	0.00	0.00	0.00
	32561	5	-0.16	3.07	0.00	0.00	0.00
	32562	6	-0.08	3.07	0.00	0.00	0.00
	32563	7	-0.10	3.19	0.00	0.00	0.00
	32564	8	-0.20	3.08	0.00	0.00	0.00
	32565	9	-0.20	3.01	-0.08	-0.02	0.00
	32566	10	-0.10	3.01	0.00	0.00	0.00
	32567	11	-0.02	3.09	0.00	0.00	0.00
	32568	12	-0.02	3.19	0.00	0.00	0.00
Clus. 4 - EI. 2715	32569	1	0.02	3.26	0.00	0.00	0.00
Concrete	32570	2	0.02	3.02	0.00	0.00	0.00
	32571	3	0.27	3.01	0.00	0.00	0.00
	32572	4	0.08	3.15	0.00	0.00	0.00
	32573	5	0.08	3.07	0.00	0.00	0.00
	32574	6	0.16	3.07	0.00	0.00	0.00
	32575	7	0.02	3.19	0.00	0.00	0.00
	32576	8	0.02	3.09	0.00	0.00	0.00
	32577	9	0.10	3.01	0.00	0.00	0.00
	32578	10	0.20	3.01	0.00	0.00	0.00
	32579	11	0.20	3.08	0.00	0.00	0.00
	32580	12	0.10	3.19	0.00	0.00	0.00
Clus. 4 - EI. 2716	32581	1	0.44	3.23	0.00	0.00	0.00

C4.7.2: Compressive stresses in final lining *(CJFL)* before prestressing (side of tunnel)

Soil element	Stress point	Local number	X [m]	y [m]	σ_1 [kN/m2)	σ_2 [kN/m2)	σ_3 [kN/m2)
Clus. 4 - El. 2775	33289	1	3.02	0.30	-87.42	-19.42	-0.86
Concrete	33290	2	3.28	0.05	-113.65	-26.72	-7.83
	33291	3	3.26	0.40	-108.21	-24.85	-4.75
	33292	4	3.13	0.26	-97.38	-22.16	-3.34
	33293	5	3.22	0.19	-105.14	-24.40	-5.76
	33294	6	3.21	0.29	-103.69	-23.88	-4.86
	33295	7	3.10	0.22	-93.75	-21.21	-2.64
	33296	8	3.20	0.12	-103.56	-24.03	-5.68
	33297	9	3.28	0.15	-111.82	-26.29	-7.69
	33298	10	3.27	0.29	-108.68	-25.30	-6.30
	33299	11	3.18	0.37	-101.62	-23.22	-3.94
	33300	12	3.09	0.33	-93.08	-20.98	-2.29
Clus. 4 - El. 2776	33301	1	2.97	0.63	-83.30	-18.50	-0.79
Concrete	33302	2	3.25	0.47	-106.86	-24.47	-4.38
	33303	3	3.18	0.81	-93.85	-21.55	-4.12
	33304	4	3.08	0.63	-90.66	-20.56	-2.81
	33305	5	3.17	0.59	-97.94	-22.41	-3.92
	33306	6	3.15	0.69	-94.45	-21.66	-4.01
	33307	7	3.05	0.58	-89.13	-20.08	-2.14
	33308	8	3.16	0.51	-98.50	-22.48	-3.66
	33309	9	3.23	0.57	-103.43	-23.76	-4.59
	33310	10	3.21	0.71	-98.55	-22.76	-4.89
	33311	11	3.11	0.76	-90.34	-20.65	-3.52
	33312	12	3.03	0.68	-86.22	-19.43	-2.11
Clus. 4 - El. 2777	33313	1	2.89	0.94	-73.11	-16.21	-0.56

C4.7.3: Compressive stresses in fmallining *(aFL)* after prestressing (tunnel crown)

Soil element	Stress point	Local number	X [m]	y [m]	°1 [kN/m2]	°2 [kN/m2]	03 [kN/m2]
Clus.4 - El. 2714	32557	1	-0.02	3.26	-4036.68	-964.37	-346.82
Concrete	32558	2	-0.27	3.01	-4685.37	-1036.85	-27.60
	32559	3	-0.02	3.02	-4656.93	-1030.87	-28.86
	32560	4	-0.08	3.15	-4317.95	-996.07	-209.63
	32561	5	-0.16	3.07	-4520.70	-1017.79	-105.62
	32562	6	-0.08	3.07	-4512.77	-1016.48	-107.58
	32563	7	-0.10	3.19	-4216.24	-984.11	-256.99
	32564	8	-0.20	3.08	-4478.01	-1014.47	-133.23
	32565	9	-0.20	3.01	-4683.82	-1035.91	-24.87
	32566	10	-0.10	3.01	-4673.39	-1033.55	-24.59
	32567	11	-0.02	3.09	-4458.04	-1011.22	-138.41
	32568	12	-0.02	3.19	-4215.20	-985.66	-265.09
Clus.4 - El. 2715	32569	1	0.02	3.26	-4051.70	-969.85	-356.70
Concrete	32570	2	0.02	3.02	-4653.38	-1030.12	-29.01
	32571	3	0.27	3.01	-4670.28	-1033.78	-28.70
	32572	4	0.08	3.15	-4318.27	-998.18	-218.90
	32573	5	0.08	3.07	-4507.24	-1016.07	-111.24
	32574	6	0.16	3.07	-4512.69	-1016.47	-107.63
	32575	7	0.02	3.19	-4215.58	-986.57	-268.83
	32576	8	0.02	3.09	-4457.13	-1011.40	-140.13
	32577	9	0.10	3.01	-4659.49	-1030.43	-24.29
	32578	10	0.20	3.01	-4666.06	-1031.91	-24.44
	32579	11	0.20	3.08	-4472.48	-1013.28	-133.36
	32580	12	0.10	3.19	-4224.29	-989.05	-271.41

C4.7.4: Compressive stresses in final lining *(aFL)* after prestressing (tunnel side)

Soil element	Stress point	Local number	X [m]	y [m]	σ_x [kN/m']	σ_y [kN/m']	σ_z [kN/m']
Clus. 4 - El. 277S	33289	1	3.02	0.30	-5307.12	-1181.47	-63.21
Concrete	33290	2	3.28	0.05	-5138.63	-1228.56	-445.72
	33291	3	3.26	0.40	-5157.91	-1234.04	-451.36
	33292	4	3.13	0.26	-5229.91	-1205.04	-247.56
	33293	5	3.22	0.19	-5181.42	-1218.40	-356.76
	33294	6	3.21	0.29	-5184.46	-1220.41	-362.85
	33295	7	3.10	0.22	-5256.79	-1195.10	-175.51
	33296	8	3.20	0.12	-5196.12	-1215.62	-329.44
	33297	9	3.28	0.15	-5139.56	-1228.93	-446.51
	33298	10	3.27	0.29	-5159.49	-1234.30	-450.96
	33299	11	3.18	0.37	-5186.40	-1216.18	-341.68
	33300	12	3.09	0.33	-5254.77	-1196.81	-185.28
Clus. 4 - El. 2776	33301	1	2.97	0.63	-5306.65	-1181.32	-63.01
Concrete	33302	2	3.25	0.47	-5136.80	-1228.30	-446.38
	33303	3	3.18	0.81	-5130.40	-1227.67	-449.91
	33304	4	3.08	0.63	-5217.92	-1201.84	-244.99
	33305	5	3.17	0.59	-5158.04	-1213.05	-355.82
	33306	6	3.15	0.69	-5157.95	-1213.96	-360.04
	33307	7	3.05	0.58	-5249.44	-1193.74	-176.67
	33308	8	3.16	0.51	-5179.41	-1212.41	-331.54
	33309	9	3.23	0.57	-5108.89	-1222.18	-446.47
	33310	10	3.21	0.71	-5118.52	-1225.00	-449.67
	33311	11	3.11	0.76	-5164.57	-1210.95	-339.74
	33312	12	3.03	0.68	-5245.33	-1194.00	-181.95
Clus. 4 - El. 2777	33313	1	2.89	0.94	-5295.39	-1178.67	-62.18

C4.8 - Internal water pressure

C4.8.1: Consolidation analyses result (Case 1)

Plastic point (Tension crack development in lining)

Pi=12 bars

Pi=20 bars

Pi=25 bars

Pi=30 bars

C4.8.2: Stresses in fmallining elements

Soil element	Stress point	Local number	X[m]	Y[m]	σ_x [kN/m']	σ_y [kN/m']	σ_z [kN/m']	$\{\sigma_x+\sigma_y\}/2$ [kN/m']	$\{\sigma_x-\sigma_y\}/2$ [kN/m']
Clus. 3 - EI.4745	56929	1	-2.34	2.27	-0.36	-0.08	0.00	-0.18	-0.18
Concrete	56930	2	-2.22	2.04	-20.48	-4.50	0.00	-10.24	-10.24
	56931	3	-2.04	2.22	-7.94	-1.75	0.00	-3.97	-3.97
	56932	4	-2.24	2.21	-6.01	-1.32	0.00	-3.00	-3.00
	56933	5	-2.21	2.14	-10.59	-2.33	0.00	-5.29	-5.29
	56934	6	-2.15	2.19	-9.01	-1.98	0.00	-4.51	-4.51
	56935	7	-2.31	2.20	-4.72	-1.04	0.00	-2.36	-2.36
	56936	8	-2.26	2.11	-10.89	-2.39	0.00	-5.44	-5.44
	56937	9	-2.17	2.09	-17.39	-3.83	0.00	-8.69	-8.70
	56938	10	-2.10	2.17	-11.18	-2.46	0.00	-5.59	-5.59
	56939	11	-2.13	2.24	-7.00	-1.54	0.00	-3.50	-3.50
	56940	12	-2.25	2.26	-3.63	-0.80	0.00	-1.81	-1.81
Clus. 3 - EI.4746	56941	1	-2.05	2.54	-1.45	-0.32	0.00	-0.73	-0.73
Concrete	56942	2	-2.00	2.26	-5.77	-1.27	0.00	-2.88	-2.88
	56943	3	-1.80	2.42	-0.14	-0.03	0.00	-0.07	-0.07
	56944	4	-1.98	2.45	-1.12	-0.25	0.00	-0.56	-0.56
	56945	5	-1.96	2.37	-2.85	-0.63	0.00	-1.42	-1.42
	56946	6	-1.90	2.42	-1.33	-0.29	0.00	-0.67	-0.67
	56947	7	-2.03	2.46	-0.62	-0.14	0.00	-0.31	-0.31
	56948	8	-2.01	2.35	-3.74	-0.82	0.00	-1.87	-1.87
	56949	9	-1.94	2.31	-3.61	-0.79	0.00	-1.80	-1.80
	56950	10	-1.86	2.38	-1.04	-0.23	0.00	-0.52	-0.52
	56951	11	-1.87	2.46	-1.08	-0.24	0.00	-0.54	-0.54
	56952	12	-1.97	2.51	-1.33	-0.29	0.00	-0.67	-0.67
Clus. 3 - EI.4747	56953	1	-1.72	2.77	-1.97	-0.43	0.00	-0.98	-0.98
Concrete	56954	2	-1.75	2.46	0.00	0.00	0.00	0.00	0.00
	56955	3	-1.53	2.60	0.00	0.00	0.00	0.00	0.00
	56956	4	-1.68	2.66	-1.31	-0.29	0.00	-0.65	-0.65
	56957	5	-1.69	2.57	-0.64	-0.14	0.00	-0.32	-0.32
	56958	6	-1.63	2.61	-0.28	-0.06	0.00	-0.14	-0.14
	56959	7	-1.73	2.68	-1.87	-0.41	0.00	-0.93	-0.93
	56960	8	-1.74	2.55	-1.12	-0.25	0.00	-0.56	-0.56
	56961	9	-1.68	2.50	0.00	0.00	0.00	0.00	0.00
	56962	10	-1.60	2.56	0.00	0.00	0.00	0.00	0.00
	56963	11	-1.59	2.65	-0.16	-0.03	0.00	-0.08	-0.08
	56964	12	-1.66	2.72	-1.37	-0.30	0.00	-0.68	-0.69

C 4.8.3: Finallining in compression due to prestressing effect

Soil element	Stress point	Local number	X[m]	Y[m]	a'_{xx} [kN/m2]	a'_{yy} [kN/m2]	o_{IZI} [kN/m2]	axv [kN/m2]	Status
Clus.4 - El. 2714	32557	1	-0.02	3.26	-4036.62	-346.88	-964.37	-14.83	Elastic
Concrete	32558	2	-0.27	3.01	-4646.47	-66.50	-1036.85	-423.89	Elastic
	32559	3	-0.02	3.02	-4656.70	-29.09	-1030.87	-32.34	Elastic
	32560	4	-0.08	3.15	-4314.98	-212.61	-996.07	-110.44	Elastic
	32561	5	-0.16	3.07	-4508.42	-117.90	-1017.79	-232.52	Elastic
	32562	6	-0.08	3.07	-4509.62	-110.74	-1016.48	-117.80	Elastic
	32563	7	-0.10	3.19	-4212.08	-261.15	-984.11	-128.34	Elastic
	32564	8	-0.20	3.08	-4458.85	-152.39	-1014.47	-287.88	Elastic
	32565	9	-0.20	3.01	-4663.29	-45.39	-1035.91	-308.54	Elastic
	32566	10	-0.10	3.01	-4668.36	-29.62	-1033.56	-152.77	Elastic
	32567	11	-0.02	3.09	-4457.83	-138.62	-1011.22	-30.37	Elastic
	32568	12	-0.02	3.19	-4215.02	-265.26	-985.66	-26.51	Elastic
Clus.4 - El. 2715	32569	1	0.02	3.26	-4051.49	-356.92	-969.85	28.37	Elastic
Concrete	32570	2	0.02	3.02	-4653.20	-29.19	-1030.13	28.99	Elastic
	32571	3	0.27	3.01	-4631.39	-67.59	-1033.78	423.06	Elastic
	32572	4	0.08	3.15	-4315.77	-221.40	-998.18	101.20	Elastic
	32573	5	0.08	3.07	-4504.37	-114.11	-1016.07	112.12	Elastic
	32574	6	0.16	3.07	-4500.51	-119.82	-1016.47	231.39	Elastic
	32575	7	0.02	3.19	-4215.53	-268.89	-986.57	15.14	Elastic
	32576	8	0.02	3.09	-4457.05	-140.21	-1011.40	18.79	Elastic
	32577	9	0.10	3.01	-4654.61	-29.17	-1030.43	150.25	Elastic
	32578	10	0.20	3.01	-4645.65	-44.86	-1031.91	307.13	Elastic
	32579	11	0.20	3.08	-4453.22	-152.62	-1013.29	288.45	Elastic
	32580	12	0.10	3.19	-4220.42	-275.28	-989.05	123.70	Elastic
Clus.4 - El. 2716	32581	1	0.44	3.23	-3979.28	-425.44	-969.04	516.34	Elastic
Concrete	32582	2	0.34	3.00	-4619.96	-92.74	-1036.79	523.40	Elastic

C 4.8.4: Final lining in elastic equilibrium due to prestressing effect (Pi = 10 bars)

Soil element	Stress point	Local number	X[m]	Y[m]	o'xx [kN/m']	O'yy [kN/m']	azz [kN/m']	Oxy [kN/m']	Status
Clus. 4 - EI. 2714	32557	1	-0.02	3.26	-1663.65	-1064.95	-600.29	4.34	Elastic
Concrete (k=le-07))	32558	2	-0.27	3.01	-2010.08	-1014.59	-665.43	-106.89	Elastic
	32559	3	-0.02	3.02	-1989.44	-999.87	-657.65	-3.83	Elastic
	32560	4	-0.08	3.15	-1823.91	-1042.67	-630.65	-31.22	Elastic
	32561	5	-0.16	3.07	-1958.17	-1031.34	-657.69	-56.71	Elastic
	32562	6	-0.08	3.07	-1948.97	-1020.83	-653.35	-28.94	Elastic
	32563	7	-0.10	3.19	-1769.84	-1049.61	-620.28	-31.13	Elastic
	32564	8	-0.20	3.08	-1934.01	-1040.34	-654.36	-63.08	Elastic
	32565	9	-0.20	3.01	-2070.19	-1017.13	-679.21	-76.37	Elastic
	32566	10	-0.10	3.01	-2061.76	-1005.76	-674.85	-26.48	Elastic
	32567	11	-0.02	3.09	-1912.88	-1022.70	-645.83	-14.32	Elastic
	32568	12	-0.02	3.19	-1778.28	-1053.28	-622.94	-10.13	Elastic
Clus. 4 - EI. 2715	32569	1	0.02	3.26	-1678.12	-1074.84	-605.65	8.61	Elastic
Concrete (k=le-07))	32570	2	0.02	3.02	-1986.05	-999.97	-656.92	0.60	Elastic
	32571	3	0.27	3.01	-1996.00	-1015.68	-662.57	106.17	Elastic
	32572	4	0.08	3.15	-1824.54	-1051.36	-632.70	22.28	Elastic
	32573	5	0.08	3.07	-1943.87	-1024.15	-652.97	23.51	Elastic
	32574	6	0.16	3.07	-1950.54	-1033.23	-656.43	55.77	Elastic
	32575	7	0.02	3.19	-1778.72	-1056.86	-623.83	-1.03	Elastic
	32576	8	0.02	3.09	-1912.11	-1024.27	-646.00	3.10	Elastic
	32577	9	0.10	3.01	-2048.53	-1005.33	-671.85	24.06	Elastic
	32578	10	0.20	3.01	-2053.43	-1016.61	-675.41	75.07	Elastic
	32579	11	0.20	3.08	-1928.57	-1040.59	-653.21	63.82	Elastic
	32580	12	0.10	3.19	-1777.74	-1063.55	-625.08	26.63	Elastic
Clus. 4 - EI. 2716	32581	1	0.44	3.23	-1660.56	-1089.19	-604.94	106.20	Elastic
Concrete (k=le-07))	32582	2	0.34	3.00	-1996.77	-1008.54	-661.17	112.52	Elastic

C 4.8.5: Tension cracks in (fmallining) due to high internal water pressure (Pi= 20 bars)

Soil element	Stress point	Local number	x lrn]	VIm]	oIxx IkN/m']	O'yy IkN/m']	oIzz IkN/m']	Oxy IkN/m']	Status
Clus. 4 - El. 2714 Concrete (k= 1e-8)	32557	1	-0.02	3.26	-0.22	-1779.84	-391.61	19.79	Tension cut-off
	32558	2	-0.27	3.01	-5.63	-1977.08	-436.19	105.46	Tension cut-off
	32559	3	-0.02	3.02	-0.42	-1982.77	-436.30	28.71	Tension cut-off
	32560	4	-0.08	3.15	-1.21	-1926.42	-424.08	48.28	Tension cut-off
	32561	5	-0.16	3.07	-5.81	-2009.30	-443.32	108.00	Tension cut-off
	32562	6	-0.08	3.07	-3.22	-1953.25	-430.42	79.27	Tension cut-off
	32563	7	-0.10	3.19	-0.67	-1932.08	-425.20	35.88	Tension cut-off
	32564	8	-0.20	3.08	-8.45	-2018.45	-445.92	130.62	Tension cut-off
	32565	9	-0.20	3.01	-6.89	-2020.89	-446.11	97.95	Elastic
	32566	10	-0.10	3.01	-7.63	-1980.08	-437.30	122.89	Tension cut-off
	32567	11	-0.02	3.09	-0.13	-1916.80	-421.72	16.03	Tension cut-off
	32568	12	-0.02	3.19	-0.08	-1837.06	-404.17	12.05	Tension cut-off
Clus. 4 - El. 2715 Concrete (k= 1e-8)	32569	1	0.02	3.26	-0.16	-1777.35	-391.05	-17.06	Tension cut-off
	32570	2	0.02	3.02	-0.41	-1982.79	-436.30	-28.34	Tension cut-off
	32571	3	0.27	3.01	-5.69	-1976.81	-436.15	-106.09	Tension cut-off
	32572	4	0.08	3.15	-1.12	-1923.32	-423.38	-46.45	Tension cut-off
	32573	5	0.08	3.07	-3.09	-1952.21	-430.16	-77.61	Tension cut-off
	32574	6	0.16	3.07	-23.14	-2012.12	-447.76	-108.20	Elastic
	32575	7	0.02	3.19	-0.04	-1836.03	-403.94	-8.61	Tension cut-off
	32576	8	0.02	3.09	-0.10	-1916.61	-421.67	-13.58	Tension cut-off
	32577	9	0.10	3.01	-7.52	-1979.13	-437.06	-121.97	Tension cut-off
	32578	10	0.20	3.01	-28.68	-2025.19	-451.85	-97.01	Elastic
	32579	11	0.20	3.08	-8.80	-2015.98	-445.45	-133.17	Tension cut-off
	32580	12	0.10	3.19	-0.64	-1926.22	-423.91	-35.21	Tension cut-off
Clus. 4 - El. 2716 Concrete (k= 1e-8)	32581	1	0.44	3.23	-28.95	-1829.46	-408.85	-230.15	Tension cut-off
	32582	2	0.34	3.00	-34.27	-1943.43	-435.10	-258.09	Tension cut-off

C 4.8.6: Tension cracks in (final lining) due to high internal water pressure (Pi = 25 bars)

Soil element	Stress point	Local number	X[m]	Y [m]	a'xx [kN/m']	*a'yy* [kN/m']	a_{zz} [kN/m']	a_{xy} [kN/m']	Status
Clus. 4 - EI. 2714 Concrete (k=le-07))	32557	1	-0.02	3.26	-0.20	-2199.64	-483.97	21.09	Tension cut-off
	32558	2	-0.27	3.01	-12.84	-2404.00	-531.70	175.68	Tension cut-off
	32559	3	-0.02	3.02	-0.54	-2460.27	-541.38	36.44	Tension cut-off
	32560	4	-0.08	3.15	-1.53	-2373.45	-522.49	60.18	Tension cut-off
	32561	5	-0.16	3.07	-139.11	-2540.66	-589.55	104.71	Elastic
	32562	6	-0.08	3.07	-3.63	-2408.09	-530.58	93.53	Tension cut-off
	32563	7	-0.10	3.19	-1.78	-2385.22	-525.14	65.11	Tension cut-off
	32564	8	-0.20	3.08	-10.21	-2494.91	-551.12	159.58	Tension cut-off
	32565	9	-0.20	3.01	-3.81	-2538.05	-559.21	98.29	Tension cut-off
	32566	10	-0.10	3.01	-28.44	-2471.41	-549.97	177.47	Elastic
	32567	11	-0.02	3.09	-0.16	-2350.06	-517.05	19.33	Tension cut-off
	32568	12	-0.02	3.19	-0.06	-2259.21	-497.04	11.85	Tension cut-off
Clus. 4 - EI. 2715 Concrete (k=le-07))	32569	1	0.02	3.26	-0.21	-2197.64	-483.53	-21.28	Tension cut-off
	32570	2	0.02	3.02	-0.47	-2459.26	-541.14	-34.00	Tension cut-off
	32571	3	0.27	3.01	-12.85	-2405.28	-531.99	-175.83	Tension cut-off
	32572	4	0.08	3.15	-1.40	-2369.16	-521.52	-57.56	Tension cut-off
	32573	5	0.08	3.07	-3.45	-2404.84	-529.82	-91.13	Tension cut-off
	32574	6	0.16	3.07	-143.77	-2538.91	-590.19	-105.90	Elastic
	32575	7	0.02	3.19	-0.04	-2257.77	-496.72	-9.42	Tension cut-off
	32576	8	0.02	3.09	-0.10	-2348.92	-516.78	-15.00	Tension cut-off
	32577	9	0.10	3.01	-36.01	-2471.53	-551.66	-177.34	Elastic
	32578	10	0.20	3.01	-3.93	-2537.65	-559.15	-99.84	Tension cut-off
	32579	11	0.20	3.08	-10.61	-2492.40	-550.66	-162.59	Tension cut-off
	32580	12	0.10	3.19	-1.62	-2380.14	-523.99	-62.10	Tension cut-off
Clus. 4 - EI. 2716 Concrete (k=le-07))	32581	1	0.44	3.23	-43.81	-2262.44	-507.38	-314.84	Tension cut-off
	32582	2	0.34	3.00	-42.66	-2419.89	-541.76	-321.29	Tension cut-off

C 4.8.7: Tension cracks in (fmallining) due to high internal water pressure (Pi = 30 bars)

Soil element	Stress point	Local number	X[m]	Y[m]	σ'''' [kN/m2]	σ'VV [kN/m2]	σ'ZZ [kN/m2]	σ'''' [kN/m2]	Status
Clus. 4 - El. 2714 Concrete (k=le-06)	32557	1	-0.02	3.26	-0.35	-2576.30	-566.86	29.82	Tension cut-off
	32558	2	-0.27	3.01	-19.22	-2837.77	-628.54	233.57	Tension cut-off
	32559	3	-0.02	3.02	-0.55	-2949.19	-648.94	40.45	Tension cut-off
	32560	4	-0.08	3.15	-2.99	-2831.68	-623.63	91.94	Tension cut-off
	32561	5	-0.16	3.07	-175.28	-3068.31	-713.59	118.67	Elastic
	32562	6	-0.08	3.07	-5.38	-2875.75	-633.85	124.35	Tension cut-off
	32563	7	-0.10	3.19	-2.87	-2864.10	-630.73	90.71	Tension cut-off
	32564	8	-0.20	3.08	-10.29	-3021.42	-666.98	176.31	Tension cut-off
	32565	9	-0.20	3.01	-16.47	-3060.55	-676.94	99.76	Elastic
	32566	10	-0.10	3.01	-17.03	-2956.38	-654.15	224.41	Tension cut-off
	32567	11	-0.02	3.09	-0.22	-2802.26	-616.55	24.97	Tension cut-off
	32568	12	-0.02	3.19	-0.11	-2666.69	-586.70	17.08	Tension cut-off
Clus. 4 - El. 2715 Concrete (k=le-06)	32569	1	0.02	3.26	-0.40	-2577.84	-567.21	-31.92	Tension cut-off
	32570	2	0.02	3.02	-0.50	-2946.72	-648.39	-38.24	Tension cut-off
	32571	3	0.27	3.01	-19.86	-2828.69	-626.68	-237.00	Tension cut-off
	32572	4	0.08	3.15	-2.71	-2831.26	-623.47	-87.66	Tension cut-off
	32573	5	0.08	3.07	-5.30	-2872.80	-633.18	-123.40	Tension cut-off
	32574	6	0.16	3.07	-186.67	-3072.39	-716.99	-115.08	Elastic
	32575	7	0.02	3.19	-0.09	-2666.16	-586.57	-15.18	Tension cut-off
	32576	8	0.02	3.09	-0.18	-2800.28	-616.10	-22.44	Tension cut-off
	32577	9	0.10	3.01	-17.60	-2955.32	-654.04	-228.03	Tension cut-off
	32578	10	0.20	3.01	-18.27	-3065.06	-678.33	-95.19	Elastic
	32579	11	0.20	3.08	-10.42	-3020.56	-666.82	-177.42	Tension cut-off
	32580	12	0.10	3.19	-2.41	-2868.05	-631.50	-83.10	Tension cut-off
Clus. 4 - El. 2716 Concrete (k=le-06)	32581	1	0.44	3.23	-66.77	-2661.33	-600.18	-421.53	Tension cut-off
	32582	2	0.34	3.00	-57.68	-2910.44	-652.99	-409.74	Tension cut-off

C 4.8.8: Tension cracks in (fmallining) due to high internal water pressure (Pi= 35 bars)

Soil element	Stress point	Local number	X[m]	Y[m]	0'XX [kN/m']	O'yy [kN/m']	aIZI [kN/m']	Oxy [kN/m']	Status
Clus. 4 - EI. 2714 Concrete (k=le-05)	32557	1	-0.02	3.26	-0.49	-2974.04	-654.40	38.02	Tension cut-off
	32558	2	-0.27	3.01	-20.79	-3310.50	-732.88	262.35	Tension cut-off
	32559	3	-0.02	3.02	-0.62	-3437.63	-756.41	46.05	Tension cut-off
	32560	4	-0.08	3.15	-4.34	-3285.94	-723.86	119.41	Tension cut-off
	32561	5	-0.16	3.07	-202.15	-3583.92	-832.93	150.02	Elastic
	32562	6	-0.08	3.07	-6.85	-3345.86	-737.60	151.40	Tension cut-off
	32563	7	-0.10	3.19	-4.23	-3329.22	-733.36	118.61	Tension cut-off
	32564	8	-0.20	3.08	-11.20	-3548.16	-783.06	199.33	Tension cut-off
	32565	9	-0.20	3.01	-3.80	-3572.52	-786.79	116.58	Tension cut-off
	32566	10	-0.10	3.01	-20.61	-3448.80	-763.27	266.59	Tension cut-off
	32567	11	-0.02	3.09	-0.27	-3263.08	-717.94	29.80	Tension cut -off
	32568	12	-0.02	3.19	-0.17	-3091.02	-680.06	22.66	Tension cut-off
Clus. 4 - EI. 2715 Concrete (k=le-05)	32569	1	0.02	3.26	-0.47	-2979.85	-655.67	-37.49	Tension cut-off
	32570	2	0.02	3.02	-0.59	-3435.74	-755.99	-44.87	Tension cut-off
	32571	3	0.27	3.01	-21.48	-3302.61	-731.30	-266.33	Tension cut-off
	32572	4	0.08	3.15	-3.94	-3291.33	-724.96	-113.87	Tension cut-off
	32573	5	0.08	3.07	-6.74	-3346.07	-737.62	-150.16	Tension cut-off
	32574	6	0.16	3.07	-217.79	-3588.99	-837.49	-142.82	Elastic
	32575	7	0.02	3.19	-0.15	-3093.43	-680.59	-21.36	Tension cut-off
	32576	8	0.02	3.09	-0.27	-3262.78	-717.87	-29.65	Tension cut-off
	32577	9	0.10	3.01	-21.07	-3447.95	-763.19	-269.54	Tension cut-off
	32578	10	0.20	3.01	-4.33	-3575.53	-787.57	-112.52	Elastic
	32579	11	0.20	3.08	-11.28	-3542.44	-781.82	-199.87	Tension cut-off
	32580	12	0.10	3.19	-3.65	-3339.23	-735.43	-110.42	Tension cut-off
Clus. 4 - EI. 2716 Concrete (k=le-05)	32581	1	0.44	3.23	-80.77	-3104.56	-700.77	-500.77	Tension cut-off
	32582	2	0.34	3.00	-67.20	-3398.91	-762.54	-477.92	Tension cut-off

C4.8.9: Final lining design (elastic analysis)

CONCRETE LINING DESIGN (Seeber Theory)

PROJECT:

INPUT PARAMETERS:			CALCULATION:			
Geometry:			Primary .tre..... In rock ma.. :			
External tunnel radius:	3.30	[mJ	Vertical	av-	5.2	(Nlmm-)
Lining Ihid",e,,:	0.30	[mJ	Horizontal	oft-	4.16	[N/mmj
Internal tunnel radius:	3.00	m	loading ea." ~Empty tunnel			
OVerbunfon:	200.00	[mJ	Groundwater pressure	Pv00-	0.98	[N/mmj
Groundwater height	too.OO	[mJ	Concrete strain	,,, '	-3.38E-04	[.J
Rockma .. :				'',''.	-3.71E-04	H
Elasticity modulus:	10000	[Nlmm1	MirWnallhiekness	t'"',-	0.18	[mJ
IPoisson's ratio~	0.20	[.J	loading ea.e - Injection			
I Unit weight	26.00	[kNlm1	Pressure on pump	~	1.50	[N/mmj
Horizontal stress ratio:	0.80	[-J	Max. allow. pressure on Ininll	Pm.'"	2.34	[Nlmm1
Defonnation modutus(Lame)	8333	[Nlmm1	Injection pressure on Inin!!	1lt1-	1.50	[N/mmj
Concrete lining:			MirWnallhiekness	t..,.	0.19	[mJ
Concrete quality	C30		Concrete strain	'',=~	-S.16E-04	[-J
Elasticity modu"':	30000	[Nlmm1		''' -	-S.66E-04	[-J
IPoisson"sratioj	0.20	-				
Thermal coemdent	1.20E-05	1rC	loading ea." - Operation			
Strength:	30.00	[Nlmm1	Inj. pressore Ioos (creep)	6i>.:-	-0.45	[N/mmj
Max. alowed ..... :	8.00E-04	I-J	Inj pressure Ioos (temp.)	APt-	-0.52	[Nlmm1
Intemal water pressure:	0.80	[Nlmm1	Rem"" inJ. pressure	IIIIIIIIII	0.53	[Nlmm1
Reduction and safety factors:			Remaind concrete strain	,,, -	-1.81E-04	[-J
Concrete .lrength reduction	0_9	-				
Concrete strain reduction	0.8	I-J	Pressure taken by rock	',__'	1.51	[N/mm1
Safety factor	1.5	I-J	Maximal allowed pressure	Plli"	2.04	[Nlmm1
Pre.. ure 10~ :						
I on pump	0	'Jl.	Intemal pressure (caleul.)	111-·	1.09	(N/mmj
Creep and shrinkege	30	'Jl.	Concreta strain	'',--	-3.26E-04	[-j
Temperature	15	·C		''''	-3.64E-04	[-J

C4_8.10: Final lining design - grouting effect

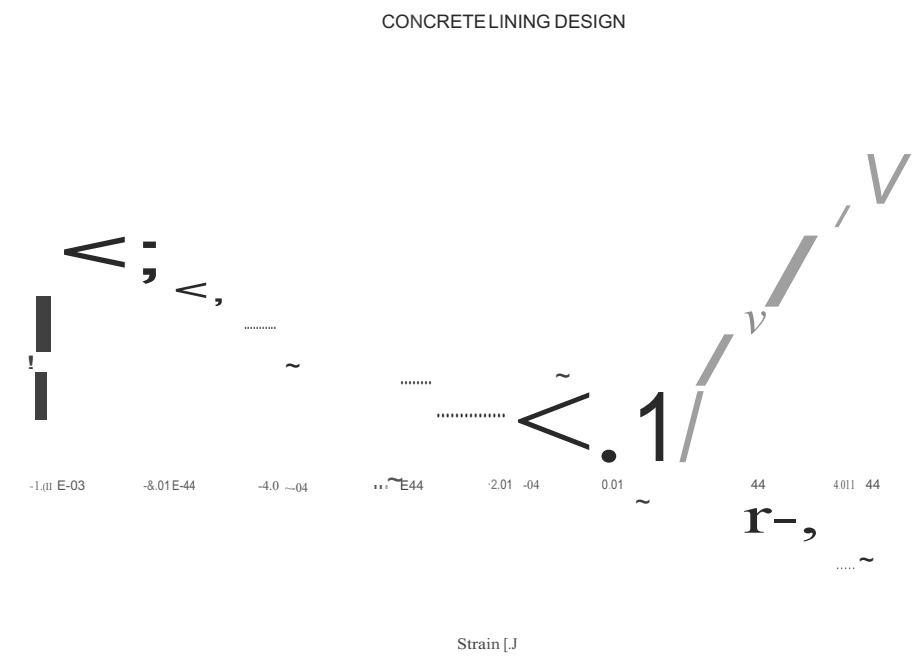

Case 1: Result of groundwater flow analysis
C4.8.11: Seepage flow Pi = 10 bars (Lining element 1422- side of tunnel)

Soilelement	Stress point	Local number	X[m]	V[m]	q. [m/s]	q, [m/s]	[q] [m/s]	Saturation [%]
Clus.4 -EI. 1422 Concrete (k= *1e-B)*	17053	1	3.03	O.OB	1.60E-06	3.39E-OB	1.60E-06	100.00
	17054	2	3.25	0.43	1.43E-06	1.79E-07	1.44E-06	100.00
	17055	3	3.19	0.77	1.40E-06	3.30E-07	1.44E-06	100.00
	17056	4	3.12	0.32	1.56E-06	1.50E-07	1.56E-06	100.00
	17057	5	3.19	0.43	1.49E-06	1.91E-07	1.50E-06	100.00
	1705B	6	3.17	0.53	1.4BE-06	2.40E-07	1.50E-06	100.00
	17059	7	3.10	O.lB	1.5BE-06	B.34E-OB	1.5BE-06	100.00
	17060	B	3.19	0.32	1.51E-06	1.42E-07	1.52E-06	100.00
	17061	9	3.24	0.54	1.42E-06	2.27E-07	1.44E-06	100.00
	17062	10	3.21	0.6B	1.41E-06	2.B7E-07	1.44E-06	100.00
	17063	11	3.15	0.56	1.50E-06	2.5BE-07	1.52E-06	100.00
	17064	12	3.09	0.2B	1.5BE-06	1.3BE-07	1.5BE-06	100.00

C48 12 Seepage flow Pi =20 bars (Linmg e ement 1422- side of tunnel)

Soilelement	Stress point	Local number	X[m]	V[m]	q.[m/s]		lql [m/s]	Saturation [%]
Clus.4 - EI. 1422 Concrete (k= *1e-B)*	17053	1	3.03	O.OB	3.34E-06	7.94E-OB	3.35E-06	100.00
	17054	2	3.25	0.43	3.00E-06	3.B7E-07	3.02E-06	100.00
	17055	3	3.19	0.77	2.94E-06	7.02E-07	3.02E-06	100.00
	17056	4	3.12	0.32	3.26E-06	3.24E-07	3.27E-06	100.00
	17057	5	3.19	0.43	3.12E-06	4.09E-07	3.15E-06	100.00
	1705B	6	3.17	0.53	3.10E-06	5.13E-07	3.14E-06	100.00
	17059	7	3.10	O.lB	3.31E-06	1.B4E-07	3.32E-06	100.00
	17060	B	3.19	0.32	3.17E-06	3.09E-07	3.1BE-06	100.00
	17061	9	3.24	0.54	2.9BE-06	4.B6E-07	3.02E-06	100.00
	17062	10	3.21	0.6B	2.95E-06	6.12E-07	3.01E-06	100.00
	17063	11	3.15	0.56	3.13E-06	5.51E-07	3.1BE-06	100.00
	17064	12	3.09	0.2B	3.30E-06	2.9BE-07	3.32E-06	100.00

C4813 Seepa e flow Pi =25 bars (L-mmg e ement 1422- sideo f tunne l)

Soil element	Stress point	local number	X[m]	V[m]	q.[m/s]	qy[m/s]	Iql [m/s]	Saturation [%]
Clus. 4 - EI. 1422 Concrete (k=le-07))	17053	1	3.03	0.08	6.25E-06	6.70E-08	6.25E-06	100.00
	17054	2	3.25	0.43	5.87E-06	6.87E-07	5.91E-06	100.00
	17055	3	3.19	0.77	5.76E-06	l.30E-06	5.91E-06	100.00
	17056	4	3.12	0.32	6.10E-06	5.34E-07	6.13E-06	100.00
	17057	5	3.19	0.43	5.97E-06	7.12E-07	6.01E-06	100.00
	17058	6	3.17	0.53	5.94E-06	9.08E-07	6.01E-06	100.00
	17059	7	3.10	0.18	6.17E-06	2.66E-07	6.18E-06	100.00
	17060	8	3.19	0.32	6.02E-06	5.14E-07	6.04E-06	100.00
	17061	9	3.24	0.54	5.84E-06	8.82E-07	5.90E-06	100.00
	17062	10	3.21	0.68	5.79E-06	l.13E-06	5.90E-06	100.00
	17063	11	3.15	0.56	5.96E-06	9.74E-07	6.04E-06	100.00
	17064	12	3.09	0.28	6.16E-06	4.80E-07	6.18E-06	100.00

C4814 Seepage flOWPi= 30 bars (L-mmge emen t 1422- sideo ftunn e1)

Soil element	Stress point	local number	X[m]	V [m]	q. [m/s]	qy[m/s]	Iql [m/s]	Saturation [%]
Clus. 4 - EI. 1422 Concrete (k=le-06)	17053	1	3.03	0.08	7.45E-06	-6.46E-07	7.48E-06	100.00
	17054	2	3.25	0.43	7.10E-06	l.66E-07	7.10E-06	100.00
	17055	3	3.19	0.77	7.03E-06	9.25E-07	7.09E-06	100.00
	17056	4	3.12	0.32	7.31E-06	-5.46E-08	7.31E-06	100.00
	17057	5	3.19	0.43	7.19E-06	l.80E-07	7.19E-06	100.00
	17058	6	3.17	0.53	7.17E-06	4.19E-07	7.18E-06	100.00
	17059	7	3.10	0.18	7.37E-06	-3.87E-07	7.38E-06	100.00
	17060	8	3.19	0.32	7.22E-06	-6.40E-08	7.22E-06	100.00
	17061	9	3.24	0.54	7.08E-06	4.06E-07	7.09E-06	100.00
	17062	10	3.21	0.68	7.05E-06	7.08E-07	7.09E-06	100.00
	17063	11	3.15	0.56	7.20E-06	4.95E-07	7.21E-06	100.00
	17064	12	3.09	0.28	7.38E-06	-l.29E-07	7.38E-06	100.00

C4.8.15: Seepa e flow Pi =35 bars (Lining element 1422- side of tunnel)

Soilelement	Stress point	local number	Xlm)	VIm)	q,lm/s)	qylm/s)	Iqllm/s)	Saturation 1%)
(Ius. 4 - EI. 1422 (oncrete(k=le-05)	17053	1	3.03	0.08	8.77E-06	-3.09E-06	9.30E-06	100.00
	17054	2	3.25	0.43	8.56E-06	-1.94E-06	8.78E-06	100.00
	17055	3	3.19	0.77	8.69E-06	-9.73E-07	8.74E-06	100.00
	17056	4	3.12	0.32	8.76E-06	-2.30E-06	9.06E-06	100.00
	17057	5	3.19	0.43	8.67E-06	-1.96E-06	8.89E-06	100.00
	17058	6	3.17	0.53	8.72E-06	-1.66E-06	8.88E-06	100.00
	17059	7	3.10	0.18	8.73E-06	-2.73E-06	9.15E-06	100.00
	17060	8	3.19	0.32	8.65E-06	-2.27E-06	8.94E-06	100.00
	17061	9	3.24	0.54	8.6IE-06	-1.63E-06	8.76E-06	100.00
	17062	10	3.21	0.68	8.66E-06	-1.25E-06	8.75E-06	100.00
	17063	11	3.15	0.56	8.78E-06	-1.58E-06	8.92E-06	100.00
	17064	12	3.09	0.28	8.82E-06	-2.42E-06	9.15E-06	100.00
(Ius. 4 - EI. 1423 (oncrete(k=le-05)	17065	1	3.14	0.92	8.71E-06	-5.28E-07	8.72E-06	100.00
	17066	2	3.03	1.25	8.64E-06	4.84E-07	8.66E-06	100.00
	17067	3	2.66	1.44	9.03E-06	1.58E-06	9.17E-06	100.00
	17068	4	3.01	1.12	8.82E-06	1.30E-07	8.82E-06	100.00
	17069	5	2.97	1.22	8.78E-06	4.58E-07	8.79E-06	100.00
	17070	6	2.86	1.28	8.93E-06	7.70E-07	8.96E-06	100.00
	17071	7	3.12	1.02	8.69E-06	-2.42E-07	8.70E-06	100.00
	17072	8	3.07	1.15	8.67E-06	1.63E-07	8.67E-06	100.00
	17073	9	2.92	1.32	8.77E-06	7.91E-07	8.81E-06	100.00
	17074	10	2.77	1.39	8.93E-06	1.23E-06	9.02E-06	100.00
	17075	11	2.81	1.29	9.03E-06	8.65E-07	9.07E-06	100.00
	17076	12	3.00	1.08	8.88E-06	1.92E-08	8.88E-06	100.00
(Ius. 4 - EI. 1424 (oncrete(k=le-05)	17077	1	2.64	1.49	8.96E-06	1.75E-06	9.12E-06	100.00
	17078	2	3.01	1.30	8.62E-06	6.42E-07	8.65E-06	100.00
	17079	3	2.85	1.62	8.41E-06	1.67E-06	8.58E-06	100.00
	17080	4	2.78	1.48	8.77E-06	1.46E-06	8.89E-06	100.00
	17081	5	2.89	1.42	8.67E-06	1.11E-06	8.74E-06	100.00
	17082	6	2.84	1.52	8.60E-06	1.45E-06	8.72E-06	100.00
	17083	7	2.75	1.43	8.89E-06	1.38E-06	9.00E-06	100.00
	17084	8	2.90	1.36	8.75E-06	9.34E-07	8.80E-06	100.00
	17085	9	2.97	1.40	8.57E-06	9.46E-07	8.62E-06	100.00
	17086	10	2.91	1.52	8.48E-06	1.36E-06	8.59E-06	100.00
	17087	11	2.79	1.58	8.57E-06	1.71E-06	8.74E-06	100.00
	17088	12	2.70	1.53	8.79E-06	1.74E-06	8.96E-06	100.00

Case 2: Results of ground flow analysis

C4.8.18: Seepage' flow calculation result (Pi = 25 bars and Kr = variable)

1: Seepage flow in lining

Soil element	Stress point	Local number	X[m]	V[m]	q,[m/s]	q, [m/s]	[q] [m/s]	Satu ration [%]
				K; = 1 X 10-7				
Clus. 4-	13633	1	0.04	3.03	8.s0E-08	6.16E-06	6.16E-06	100.00
EI. 1137	13634	2	0.60	3.22	1.09E-06	s.74E-06	s.84E-06	100.00
	13635	3	0.04	3.28	8.01E-08	s.84E-06	s.84E-06	100.00
	13636	4	0.17	3.14	3.39E-07	6.04E-06	6.0sE-06	100.00
Concrete	13637	5	0.34	3.20	6.s1E-07	s.91E-06	s.94E-06	100.00
(k=le-07))	13638	6	0.17	3.22	3.2sE-07	s.93E-06	s.94E-06	100.00
	13639	7	0.21	3.09	4.32E-07	6.09E-06	6.11E-06	100.00
	13640	8	0.44	3.16	8.33E-07	s.92E-06	s.98E-06	100.00
	13641	9	0.44	3.25	7.93E-07	s.78E-06	s.84E-06	100.00
	13642	10	0.21	3.28	3.90E-07	s.82E-06	s.83E-06	100.00
				tc; = 5 X 10-6				
Clus. 4-	13633	1	0.04	3.03	1.28E-07	9.33E-06	9.33E-06	100.00
EI. 1137	13634	2	0.60	3.22	1.76E-06	9.34E-06	9.s0E-06	100.00
	13635	3	0.04	3.28	1.28E-07	9.48E-06	9.48E-06	100.00
	13636	4	0.17	3.14	s.29E-07	9.s2E-06	9.54E-06	100.00
Concrete	13637	5	0.34	3.20	1.04E-06	9.49E-06	9.5sE-06	100.00
(k=le-07))	13638	6	0.17	3.22	s.17E-07	9.s4E-06	9.ssE-06	100.00
	13639	7	0.21	3.09	6.62E-07	9.46E-06	9.48E-06	100.00
	13640	8	0.44	3.16	l.32E-06	9.47E-06	9.56E-06	100.00
	13641	9	0.44	3.25	l.28E-06	9.40E-06	9.48E-06	100.00
	13642	10	0.21	3.28	6.27E-07	9.46E-06	9.48E-06	100.00
				K; = 1 X 10-6				
Clus.4	13633	1	0.04	3.03	l.31E-07	9.47E-06	9.47E-06	100.00
- EI. 1137	13634	2	0.60	3.22	1.76E-06	9.38E-06	9.54E-06	100.00
	13635	3	0.04	3.28	1.28E-07	9.s3E-06	9.s3E-06	100.00
Concrete	13636	4	0.17	3.14	s.33E-07	9.s9E-06	9.60E-06	100.00
(k=le-07))	13637	5	0.34	3.20	1.04E-06	9.s4E-06	9.s9E-06	100.00
	13638	6	0.17	3.22	s.19E-07	9.s8E-06	9.s9E-06	100.00
	13639	7	0.21	3.09	6.70E-07	9.ssE-06	9.s7E-06	100.00
	13640	8	0.44	3.16	1.33E-06	9.s1E-06	9.60E-06	100.00
	13641	9	0.44	3.25	1.29E-06	9.44E-06	9.s3E-06	100.00
	13642	10	0.21	3.28	6.29E-07	9.s1E-06	9.s3E-06	100.00
				K; = 5 x 10-s				
Clus.4	13633	1	0.04	3.03	1.21E-07	8.82E-06	8.82E-06	100.00
- EI. 1137	13634	2	0.60	3.22	1.67E-06	8.83E-06	8.98E-06	100.00
	13635	3	0.44	3.28	1.21E-07	8.9sE-06	8.9sE-06	100.00
	13636	4	0.17	3.14	s.01E-07	9.03E-06	9.04E-06	100.00
Concrete	13637	5	0.35	3.20	9.8sE-07	8.99E-06	9.0sE-06	100.00
(k=le-07))	13638	6	0.17	3.22	4.90E-07	9.03E-06	9.04E-06	100.00
	13639	7	0.21	3.09	6.27E-07	8.96E-06	8.99E-06	100.00
	13640	8	0.44	3.16	1.26E-06	8.98E-06	9.06E-06	100.00
	13641	9	0.44	3.25	l.22E-06	8.88E-06	8.96E-06	100.00
	13642	10	0.21	3.28	s.94E-07	8.93E-06	8.9sE-06	100.00

2: Seepage flow in grouted zone

Soil element	Stress point	Local number	X[m]	Y[m]	q_s[m/s]	q [m/s]	[q] [m/s]	Saturation [%]
				$K = 1 \times 10^{-7}$				
(Ius. 2 - EI.893	1070S	1	4.37	-0.73	2.90E-06	-S.74E-07	2.96E-06	100
Rock k=1e-07	10706	2	4.36	0.03	3.13E-06	-6.70E-08	3.13E-06	100
	10707	3	3.S1	-0.3S	S.36E-06	-6.32E-07	S.40E-06	100
Grouted zone	10708	4	4.17	-0.47	3.S4E-06	-4.88E-07	3.58E-06	100
	10709	S	4.16	-0.23	3.63E-06	-2.91E-07	3.64E-06	100
	10710	6	3.90	-O.3S	4.32E-06	-4.80E-07	4.3SE-06	100
	10711	7	4.37	-O.Sl	2.99E-06	-4.32E-07	3.02E-06	100
	10712	8	4.37	-0.20	3.08E-06	-2.27E-07	3.09E-06	100
	10713	9	4.10	-0.08	3.83E-06	-l.60E-07	3.84E-06	100
	10714	10	3.76	-0.23	4.7SE-06	-3.87E-07	4.77E-06	100
				$K_s = 5 \times 10^{-6}$				
(Ius. 2 - EI.893	1070S	1	4.37	-0.73	8.13E-06	-6.36E-06	l.03E-OS	100
Rock k= Se-06	10706	2	4.36	0.03	8.82E-06	-S.06E-06	1.02E-OS	100
	10707	3	3.51	-0.3S	9.61E-06	-6.80E-06	1.18E-OS	100
	10708	4	4.17	-0.47	8.62E-06	-6.1SE-06	1.06E-OS	100
Grouted zone	10709	S	4.16	-0.23	8.86E-06	-S.72E-06	l.OSE-OS	100
	10710	6	3.90	-0.3S	9.07E-06	-6.24E-06	l.10E-OS	100
	10711	7	4.37	-O.Sl	8.3SE-06	-6.00E-06	l.03E-OS	100
	10712	8	4.37	-0.20	8.63E-06	-S.48E-06	l.02E-OS	100
	10713	9	4.10	-0.08	9.09E-06	-S.47E-06	l.06E-OS	100
	10714	10	3.76	-0.23	9.42E-06	-6.17E-06	1.13E-OS	100
				$K_s = 1 \times 10^{-6}$				
(Ius. 2 - EI.893	1070S	1	4.37	-0.73	7.96E-06	-2.21E-06	8.26E-06	100
Rock k = 1e-06	10706	2	4.36	0.03	8.24E-06	-8.41E-07	8.28E-06	100
	10707	3	3.S1	-0.3S	9.SSE-06	-1.93E-06	9.74E-06	100
	10708	4	4.17	-0.47	8.43E-06	-1.8SE-06	8.63E-06	100
	10709	S	4.16	-0.23	8.S2E-06	-1.38E-06	8.63E-06	100
Grouted zone	10710	6	3.90	-0.3S	8.91E-06	-1.73E-06	9.08E-06	100
	10711	7	4.37	-O.Sl	8.07E-06	-1.82E-06	8.28E-06	100
	10712	8	4.37	-0.20	8.19E-06	-1.26E-06	8.28E-06	100
	10713	9	4.10	-0.08	8.67E-06	-l.08E-06	8.73E-06	100
	10714	10	3.76	-0.23	9.20E-06	-l.SlE-06	9.32E-06	100
				$K_s = 5 \times 10^{-8}$				
(Ius. 2 - EI.893	1070S	1	4.37	-0.73	2.77E-06	-S.62E-OS	S.63E-OS	100
Rock k=Se-OS	10706	2	4.36	0.03	9.SSE-06	-S.71E-OS	S.79E-OS	100
	10707	3	3.S1	-0.3S	3.97E-06	-6.76E-OS	6.78E-OS	100
	10708	4	4.17	-0.47	4.54E-06	-S.87E-OS	S.89E-OS	100
	10709	S	4.16	-0.23	6.96E-06	-S.91E-OS	S.9SE-OS	100
Grouted zone	10710	6	3.90	-0.3S	S.20E-06	-6.20E-OS	6.22E-OS	100
	10711	7	4.37	-0.51	4.70E-06	-S.68E-OS	S.70E-OS	100
	10712	8	4.37	-0.20	7.4SE-06	-S.71E-OS	S.76E-OS	100
	10713	9	4.10	-0.08	8.63E-06	-S.99E-OS	6.0SE-OS	100
	10714	10	3.76	-0.23	6.53E-06	-6.41E-OS	6.44E-OS	100
	1071S	11	3.76	-0.47	3.18E-06	-6.34E-OS	6.3SE-OS	100
	10716	12	4.11	-0.63	2.79E-06	-S.89E-OS	S.90E-OS	100

3: Seepage flow in rock zone

Soil element	Stress point	Local number	X [m]	Y[m]	q,[m/s]	qy [m/s]	[q] [m/s]	Saturation [%]
				K = 1 x 10-7				
Clus. 3 - EI. 1089	130S7	1	-3.2S	-0.96	-S.48E-06	-1.70E-D6	S.74E-06	100
Rock k=le-07	130S8	2	-3.29	-0.39	-S.83E-06	-7.82E-07	S.88E-06	100
	130S9	3	-3.37	-0.40	-S.66E-06	-7.66E-07	S.71E-06	100
	13060	4	-3.29	-0.70	-S.63E-06	-1.29E-06	S.77E-06	100
	13061	S	-3.30	-0.S2	-S.73E-06	-1.00E-06	S.82E-06	100
	13062	6	-3.33	-0.S3	-S.68E-06	-9.90E-07	S.76E-06	100
	13063	7	-3.26	-0.80	-S.61E-06	-1.4SE-06	S.79E-06	100
	13064	8	-3.28	-0.S7	-S.7SE-06	-1.08E-06	S.8SE-06	100
	1306S	9	-3.31	-0.39	-S.78E-06	-7.66E-07	S.83E-06	100
	13066	10	-3.3S	-0.39	-S.71E-06	-7.60E-07	S.76E-06	100
				$ic;$ = 5 x 10-6				
Clus. 3 - EI. 1089	130S7	1	-3.2S	-0.96	-S.48E-06	-1.70E-06	S.74E-06	100
Rock k=le-07	130S8	2	-3.29	-0.39	-S.83E-06	-7.82E-07	S.88E-06	100
	130S9	3	-3.37	-0.40	-S.66E-06	-7.66E-07	S.71E-06	100
	13060	4	-3.29	-0.70	-S.63E-06	-1.29E-06	S.77E-06	100
	13061	S	-3.30	-0.S2	-S.73E-06	-1.00E-06	S.82E-06	100
	13062	6	-3.33	-0.S3	-S.68E-06	-9.90E-07	S.76E-06	100
	13063	7	-3.26	-0.80	-S.61E-06	-1.4SE-06	S.79E-06	100
	13064	8	-3.28	-0.S7	-S.7SE-06	-1.08E-06	S.8SE-06	100
	1306S	9	-3.31	-0.39	-S.78E-06	-7.66E-07	S.83E-06	100
	13066	10	-3.3S	-0.39	-S.71E-06	-7.60E-07	S.76E-06	100
				$K;$ = 1 x 10-6				
Clus. 3 - EI. 1089	130S7	1	-3.2S	-0.96	-9.36E-06	-3.73E-06	1.01E-OS	100
Rock k = 1e-06	130S8	2	-3.29	-0.39	-9.89E-06	-2.16E-06	1.01E-OS	100
	130S9	3	-3.37	-0.40	-9.7SE-06	-2.14E-06	9.98E-06	100
	13060	4	-3.29	-0.70	-9.60E-06	-3.02E-06	1.01E-OS	100
	13061	S	-3.30	-0.S2	-9.76E-06	-2.S3E-06	1.01E-OS	100
	13062	6	-3.33	-0.S3	-9.72E-06	-2.S2E-06	1.00E-OS	100
	13063	7	-3.26	-0.80	-9.SSE-06	-3.29E-06	1.01E-OS	100
	13064	8	-3.28	-0.S7	-9.76E-06	-2.67E-06	1.01E-OS	100
	1306S	9	-3.31	-0.39	-9.8SE-06	-2.14E-06	1.01E-OS	100
	13066	10	-3.3S	-0.39	-9.80E-06	-2.13E-06	1.00E-OS	100
				$K;$ = 5 x IO-s				
Clus. 3 - EI. 1089	130S7	1	-3.2S	-0.96	7.97E-06	-6.6SE-OS	6.70E-OS	100
Rock k=Se-OS	130S8	2	-3.29	-0.39	-2.20E-06	-7.16E-OS	7. 17E-OS	100
	130S9	3	-3.37	-0.40	-2.S1E-06	-7.00E-OS	7.00E-OS	100
	13060	4	-3.29	-0.70	3.S1E-06	-6.89E-OS	6.90E-OS	100
	13061	S	-3.30	-0.S2	2.83E-07	-7.04E-OS	7.04E-OS	100
	13062	6	-3.33	-0.S3	l.18E-07	-6.99E-OS	6.99E-OS	100
	13063	7	-3.26	-0.80	S.3SE-06	-6.84E-OS	6.86E-OS	100
	13064	8	-3.28	-0.S7	1.23E-06	-7.0SE-OS	7.0SE-OS	100
	1306S	9	-3.31	-0.39	-2.44E-06	-7.12E-OS	7.12E-05	100
	13066	10	-3.3S	-0.39	-2.S6E-06	-7.0SE-05	7.06E-05	100
	13067	11	-3.35	-0.57	8.llE-07	-6.92E-OS	6.93E-OS	100
	13068	12	-3.30	-0.80	5.04E-06	-6.78E-05	6.80E-OS	100

C4.8.l9: Stress field in elements

1. Lining

10 bars

Soil element	Stress point	local number	X[m]	V [m]	0, [kN/mA2)	0, [kN/mA2)	0, [kN/mA2)	10,+o.ll2 [kN/mA2)	10,-<1,)/2 [kN/mA2)
Clus.4 - El. 2715	32569	1	0.02	3.26	-1677.59	-1074.06	-605.00	-1141.29	-536.30
Concrete Ik;le-07))	32570	2	0.Q2	3.02	-1985.85	-999.77	-656.73	-1321.29	-664.56
	32571	3	0.27	3.01	-2007.18	-1004.13	-662.38	-1334.78	-672.40
	32572	4	0.08	3.15	-1824.28	-1049.82	-631.80	-1228.04	-596.24
	32573	5	0.08	3.07	-1943.85	-1022.93	-652.34	-1298.09	-645.75
	32574	6	0.16	3.07	-1953.30	-1029.24	-655.81	-1304.56	-648.74
	32575	7	0.02	3.19	·1777.82	-1055.96	-622.93	-1200.38	-577.45
	32576	8	0.02	3.09	-1911.39	·1023.53	-645.27	-1278.33	-633.06
	32577	9	0.10	3.01	-2048.92	-1004.61	-671.68	-1360.30	-688.62
	32578	10	0.20	3.01	-2058.68	-1011.04	-675.25	-1366.96	-691.72
					20 bars				
Clus.4 - El. 2715	32569	1	0.Q2	3.26	-1757.66	-371.20	19.85	-868.91	-888.76
Concrete Ik; 1e-8)	32570	2	0.Q2	3.02	-1971.35	-424.47	11.84	-979.76	-991.60
	32571	3	0.27	3.01	-1973.44	-427.08	9.07	-982.18	-991.25
	32572	4	0.08	3.15	-1890.51	-389.44	33.93	-928.29	-962.22
	32573	5	0.08	3.07	-1929.72	-404.60	25.57	-952.08	-977.65
	32574	6	0.16	3.07	-1998.39	-428.15	2.33	-998.03	-1000.36
	32575	7	0.02	3.19	-1798.50	-366.37	37.57	-880.47	-918.03
	32576	8	0.02	3.09	-1878.83	-383.80	37.87	-920.48	-958.35
	32577	9	0.10	3.01	-1980.15	-430.56	6.50	-986.82	-993.33
	32578	10	0.20	3.01	-2025.04	-447.00	-19.13	-1022.08	-1002.96
					25 bars				
Clus.4 - El. 2715	32569	1	0.02	3.26	-2194.17	-479.85	3.67	-1095.25	-1098.92
Concrete Ik;le-0711	32570	2	0.02	3.02	-2458.19	-539.60	1.54	-1228.33	-1229.86
	32571	3	0.27	3.01	-2417.07	-530.92	1.07	-1208.00	-1209.07
	32572	4	0.08	3.15	-2365.86	-516.83	4.69	-1180.59	-1185.28
	32573	5	0.08	3.07	-2404.93	-526.46	3.37	-1200.78	·1204.15
	32574	6	0.16	3.07	-2541.16	-587.77	-136.68	-1338.92	-1202.24
	32575	7	0.02	3.19	-2252.23	-491.13	5.59	-1123.32	-1128.91
	32576	8	0.02	3.09	-2343.89	-511.66	5.12	-1169.38	-1174.51
	32577	9	0.10	3.01	-2483.55	-550.84	-22.34	-1252.95	-1230.60
	32578	10	0.20	3.01	-2541.02	-558.58	0.56	-1270.23	-1270.79
					30 bars				⁻.
Clus.4 - El. 2715	32569	1	0.02	3.26	-2577.03	-566.01	1.20	-1287.91	-1289.12
Concrete(k=le-06)	32570	2	0.02	3.02	-2946.97	-648.13	0.25	-1473.36	-1473.61
	32571	3	0.27	3.01	-2848.36	-626.49	0.19	-1424.09	-1424-27
	32572	4	0.08	3.15	-2832.94	-622.44	1.03	-1415.95	-1416.99
	32573	5	0.08	3.07	-2877.44	-632.53	0.65	-1438.40	-1439.05
	32574	6	0.16	3.07	-3076.44	-716.46	-181.56	-1629.00	-1447.44
	32575	7	0.02	3.19	-2664.99	-585.32	1.25	-1331.87	-1333.12
	32576	8	0.02	3.09	-2799.53	-615.17	0.93	-1399.30	-1400.23
	32577	9	0.10	3.01	-2972.76	-653.89	0.16	-1486.30	-1486.46
	32578	10	0.20	3.01	-3067.91	-678.21	-15.18	-1541.54	-1526.36
					35 bars				
Clus.4 - El. 2715	32569	1	0.Q2	3.26	-2980.11	-655.46	0.21	-1489.95	-1490.16
Concretelk;le-05)	32570	2	0.02	3.02	-3436.29	-755.96	0.04	-1718.13	-1718.16

2. Grouted zone

10 bars

Soil element	Stress point	local number	X [m]	Vlm]	0, IkN/mA2]	0, IkN/mA2]	0, IkN/mA2]	(0,+0,)/2 IkN/mA2]	(0,-0,)/2 IkN/mA2]
Clus.2 - EI.1650	19789	1	0.27	3.59	-9042.32	-8482.63	-1572.23	-5307.27	-3735.04
Rock	19790	2	0.23	3.41	-7160.04	-6534.51	-1245.12	-4202.58	-2957.46
	19791	3	0.40	3.39	-7215.76	-6590.63	-1251.65	-4233.71	-2982.06
	19792	4	0.29	3.50	-8190.81	-7601.52	-1417.17	-4803.99	-3386.82
	19793	5	0.28	3.45	-7603.23	-6993.33	-1315.95	-4459.59	-3143.64
	19794	6	0.33	3.44	-7594.96	-6985.05	-1314.48	-4454.72	-3140.24
	19795	7	0.26	3.54	-8500.73	-7923.20	-1471.35	-4986.04	-3514.69
	19796	8	0.24	3.46	-7760.87	-7156.22	-1342.13	-4551.50	-3209.37
	19797	9	0.28	3.40	-7132.75	-6506.62	-1238.62	-4185.69	-2947.06

20 bars

Clus.2 - EI.1650	19789	1	0.27	3.59	-9022.42	-7799.64	-2160.42	-5591.42	-3431.00
Rock	19790	2	0.23	3.41	-7138.11	-5754.21	-1920.60	-4529.36	-2608.76
	19791	3	0.40	3.39	-7191.66	-5817.50	-1909.00	-4550.33	-2641.33
	19792	4	0.29	3.50	-8169.50	-6877.47	-2039.42	-5104.46	-3065.04
	19793	5	0.28	3.45	-7581.01	-6238.68	-1964.28	-4772.64	-2808.37
	19794	6	0.33	3.44	-7572.39	-6233.51	-1957.90	-4765.14	-2807.25
	19795	7	0.26	3.54	-8480.00	-7213.68	-2081.90	-5280.95	-3199.05
	19796	8	0.24	3.46	-7739.24	-6407.71	-1987.23	-4863.23	-2876.00
	19797	9	0.28	3.40	-7109.68	-5727.26	-1907.45	-4508.56	-2601.12

25 bars

Clus.2 - EI.1650	19789	1	0.27	3.59	-9023.82	-7418.06	-2547.69	-5785.75	-3238.06
Rock	19790	2	0.23	3.41	-7142.82	-5330.44	-2366.61	-4754.71	-2388.10
	19791	3	0.40	3.39	-7190.25	-5404.35	-2313.87	-4752.06	-2438.19
	19792	4	0.29	3.50	-8171.00	-6479.61	-2443.49	-5307.24	-2863.75
	19793	5	0.28	3.45	-7582.88	-5827.90	-2383.16	-4983.02	-2599.86
	19794	6	0.33	3.44	-7572.89	-5827.65	-2365.01	-4968.95	-2603.94
	19795	7	0.26	3.54	-8481.66	-6820.35	-2482.27	-5481.96	-2999.70
	19796	8	0.24	3.46	-7741.96	-5997.01	-2410.29	-5076.13	-2665.83
	19797	9	0.28	3.40	-7111.42	-5306.30	-2335.83	-4723.62	-2387.79

30 bars

Clus.2 - El. 1650	19789	1	0.27	3.59	-9024.36	-7039.41	-2927.52	-5975.94	-3048.42
Rock	19790	2	0.23	3.41	-7145.71	-4898.13	-2811.77	-4978.74	-2166.97
	19791	3	0.40	3.39	-7187.09	-4994.12	-2706.66	-4946.88	-2240.21
	19792	4	0.29	3.50	-8171.32	-6081.33	-2841.79	-5506.55	-2664.76
	19793	5	0.28	3.45	-7583.42	-5413.62	-2798.52	-5190.97	-2392.45
	19794	6	0.33	3.44	-7572.32	-5421.89	-2766.31	-5169.32	-2403.00
	19795	7	0.26	3.54	-8482.07	-6427.45	-2875.66	-5678.87	-2803.21
	19796	8	0.24	3.46	-7742.87	-5581.48	-2828.79	-5285.83	-2457.04
	19797	9	0.28	3.40	-7112.12	-4881.09	-2762.93	-4937.52	-2174.60

35 bars

Clus.2 - EI.1650	19789	1	0.27	3.59	-9025.94	-6661.98	-3310.45	-6168.20	-2857.74
Rock	19790	2	0.23	3.41	-7149.79	-4473.05	-3254.82	-5202.31	-1947.49
	19791	3	0.40	3.39	-7185.71	-4583.69	-3107.78	-5146.74	-2038.97
	19792	4	0.29	3.50	-8172.80	-5685.64	-3242.48	-5707.64	-2465.16
	19793	5	0.28	3.45	-7585.15	-5003.69	-3214.69	-5399.92	-2185.23
	19794	6	0.33	3.44	-7572.94	-5017.69	-3171.18	-5372.06	-2200.88

3.Rock zone

10 bars

Soil element	Stress point	local number	X[m]	y [m]	0, [kN/m^2]	0, [kN/m^2]	0, [kN/m^2]	(0,+0,)/2 [kN/m^2]	(0,-0,)/2 [kN/m^2]
(lus. 1- El. 150	1789	1	6.62	-44.83	-6383.37	-5092.85	-5076.46	-5729.92	-653.45
Rock	1790	2	3.96	-49.63	-6501.23	-5194.73	-5193.39	-5847.31	-653.92
	1791	3	9.37	-49.63	-6498.60	-5194.07	-5192.81	-5845.70	-652.90
	1792	4	6.64	-47.03	-6436.92	-5139.49	-5129.99	-5783.46	-653.47
	1793	5	5.81	-48.52	-6473.72	-5171.18	-5166.25	-5819.99	-653.74
	1794	6	7.49	-48.52	-6472.80	-5171.01	-5166.30	-5819.55	-653.25
	1795	7	5.77	-46.23	-6418.02	-5122.63	-5110.32	-5764.17	-653.85
	1796	8	4.70	-48.16	-6465.43	-5163.61	-5157.35	-5811.39	-654.04
	1797	9	5.58	-49.69	-6502.09	-5195.83	-5194.70	-5848.39	-653.69

20 bars

(lus. 1 - El. 150	1789	1	6.62	-44.83	-6385.57	-5093.18	-5075.66	-5730.62	-654.95
Rock	1790	2	3.96	-49.63	-6502.98	-5195.21	-5193.77	-5848.38	-654.60
	1791	3	9.37	-49.63	-6500.08	-5194.48	-5193.11	-5846.59	-653.48
	1792	4	6.64	-47.03	-6438.86	-5139.87	-5129.70	-5784.28	-654.58
	1793	5	5.81	-48.52	-6475.54	-5171.62	-5166.33	-5820.93	-654.60
	1794	6	7.49	-48.52	-6474.52	-5171.42	-5166.37	-5820.44	-654.07
	1795	7	5.77	-46.23	-6420.10	-5123.00	-5109.84	-5764.97	-655.13
	1796	8	4.70	-48.16	-6467.34	-5164.05	-5157.34	-5812.34	-655.00
	1797	9	5.58	-49.69	-6503.77	-5196.30	-5195.09	-5849.43	-654.34

25 bars

(lus. 1- El. 150	1789	1	6.62	-44.83	-6387.08	-5093.42	-5075.16	-5731.12	-655.96
Rock	1790	2	3.96	-49.63	-6504.19	-5195.57	-5194.06	-5849.13	-655.07
	1791	3	9.37	-49.63	-6501.09	-5194.77	-5193.33	-5847.21	-653.88
	1792	4	6.64	-47.03	-6440.19	-5140.15	-5129.54	-5784.87	-655.32
	1793	5	5.81	-48.52	-6476.78	-5171.93	-5166.41	-5821.60	-655.19
	1794	6	7.49	-48.52	-6475.70	-5171.71	-5166.44	-5821.07	-654.63
	1795	7	5.77	-46.23	-6421.53	-5123.27	-5109.54	-5765.54	-655.99
	1796	8	4.70	-48.16	-6468.65	-5164.36	-5157.36	-5813.01	-655.65
	1797	9	5.58	-49.69	-6504.93	-5196.64	-5195.37	-5850.15	-654.78

30 bars

(lus. 1 - El. 150	1789	1	6.62	-44.83	-6388.80	-5093.73	-5074.66	-5731.73	-657.07
Rock	1790	2	3.96	-49.63	-6505.61	-5195.99	-5194.42	-5850.01	-655.60
	1791	3	9.37	-49.63	-6502.27	-5195.13	-5193.61	-5847.94	-654.33
	1792	4	6.64	-47.03	-6441.72	-5140.50	-5129.41	-5785.56	-656.16
	1793	5	5.81	-48.52	-6478.23	-5172.32	-5166.54	-5822.38	-655.85
	1794	6	7.49	-48.52	-6477.07	-5172.08	-5166.56	-5821.81	-655.25
	1795	7	5.77	-46.23	-6423.18	-5123.62	-5109.26	-5766.22	-656.96
	1796	8	4.70	-48.16	-6470.17	-5164.75	-5157.42	-5813.80	-656.37
	1797	9	5.58	-49.69	-6506.29	-5197.06	-5195.72	-5851.00	-655.29

35 bars

(lus. 1 - El. 150	1789	1	6.62	-44.83	-6390.51	-5094.02	-5074.15	-5732.33	-658.18
Rock	1790	2	3.96	-49.63	-6507.01	-5196.40	-5194.75	-5850.88	-656.13
	1791	3	9.37	-49.63	-6503.45	-5195.47	-5193.87	-5848.66	-654.79
	1792	4	6.64	-47.03	-6443.25	-5140.83	-5129.26	-5786.25	-657.00

C4.9 - Schleiss analytical solution

Water losses through concrete liner, grouted zone and rock mass zone are computed iteratively from the equation below.

$$\frac{P_i}{P_{wg}} - \frac{3}{4}\frac{T_g}{} = \frac{q}{2\pi K_T}\ln\frac{T_a}{T_i} + \frac{q}{2\pi K_c}\left[1 - \left(\frac{T_a}{T_i}\right)^2\right] + \frac{1}{2\pi K_g}\ln\left(\frac{T_g}{T_a}\right)$$

Whereas P_i is the internal water pressure

q is the seepage loss

K_T I K_c and K_g are permeability coefficients for rock mass, concrete and grouted rock zone respectively. $K_T = K_g$ an assumption based on Schleiss, 1986.

T_i I T_a and T_g are internal, external and grouted zone radii with reference to the centre of the tunnel.

$T_i = 3.0m$, $T_a = 3.3m$ and $T_g = 5.5m$. The values of permeability coefficient and corresponding internal water pressure are as shown in table 6.3.

$$\ln\left(\frac{T_a}{T_i}\right) = 0.0953 \quad \text{and} \quad \ln\left(\frac{T_g}{T_a}\right) = 0.5108$$

Seepage loss is computed as follows:

For $P_i = 10$ *bars;*

$$q \times 10^6 \left[1.592 \ln\left(\frac{q}{1.728 \times 10^{-6}}\right) + 2.3297\right] = 5.875$$

By trial and error:

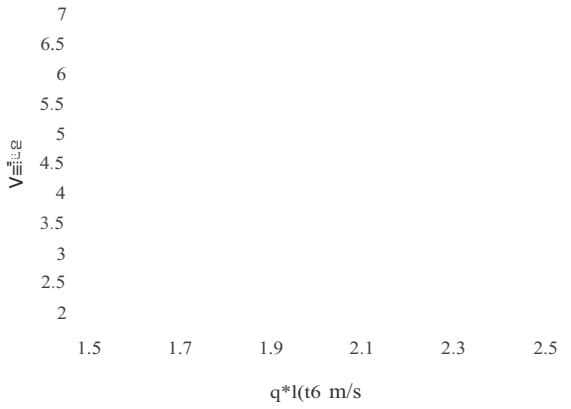

Seepage flow for $P_i = 10$ *bars* is = 2.175 x 10-6 *mf s*

For $P_i = 20$ *bars;*

$$q \times 10^6 \left[1.592 \ln\left(\frac{1.728 \sim 10^{-6}}{}\right) + 2.3297\right] = 15.875$$

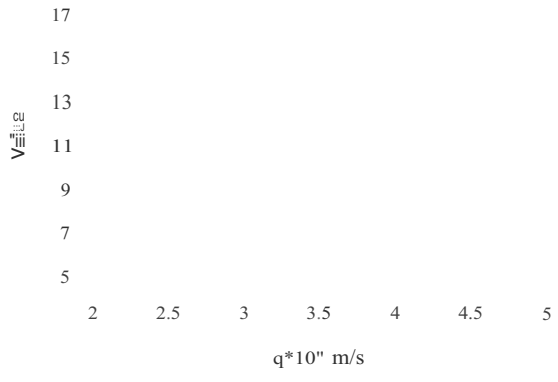

Seepage flow for $P_i = 20$ *bars* is = 4.220 x *10-6m/s*

For *Pi* = 25 *bars;*

q X 105 [15.92In (1.728q x 10-6) + 9.6462] = 20.875

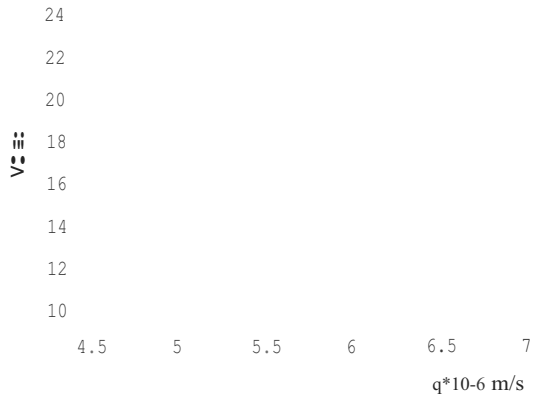

Seepage flow for *Pi* = 25 *bars* is = 6.680 x *10-6m/s*

For *Pi* = 30 *bars;*

q X 105 [15.92 In (1.728q x 10-6) + 8.2810] = 25.875

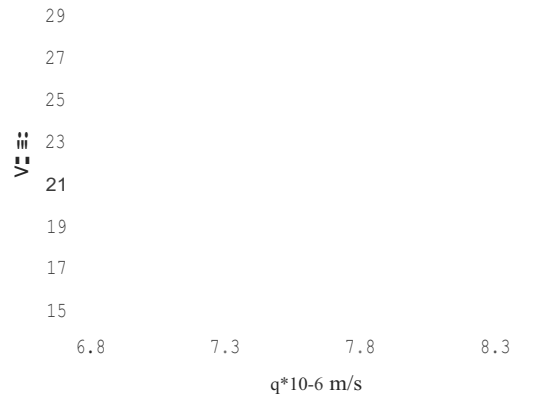

Seepage flow for *Pi* = 30 *bars* is = 7.950 x *10-6m/s*

For *Pi* = 35 *bars;*

q X 105 [15.92In (1.728q x 10-6) + 8.1510] = 30.875

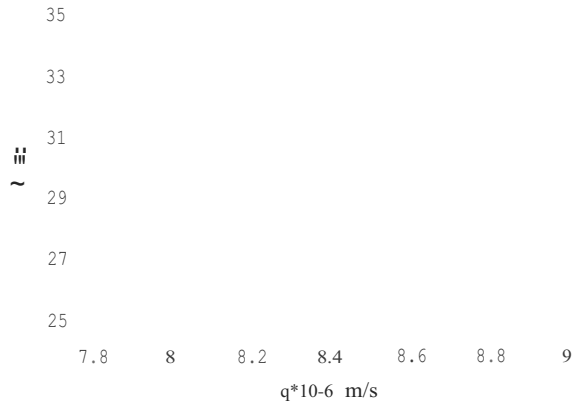

Seepage flow for *Pi* = 35 *bars* is = 8.970 x *10-6m/s*

Water losses = *q* x rrDd x 10$_6$ *ljsjkmjbar*

Where D= 6m, tunnel internal diameter and d = 30 cm, equivalent thickness of the lining

Pi (bars)	Seepage loss, *q (m/s)*	Water losses
10	2.175 x 10-6	1.230
20	4.220 x 10-6	1.193
25	6.680 x 10-6	1.511
30	7.950 x 10-6	1.499
35	8.970 x 10-6	1.449